

Title	Lipase/H ₂ S ₀₄ -Cocatalyzed Dynamic Kinetic Resolution of Alcohols in Pickering Emulsion
Author(s)	Moon, Jihoon; Kin, Takusho; Mizuno, Karin et al.
Citation	ChemCatChem. 2023, 15(18), p. e202300878
Version Type	AM
URL	https://hdl.handle.net/11094/94659
rights	© 2023 Wiley-VCH GmbH
Note	

Osaka University Knowledge Archive : OUKA

<https://ir.library.osaka-u.ac.jp/>

Osaka University

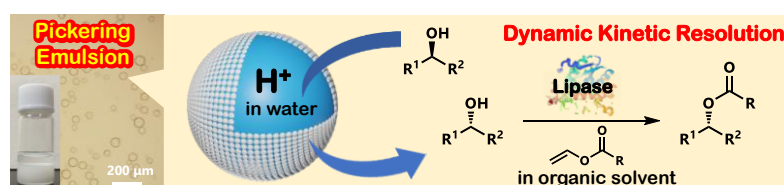
Lipase/H₂SO₄-Cocatalyzed Dynamic Kinetic Resolution of Alcohols in Pickering Emulsion

Jihoon Moon, Takusho Kin, Karin Mizuno, Shuji Akai*, Kyohei Kanomata*

Graduate School of Pharmaceutical Sciences, Osaka University, 1-6 Yamadaoka, Suita, Osaka 565-0871, Japan

Abstract

This study reports the first chemoenzymatic dynamic kinetic resolution (DKR) of racemic *sec*-alcohols by simultaneously using immobilized lipase and aqueous sulfuric acid as catalysts for kinetic resolution and racemization, respectively. The nanoparticle-stabilized phase separation in a Pickering emulsion enabled the use of these inherently incompatible catalysts in a single vessel. The racemization reaction in the aqueous sulfuric acid solution significantly suppressed the dehydrative side reactions that form alkenes and dimeric ethers, which are often observed in racemization using Brønsted/Lewis acids or oxovanadium compounds in organic solvents. The efficacy of the Pickering emulsion was confirmed by the significantly lower catalytic performance in DKR without emulsification. This method achieved high yields and high optical purities in the production of a wide range of *sec*-alcohols.



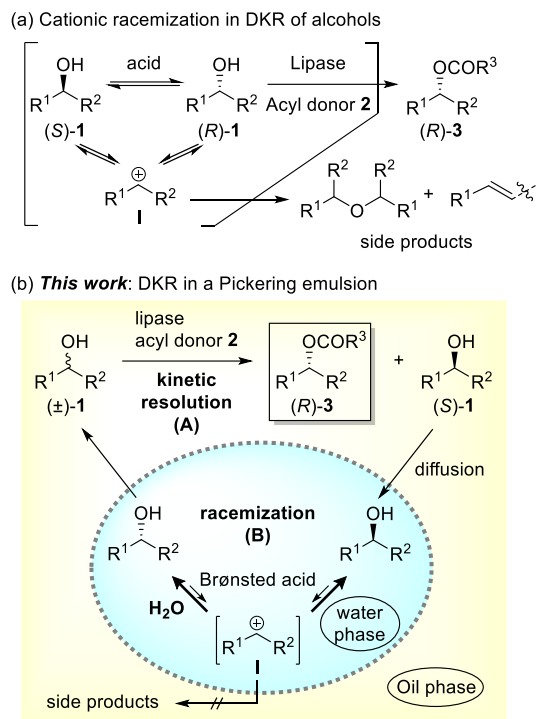
Introduction

Chemoenzymatic dynamic kinetic resolution (DKR) combines enzymatic kinetic resolution (KR) and rapid racemization of the starting materials in a one-pot system to obtain optically active compounds in quantitative yields.^[1–3] In particular, the DKR of alcohols has been intensively studied because alcohols play a pivotal role in the synthesis of various biologically active compounds such as natural products and pharmaceuticals.^[4–6] Lipase-catalyzed enantioselective acylation in organic solvents is a well-established method for the DKR of various alcohols because of its high enantioselectivity and wide substrate scope.^[7]

Typical racemization for DKR include catalysis via redox pathways^[8–13] and carbocation intermediates.^[14–18] Hydrogen-transfer catalysts such as ruthenium complexes have been intensively studied for the redox racemization of *sec*-alcohols. Although racemization via the carbocation intermediate **I** indicates a different scope for redox catalysis, such as the applicability to *tert*-alcohols,^[19,20] it has not been fully explored in DKR, mainly for the following two reasons: (i) low

compatibility of the racemization catalysts with lipases and (ii) dehydrative side reactions that form alkenes and dimeric ethers (Scheme 1a). Several efforts have been made to improve the compatibility between these two catalysts. Elaborate apparatuses, including Teflon tubes and inox baskets, have been used to physically separate lipases from racemization catalysts such as vanadyl sulfate (VOSO₄) and resin-supported Brønsted acids.^[15,21–23] Compartmentalization by immobilizing racemization catalysts and/or lipases inside mesoporous materials has also been reported,^[24–26] including our original mesoporous silica-supported oxovanadium catalyst (V-MPS4), in which an oxovanadium species was covalently bound to the surface of the 4-nm-sized pores in mesoporous silica.^[27–29] However, although highly compatible with lipases, V-MPS4 is prone to side reactions such as ether formation during the racemization process.^[30–33] In addition, its racemization profile is limited by the electronic nature of the substrates, with slow racemization observed for simple 1-phenylethanol (**1a**: R¹ = Ph, R² = Me, Table S2).

Although the processes described above address the low compatibility of lipases and racemization catalysts, the side reactions during racemization remain a considerable challenge.^[22,23,30–33] To solve this problem, we envisioned a new strategy using an oil/water biphasic medium for chemoenzymatic DKR (Scheme 1b). In this biphasic DKR, lipase-catalyzed KR of (±)-**1** proceeds in the oil phase (A) while Brønsted acid-catalyzed racemization occurs in the aqueous phase (B). Importantly, the side reactions during racemization would be significantly suppressed because cation intermediate **I** would be rapidly captured by a solvent water molecule to re-form (±)-**1**.^[19] Phase separation ensures the compatibility of the two catalysts. To implement this biphasic DKR concept, a Pickering emulsion was used as the reaction medium. Pickering emulsions are oil/water mixtures in which micrometer-sized droplets are stabilized by the irreversible adsorption of nanoparticles at the interface.^[34–37] We anticipated that this nanoparticle layer would form a robust barrier to physically separate the lipase from the acid solution, allowing them to coexist in a single medium while still enabling small molecules such as **1** to easily diffuse through the layer.^[38] Furthermore, the produced ester (*R*)-**3** would remain in the oil phase because of its high hydrophobicity, avoiding acid-catalyzed side reactions such as hydrolysis and elimination. Herein, we report the DKR of racemic *sec*-alcohols **1** in a Pickering emulsion using immobilized lipase/aqueous sulfuric acid as the catalysts. We confirmed that emulsification by nanoparticles is essential for combining these two inherently incompatible catalysts in a single vessel. This methodology, which uses aqueous sulfuric acid as the racemization catalyst, has the additional advantage of extending its substrate scope by simply tuning the acid concentration based on the racemization reactivity of the substrates.



Scheme 1. Chemoenzymatic dynamic kinetic resolution (DKR) of alcohols

Results and Discussion

The Pickering emulsions were prepared by homogenizing a mixture of methyl-modified silica nanoparticles (Fig. S1), *n*-octane, and aqueous sulfuric acid (aq. H₂SO₄) at concentrations of up to 5.0 M (Fig. 1).^[37] The emulsion was stable, and the droplet size distribution did not change significantly after incubation under the reaction conditions (Table S1). The emulsion was confirmed to be a water-in-oil (w/o) type via fluorescence imaging using water-soluble FITC-dextran (Fig. 1b, inset).

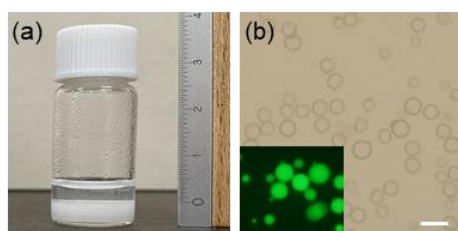


Fig. 1 (a) Silica nanoparticle-stabilized Pickering emulsions using 1.0 M H₂SO₄ as aqueous phase; (b) microscopic image of emulsion and (inset) fluorescent image using FITC-dextran solution (6 μM) as aqueous phase. Scale bar: 100 μm.

We then investigated the racemization of an alcohol in a Pickering emulsion using optically pure (*R*)-1-phenylethanol (**1a**) as a typical substrate (Fig. 2 and S2). Each reaction was prepared in a

Pickering emulsion comprising silica nanoparticles (30 mg), *n*-octane (600 μ L), and aqueous acid solution (300 μ L) using (*R*)-**1a** (0.10 mmol), and conducted in an incubator without stirring.^[39] Aqueous Brønsted acid solutions were found to be effective for the racemization. As a typical example, facile racemization of (*R*)-**1a** occurred in a Pickering emulsion of *n*-octane and 1.0 M aq. H₂SO₄ at 50 °C, with an enantiomeric excess (% ee) half-life of 3.8 h (Fig. 2, square markers). The racemization using 1.0 M aq. HCl as the aqueous phase at 50 °C (unshaded circles) proceeded at a comparable rate to that using 1.0 M aq. H₂SO₄. However, ca. 5% of a chlorinated side product, (1-chloroethyl)benzene, was observed after 4 h, and the yield of the chlorinated product markedly increased as the HCl concentration increased above 1.5 M. The racemization rate was significantly affected by the acid concentration and reaction temperature. Changing the conditions to 0.5 M aq. H₂SO₄ at 50 °C (shaded circles) or 1.0 M aq. H₂SO₄ at 35 °C (triangles) resulted in a significantly lower racemization rate. An aqueous VOSO₄ solution did not promote racemization (crosses), despite solid VOSO₄ hydrate often being used as a racemization catalyst for the DKR of *sec*-alcohols in organic solvents.^[17,21–23] Notably, during the racemization of (*R*)-**1a** in a Pickering emulsion of 1.0 M aq. H₂SO₄, side products such as styrene and bis(1-phenylethyl) ether, were not observed even after 18 h when the racemization was complete. In contrast, the formation of these side products has often been reported in similar racemization reactions via cationic intermediate **I** using catalysts such as VOSO₄, zeolites, and resin-supported Brønsted acids.^[15–18,21–23] In addition, using V-MPS4^[28,29] as the catalyst resulted in no racemization of (*R*)-**1a** under typical DKR conditions (Table S2), despite its efficiency for the racemization of allylic alcohols.^[29]

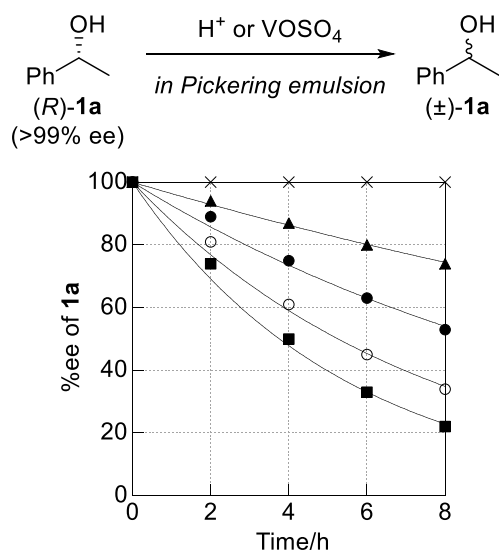


Fig. 2 Racemization of (*R*)-**1a** in Pickering emulsions over time: 1.0 M aq. H₂SO₄ at 50 °C (■); 1.0 M aq. HCl at 50 °C (○); 0.5 M aq. H₂SO₄ at 50 °C (●); 1.0 M aq. H₂SO₄ at 35 °C (▲); and 1.0 M aq. VOSO₄ at 50 °C (×). Lines indicate exponential curve fitting for each plot. Each reaction was conducted in a Pickering emulsion of silica nanoparticles (30 mg)/*n*-octane (600 μ L)/indicated aqueous solution (300 μ L) using (*R*)-**1a** (0.10 mmol).

We used the procedure described below to confirm that the racemization occurred inside the emulsion droplets rather than in the outer oil phase (Fig. S3). Using (*R*)-**1a** (>99% ee) as the substrate, the optical purity decreased to 79% ee after 2 h in a Pickering emulsion of *n*-octane/aq. H₂SO₄ (1.0 M) at 50 °C. At this stage, the emulsion and the supernatant oil phase were separated, and each was incubated at 50 °C. After 6 h, the optical purity of **1a** in the Pickering emulsion further decreased to 20% ee, whereas that of **1a** in the supernatant remained unchanged (79% ee). These results clearly indicated that racemization occurred exclusively inside the emulsion droplets.

Next, we investigated the lipase-catalyzed KR of (\pm)-**1a** using vinyl ester **2** and commercially available immobilized *Candida antarctica* lipase B (CAL-B) under a standard condition of lipase-catalyzed acylative kinetic resolution (Fig. 3). The KR of (\pm)-**1a** with **2a** (R = *n*-C₃H₇) in anhydrous *n*-octane was highly enantioselective, and the yield of (*R*)-**3aa** (R = *n*-C₃H₇) reached 50% within 1 h along with 50% unreacted (*S*)-**1a**; both compounds were optically pure (unshaded circles). We then examined the KR in a Pickering emulsion of *n*-octane/deionized water (DW). The reaction was initiated by adding CAL-B in the outer organic phase containing (\pm)-**1a** and **2a** (see the ESI for the detailed procedure). The rate of KR in the Pickering emulsion was significantly lower than that in anhydrous *n*-octane, and the yield of **3aa** did not exceed 40% (unshaded circles). Using vinyl decanoate (**2b**: R = *n*-C₉H₁₉) instead of **2a** slightly improved the yield of **3**, although it remained below 40% (triangles). We attributed this insufficient conversion to the concomitant hydrolysis of product **3** under these reaction conditions because the emulsion oil phase was oversaturated with water (109 ppm, Fig. S4). The rate of the reaction using **2b** was significantly improved by adding placing anhydrous magnesium sulfate on top of the emulsion as a dehydrating reagent, and the yield of **3ab** reached 50% (squares).

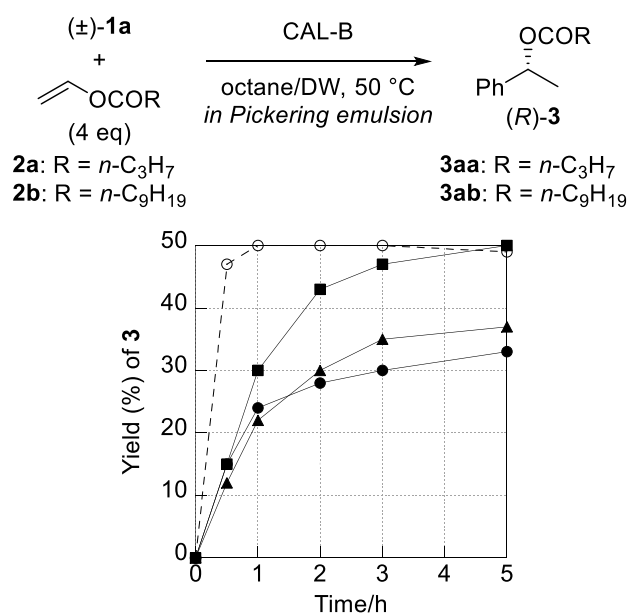


Fig. 3 Lipase-catalyzed KR of (\pm)-**1a** over time: **2a** in anhydrous *n*-octane (○); **2a** in Pickering emulsion of *n*-octane/DW (●); **2b** in Pickering emulsion of *n*-octane/DW (▲); and **2b** in Pickering emulsion of *n*-octane/DW with MgSO₄ (■). The yield of **3** was determined by GC-FID analysis, and

the *E*-values were >200 in all cases (**3** was >99% ee, which was determined by chiral HPLC analysis). Each reaction was conducted in a Pickering emulsion of silica nanoparticles (30 mg)/*n*-octane (600 μL)/DW (300 μL) using (±)-**1a** (0.10 mmol) and immobilized CAL-B (2.0 mg). DW: deionized water.

After establishing the racemization and KR conditions, the DKR of (±)-**1a** in a Pickering emulsion was investigated (Table 1). The reactions were conducted at 50 °C for 21 h using **2b** (4.0 eq), immobilized CAL-B (20 mg/mmol), *n*-octane, and 1.0 M aq. H₂SO₄. The reaction proceeded smoothly to afford **3ab** in 91% yield with >99% ee (Entry 1). In contrast, a biphasic mixture of *n*-octane and 1.0 M aq. H₂SO₄ without emulsification resulted in incomplete conversion (Entry 2). The efficacy of the emulsification was further demonstrated using non-immobilized CAL-B. In a Pickering emulsion, **3ab** was obtained in 78% yield (Entry 3), whereas the reaction did not proceed in the biphasic mixture without emulsification (Entry 4). These results indicated that the phase separation in a Pickering emulsion was essential for promoting CAL-B/H₂SO₄-cocatalyzed DKR because lipases are readily inactivated by acids.

Table 1. DKR of (±)-**1a** in Pickering emulsions^[a]

$$(\pm)\text{-1a} + \text{2b} \xrightarrow[\substack{\text{octane/aq. H}_2\text{SO}_4 (1.0 \text{ M}) \\ 50 \text{ }^\circ\text{C, 21 h}}]{\text{CAL-B}} (R)\text{-3ab}$$

(4 eq)

Entry	CAL-B	Medium	% Yield of 3ab ^[b]
1	immobilized	Pickering emulsion ^[c]	91 ^[d]
2	immobilized	biphasic mixture	64
3	non-immobilized	Pickering emulsion ^[c]	78
4	non-immobilized	biphasic mixture	no reaction

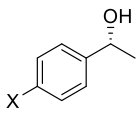
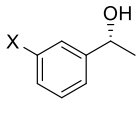
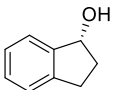
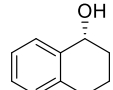
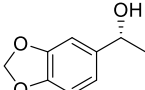
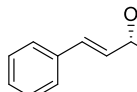
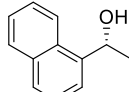
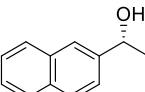
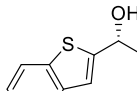
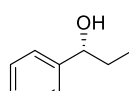
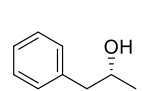
^[a]The reaction was conducted in a Pickering emulsion of silica nanoparticles (30 mg)/*n*-octane (600 μL)/1.0 M aq. H₂SO₄ (300 μL) using (±)-**1a** (0.10 mmol), **2b** (4.0 eq), and CAL-B (2.0 mg). In Entries 2 and 4, a biphasic mixture without silica nanoparticles was used. ^[b]Determined by GC-FID analysis. ^[c]Pickering emulsion with MgSO₄ (150 mg) on the emulsion droplets. ^[d]>99% ee.

The present DKR method was successfully applied to a wide range of alcohols. To effectively promote DKR, we found that tuning the acid concentration to ensure a moderate rate of racemization was critical (Table 2). An acid concentration of 1.0 M was suitable for 4-Me-substituted phenylethanol (±)-**1b**, and optically pure (*R*)-**1b** was obtained in 82% isolated yield after methanolysis of the produced ester. The substrates (±)-**1c–1e** and **1h**, which bear a halogen atom at either the *para*-

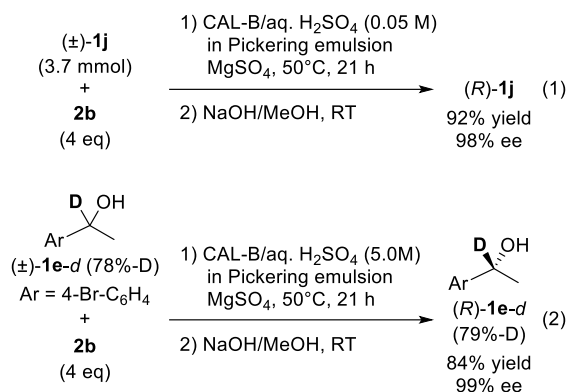
or *meta*-position, required higher acid concentrations for racemization, and using 1.5–5.0 M aq. H₂SO₄ afforded (*R*)-**1c–1e** and (*R*)-**1h** in 73–90% yields with >96% ee. Notably, our previous lipase/V-MPS4 conditions resulted in unsuccessful DKR of these electron-withdrawing-group-bearing alcohols because racemization did not proceed with the V-MPS4 catalyst.^[29] Electron-donating 4-MeO-substituted phenylethanol (±)-**1f** required a highly dilute acid (0.002 M aq. H₂SO₄) to afford (*R*)-**1f** (67% yield, 99% ee), with more concentrated acid solutions resulting in the decomposition of **1f**. The reactions of 1-indanol ((±)-**1j**) and allyl alcohol (±)-**1m** afforded (*R*)-**1j** (97% yield, >99% ee) and (*R*)-**1m** (82% yield, 98% ee), respectively. The reactions of 1-tetralol ((±)-**1k**) and benzodioxole-substituted alcohol (±)-**1l** resulted in moderate yields, although the optical purities were high (97% ee each). The DKR of 1-naphthyl-substituted alcohol (±)-**1n** proceeded with 0.5 M aq. H₂SO₄, whereas 2-naphthyl-substituted alcohol (±)-**1o** required a higher acid concentration (2.0 M). Heterocyclic substrate (±)-**1p** containing 2-benzothiophenyl group was also tolerated under these conditions, affording (*R*)-**1p** in 70% yield with 98% ee. Ethyl-substituted alcohol (±)-**1q** required a high acid concentration (2.5 M) to promote racemization and obtain (*R*)-**1q** (65% yield, 98% ee). The reaction of 3-NO₂-substituted phenylethanol (±)-**1i** produced (*R*)-**1i** (56% yield, 97% ee), with (*S*)-**1i** (39%, 45% ee) remaining, indicating that the racemization of **1i** did proceed, albeit slowly. Aliphatic *sec*-alcohol (±)-**1r** was converted to (*R*)-**1r** (97% ee) in a lower yield of 47%, because racemization was slow.

The present DKR in a Pickering emulsion was scalable without any loss of yield (Scheme 2-1). The reaction using (±)-**1j** was conducted on a 0.5-g scale (3.7 mmol) in an open beaker using the protocol described in Table 2 (Fig. S5). Optically pure (*R*)-**1j** was obtained in 92% isolated yield after methanolysis. The advantages of the Pickering emulsion method were further demonstrated by the DKR of a deuterated substrate (Scheme 2-2). The DKR of (±)-**1e-d** and subsequent methanolysis afforded the corresponding optically pure (*R*)-**1e-d** in 84% yield without any loss of the deuterium content.

Table 2. Scope and limitations of CAL-B/H₂SO₄-cocatalyzed DKR of alcohols (\pm)-**1** in a Pickering emulsion^[a]

$ \begin{array}{c} \text{OH} \\ \\ \text{R}^1\text{---}\text{C}\text{---}\text{R}^2 \\ (\pm)\text{-1} \end{array} \xrightarrow[2) \text{ NaOH/MeOH, RT}]{1) \text{ 2b (4 eq), CAL-B/aq. H}_2\text{SO}_4 \text{ in Pickering emulsion MgSO}_4, 50^\circ\text{C, 21 h}} \begin{array}{c} \text{OH} \\ \\ \text{R}^1\text{---}\text{C}\text{---}\text{R}^2 \\ (R)\text{-1} \end{array} $		
	1b (X = Me): 0.75 M	82% (84%), >99% ee
	1c (X = F): 1.5 M	87% (87%), >99% ee
	1d (X = Cl): 3.0 M	84% (88%), 96% ee
	1e (X = Br): 5.0 M	90% (90%), 99% ee
	1f (X = MeO): 0.002 M	67% (68%), >99% ee
	1g (X = Me): 1.5 M	88% (88%), 98% ee
	1h (X = Br): 5.0 M	70% (73%), >99% ee
	1i (X = NO ₂): 5.0 M	56% (56%), 97% ee ^[b]
	1j (0.05 M)	97% (93%), >99% ee
	1k (0.02 M)	78% (78%), 97% ee
	1l (0.02 M)	61% (63%), 97% ee
	1m ^[c] (0.03 M)	82% (82%), 98% ee
	1n ^[c] (0.5 M)	62% (68%), 95% ee
	1o (2.0 M)	87% (88%), 89% ee
	1p ^[c] (0.4 M)	70% (74%), 98% ee
	1q ^[c] (2.5 M)	65% (67%), 98% ee
	1r ^[c] (5.0 M)	47% (48%), 97% ee

^[a] DKR was performed in a Pickering emulsion of silica nanoparticles (30 mg)/*n*-octane (600 μ L)/aq. H₂SO₄ (300 μ L, acid concentration for each compound is shown in the Table)/MgSO₄ (150 mg) using (\pm)-**1a** (0.10 mmol), **2b** (4.0 eq), and immobilized CAL-B (2.0 mg). The isolated yields of (*R*)-**1** after methanolysis with NaOH are shown, with the yields of (*R*)-**3** after DKR in parentheses. Yields were determined using ¹H NMR with trichloroethylene as the internal standard. ^[b]The optical purity of the recovered **1** in DKR was 45% ee. ^[c]5.0 mg of CAL-B was used.



Scheme 2. Scale-up experiment conducted in Pickering emulsion. Reaction conditions: $(\pm)\text{-1j}$ (3.7 mmol, 0.50 g), $\mathbf{2b}$ (3.0 eq), immobilized CAL-B (70 mg), silica nanoparticles (1.1 g), *n*-octane (22 mL), aq. H_2SO_4 (0.05 M, 11 mL), and MgSO_4 (5.5 g); (2) DKR of deuterated substrate $(\pm)\text{-1e-d}$.

Conclusions

We used a Pickering emulsion to successfully achieve the first reported lipase/ H_2SO_4 -cocatalyzed DKR of alcohols. Racemization in the acidic aqueous phase significantly suppressed side reactions that form alkenes and dimeric ethers, which are often observed in the DKR of alcohols via cationic intermediates in organic solvents. In addition, the concomitant use of two inherently incompatible catalysts was achieved via phase separation due to the nanoparticles in the Pickering emulsion. The advantages of the present DKR include the expanded substrate scope of *sec*-alcohols and easy optimization of the racemization conditions by tuning the acid concentration based on the racemization reactivity of the substrates. In particular, racemization was successfully achieved using 1-phenylethanol ($\mathbf{1a}$) and its derivatives bearing electron-withdrawing groups were applicable, whereas our previous racemization using V-MPS4 was unsuccessful with these alcohols.^[28,29] The application of this Pickering emulsion-mediated strategy to various biphasic multicomponent catalyses is ongoing in our laboratory.

Experimental section

General procedure for DKR in a Pickering emulsion: A Pickering emulsion was prepared in a screw-capped vial ($\phi = 15$ mm) by mixing methyl-modified silica nanoparticles (30 mg), aqueous sulfuric acid (0.30 mL), and *n*-octane (1.0 mL) at 20,000 rpm for 90 sec using a T10 basic ULTRA-TURRAX homogenizer (IKA) equipped with a S10N-5G Dispersing tool ($\phi = 5$ mm). After the supernatant organic layer was removed, *n*-octane (600 μL) containing $(\pm)\text{-1}$ (0.10 mmol) and $\mathbf{2b}$ (0.40 mmol, 4.0 eq) was gently added to the vial. Anhydrous MgSO_4 (150 mg) was placed on top of the emulsion to cover the droplets, followed by addition of CAL-B (2.0 mg). The vial was stood in an incubator at 50°C without stirring. After 21 h, the reaction mixture was diluted with Et_2O and

naturized by solid NaHCO₃. The resulting mixture was dried over anhydrous MgSO₄, filtrated, and evaporated. The residue was purified by silica gel column chromatography to remove unreacted **1**. The purified ester **3** was then subjected to methanolysis by adding MeOH (3 mL) and NaOH (0.4 mmol). After stirring for 1 h at room temperature, the reaction was quenched by adding saturated aq. NH₄Cl, and the mixture was extracted with Et₂O (x 3 times). The combined organic layer was dried over anhydrous Na₂SO₄, filtrated, and evaporated in vacuo. The residue was purified by silica gel column chromatography to give enantiomerically enriched alcohol (*R*)-**1**.

Conflict of Interest

The authors declare no conflict of interest.

Data Availability Statement

The data that support the findings of this study are available in the supplementary material of this article.

Acknowledgments

We would like to appreciate Dr. Harald Gröger (Bielefeld University, Germany) and Dr. Yoshinari Sawama (Osaka University, Japan) for fruitful discussion. This work was financially supported in part by the JSPS KAKENHI (Grant Numbers T22K146810, A21H026050, and 22KK0073), Kansai Research Foundation for technology promotion, The Research Foundation for Pharmaceutical Sciences, and the Platform Project for Supporting Drug Discovery and Life Science Research (Basis for Supporting Innovative Drug Discovery and Life Science Research (BINDS)) from AMED (Grant Number JP23ama121054).

References

- [1] O. Verho, J. E. Bäckvall, *J. Am. Chem. Soc.* **2015**, *137*, 3996–4009.
- [2] L. C. Yang, H. Deng, H. Renata, *Org. Process Res. Dev.* **2022**, *26*, 1925–1943.
- [3] J. E. Bäckvall, Ed. , *Dynamic Kinetic Resolution (DKR) and Dynamic Kinetic Asymmetric Transformations (DYKAT)*, Thieme: Stuttgart, **2023**.
- [4] S. Akai, G. A. I. Moustafa, in *Kinetic Control in Synthesis and Self-Assembly* (Eds.: M. Numata, S. Yagai, T. Hamura), Academic Press, **2019**, pp. 21–43.
- [5] R. Ferraccioli, *Symmetry* **2021**, *13*, 1744:1–22.
- [6] K. Kanomata, S. Akai, in *Sci. Synth. Dyn. Kinet. Resolut. Dyn. Kinet. Asymmetric Transform.* (Ed.: J.E. Bäckvall), Thieme: Stuttgart, **2023**, pp. 181–217.
- [7] K. Faber, *Biotransformations in Organic Chemistry: 7th Edition*, Springer, **2018**.

- [8] M. C. Warner, J. E. Bäckvall, *Acc. Chem. Res.* **2013**, *46*, 2545–2555.
- [9] A. Berkessel, M. L. Sebastian-Ibarz, T. N. Müller, *Angew. Chem. Int. Ed.* **2006**, *45*, 6567–6570.
- [10] R. M. Haak, F. Berthiol, T. Jerphagnon, A. J. A. Gayet, C. Tarabiono, C. P. Postema, V. Ritleng, M. Pfeffer, D. B. Janssen, A. J. Minnaard, B. L. Feringa, J. G. De Vries, *J. Am. Chem. Soc.* **2008**, *130*, 13508–13509.
- [11] Y. Sato, Y. Kayaki, T. Ikariya, *Chem. Commun.* **2012**, *48*, 3635–3637.
- [12] O. El-Sepelgy, N. Alandini, M. Rueping, *Angew. Chem. Int. Ed.* **2016**, *55*, 13602–13605.
- [13] K. P. J. Gustafson, A. Guðmundsson, K. Lewis, J. E. Bäckvall, *Chem. Eur. J.* **2017**, *23*, 1048–1051.
- [14] O. Långvik, T. Saloranta, D. Y. Murzin, R. Leino, *ChemCatChem* **2015**, *7*, 4004–4015.
- [15] C. M. Sapu, T. Görbe, R. Lihammar, J. E. Bäckvall, J. Deska, *Org. Lett.* **2014**, *16*, 5952–5955.
- [16] P. Ödman, L. A. Wessjohann, U. T. Bornscheuer, *J. Org. Chem.* **2005**, *70*, 9551–9555.
- [17] S. Wuyts, K. De Temmerman, D. E. De Vos, P. A. Jacobs, *Chem. Eur. J.* **2005**, *11*, 386–397.
- [18] Y. Zhu, K. L. Fow, G. K. Chuah, S. Jaenicke, *Chem. Eur. J.* **2007**, *13*, 541–547.
- [19] T. Görbe, R. Lihammar, J. E. Bäckvall, *Chem. Eur. J.* **2018**, *24*, 77–80.
- [20] F. Kühn, S. Katsuragi, Y. Oki, C. Scholz, S. Akai, H. Gröger, *Chem. Commun.* **2020**, *56*, 2885–2888.
- [21] S. Wuyts, J. Wahlen, P. A. Jacobs, D. E. De Vos, *Green Chem.* **2007**, *9*, 1104–1108.
- [22] A. S. De Miranda, M. V. M. De Silva, F. C. Dias, S. P. De Souza, R. A. C. Leão, R. O. M. A. De Souza, *React. Chem. Eng.* **2017**, *2*, 375–381.
- [23] L. A. De Almeida, T. H. Marcondes, C. D. F. Milagre, H. M. S. Milagre, *ChemCatChem* **2020**, *12*, 2849–2858.
- [24] K. Engström, E. V. Johnston, O. Verho, K. P. J. Gustafson, M. Shakeri, C. W. Tai, J. E. Bäckvall, *Angew. Chem. Int. Ed.* **2013**, *52*, 14006–14010.
- [25] H. Cao, X. H. Zhu, D. Wang, Z. Sun, Y. Deng, X. F. Hou, D. Zhao, *ACS Catal.* **2015**, *5*, 27–33.
- [26] M. Zhang, R. Ettelaie, L. Dong, X. Li, T. Li, X. Zhang, B. P. Binks, H. Yang, *Nat. Commun.* **2022**, *13*, 475.
- [27] S. Akai, *Chem. Lett.* **2014**, *43*, 746–754.
- [28] M. Egi, K. Sugiyama, M. Saneto, R. Hanada, K. Kato, S. Akai, *Angew. Chem. Int. Ed.* **2013**, *52*, 3654–3658.
- [29] K. Sugiyama, Y. Oki, S. Kawanishi, K. Kato, T. Ikawa, M. Egi, S. Akai, *Catal. Sci. Technol.* **2016**, *6*, 5023–5030.
- [30] S. Kawanishi, S. Oki, D. Kundu, S. Akai, *Org. Lett.* **2019**, *21*, 2978–2982.
- [31] K. Higashio, S. Katsuragi, D. Kundu, N. Adebar, C. Plass, F. Kühn, H. Gröger, S. Akai, *Eur. J. Org. Chem.* **2020**, 1961–1967.
- [32] I. Tsuchimochi, S. Hori, Y. Takeuchi, M. Egi, T. O. Satoh, K. Kanomata, T. Ikawa, S. Akai, *Synlett* **2021**, *32*, 822–828.

- [33] S. Horino, T. Nishio, S. Kawanishi, S. Oki, K. Nishihara, T. Ikawa, K. Kanomata, K. Wagner, H. Gröger, S. Akai, *Chem. Eur. J.* **2022**, *28*, e202202437.
- [34] M. Pera-Titus, L. Leclercq, J. M. Clacens, F. De Campo, V. Nardello-Rataj, *Angew. Chem. Int. Ed.* **2015**, *54*, 2006–2021.
- [35] A. M. B. Rodriguez, B. P. Binks, *Soft Matter* **2020**, *16*, 10221–10243.
- [36] L. Ni, C. Yu, Q. Wei, D. Liu, J. Qiu, *Angew. Chem. Int. Ed.* **2022**, *61*, e202115885.
- [37] H. Yang, L. Fu, L. Wei, J. Liang, B. P. Binks, *J. Am. Chem. Soc.* **2015**, *137*, 1362–1371.
- [38] B. P. Binks, *Curr. Opin. Colloid Interface Sci.* **2002**, *7*, 21–41.
- [39] L. Wei, M. Zhang, X. Zhang, H. Xin, H. Yang, *ACS Sustain. Chem. Eng.* **2016**, *4*, 6838–6843.

Supporting Information

Table of Contents

1. General information.....	14
2. Preparation and characterization of silica nanoparticles	14
3. Preparation and microscopic observation of Pickering emulsions	15
4. Racemization in Pickering emulsions	15
5. Racemization of (<i>R</i>)-1a catalyzed by V-MPS4	16
6. Kinetic resolution in Pickering emulsions	17
7. Substrate synthesis	18
8. Dynamic kinetic resolution in Pickering emulsions.....	19
9. NMR spectra	26
10. HPLC spectra	45

1. General information

^1H and ^{13}C NMR spectra were measured on a JEOL JMN-ECS300 instrument (^1H : 300 MHz, ^{13}C : 75 MHz). ^2H NMR spectrum was measured on a JEOL-ECA500 instrument (^1H : 500 MHz, ^2H : 77 MHz). Chemical shifts were reported in δ (ppm). HPLC analyses were carried out using a JASCO LC-2000 Plus system (HPLC pump: PU-2080, UV detector: MD-2018) equipped with a chiral stationary phase column (4.6 \times 250 mm). Optical rotations were measured on a JASCO P-1020 polarimeter. Mass spectrum was measured on a JEOL JMS-S3000 (MALDI) with a time of flight (TOF) mass analyzer.

All reagents were purchased from Tokyo Chemical Industry Co., Ltd. (Tokyo, Japan), FUJIFILM Wako Chemical Co., Ltd. (Osaka, Japan), NACALAI TESQUE, INC. (Kyoto, Japan), and Merck Co., LLC (U.S.A.), and used without further purification. Flash chromatography was performed on silica gel 60N (particle size 40–50 μm) purchased from Kanto Chemical Co., Inc. (Tokyo, Japan)

2. Preparation and characterization of silica nanoparticles

Silica nanoparticles were prepared according to the literature method with a slight modification.^[1,2] In brief, a mixture of EtOH (200 mL), deionized water (50 mL), aq. 27% NH_3 (11.2 mL), and $\text{Si}(\text{OEt})_4$ (8.32 g) were stirred 12 h at room temperature. The formed nanoparticles were collected by centrifugation at 12,000 rpm for 5 min (KUBOTA 6200). The precipitate was washed by deionized water for 3 times, and then EtOH for 2 times by centrifugation. Then the precipitate was dried overnight at 120°C under vacuum (5 mmHg).

Hydrophobic modification of the silica nanoparticles was conducted according to the literature method.^[1] The dried silica nanoparticles (1.0 g), $\text{MeSi}(\text{OMe})_3$ (3.0 mmol) and Et_3N (3.0 mmol) were added to anhydrous toluene (6 mL), and the resultant suspension was refluxed with vigorous stirring for 4 h under argon atmosphere. After that, the suspension was centrifuged at 12,000 rpm for 10 min, and the precipitate was washed by EtOH for 5 times. The resultant precipitate was dried at 60°C overnight under vacuum (5 mmHg).

Scanning electron microscopy (SEM) was performed using a JEOL JSM-F100 microscope, operated at an accelerating voltage of 10 kV and working distance of 4 mm. The samples were coated by osmium prior to observation (5 nm thickness).

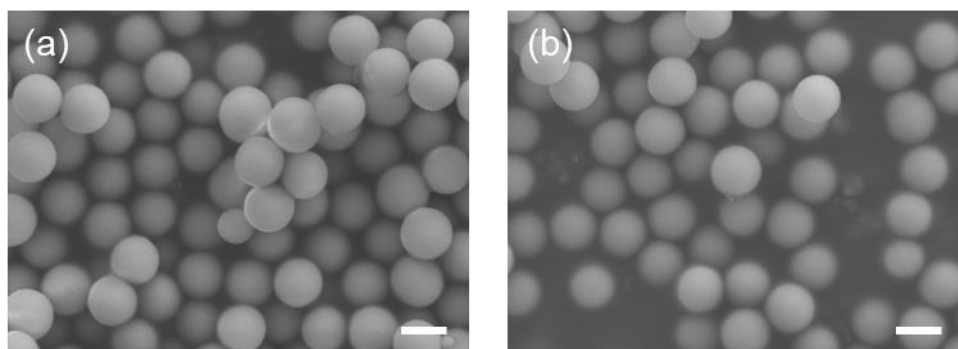


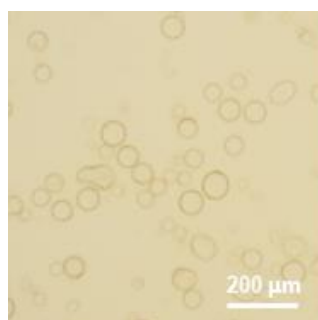
Figure S1. SEM images of (a) unmodified and (b) methyl-modified silica nanoparticles. Scale bar: 400 nm.

3. Preparation and microscopic observation of Pickering emulsions

Methyl-modified silica nanoparticles (30 mg) was added to a screw-capped vial (ϕ 15 mm) containing 1.0 M aq. H_2SO_4 (0.30 mL), and *n*-octane (1.0 mL). The mixture was homogenized at 20,000 rpm for 90 sec using a T10 basic ULTRA-TURRAX homogenizer (IKA) equipped with a S10N-5G Dispersing tool. The prepared emulsion droplets were observed using an Olympus FSX100 optical microscope (Table S1, Entry 1). The droplet size distribution did not change significantly after incubation under the reaction conditions (Entry 2). The obtained images were analyzed by an image processing software (Image-J, version 1.53k) to measure the particle size distribution. For a fluorescent imaging, a solution of fluorescein isothiocyanate-dextran (FITC-dextran, 4 kDa, 0.05 M phosphate buffer solution, Chondrex) in deionized water (6 μM) was used as the aqueous phase.

Table S1. Size of emulsion droplets

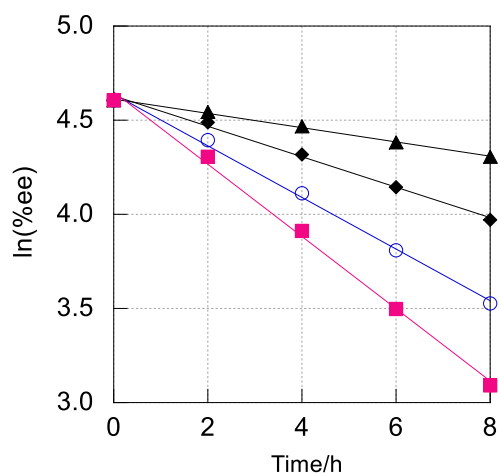
Entry	Observation	Droplet size/ μm
1	after emulsification	56.5 ± 12.8
2	after incubation for 22 h at 50°C	43.9 ± 13.9



A representative microscopic image of Entry 2.
See Figure 1 for the image of Entry 1.

4. Racemization in Pickering emulsions

Experimental procedure: A Pickering emulsion was prepared in a screw-capped vial (ϕ 15 mm) by mixing methyl-modified silica nanoparticles (30 mg), aqueous acid solution (0.30 mL), and *n*-octane (1.0 mL) at 20,000 rpm for 90 sec using a homogenizer. After the supernatant organic layer was removed, *n*-octane (0.60 mL) containing (*R*)-**1a** (0.10 mmol) was gently added to the vial. The vial was stood in an incubator (YAMATO IC101W), and the reaction was monitored by taking aliquot samples from the supernatant, which were analyzed using chiral HPLC (DAICEL CHIRALPAK IJ-3, Hexane/*i*-PrOH = 95/5, 1.0 mL/min, 220 nm, 30°C).



Conditions	k_{rac}/h^{-1}	$t_{1/2}/h$
1.0 M H ₂ SO ₄ , 50°C	0.1845	3.76
1.0 M HCl, 50°C	0.1318	5.26
0.5 M H ₂ SO ₄ , 50°C	0.0770	9.00
1.0 M H ₂ SO ₄ , 35°C	0.0369	18.78

Figure S2. Log plot for racemization time course of (*R*)-**1a**: 1.0 M H₂SO₄ at 50°C (■); 1.0 M HCl at 50°C (○); 0.5 M H₂SO₄ at 50°C (◆); 1.0 M H₂SO₄ at 35°C (▲).

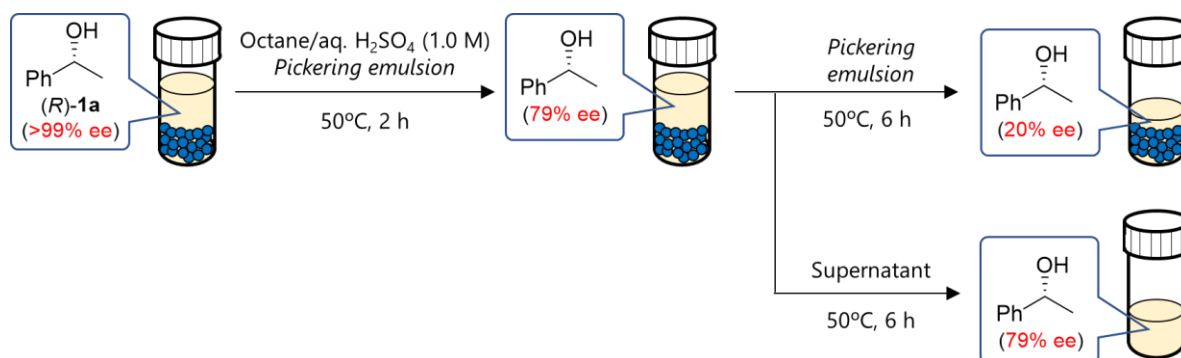


Figure S3. Racemization of (*R*)-**1a** in a Pickering emulsion and in the supernatant.

5. Racemization of (*R*)-**1a** catalyzed by V-MPS4

The racemization reaction conducted using (*R*)-**1a** (0.10 mmol) and V-MPS4 (4.5 mg, containing 0.22 mmol/g of vanadium) in anhydrous solvents (1.0 mL) at 50°C for 8 h. The racemization did not proceed in all cases (Table S2).

Table S2. Racemization of (*R*)-**1a** catalyzed by V-MPS4

Entry	Solvent	%ee of 1a after 8 h
1	MeCN	99
2	ClCH ₂ CH ₂ Cl	99
3	<i>i</i> -PrOH	99
4	octane	99

6. Kinetic resolution in Pickering emulsions

Experimental procedure of kinetic resolution: A Pickering emulsion was prepared in a screw-capped vial (ϕ 15 mm) by mixing methyl-modified silica nanoparticles (30 mg), deionized water (0.30 mL), and *n*-octane (1 mL) at 20,000 rpm for 90 sec using a homogenizer. After the supernatant organic layer was removed, *n*-octane (0.60 mL) containing (\pm)-**1a** (0.10 mmol) and vinyl decanoate (**2b**; 0.20 mmol, 2.0 eq) was gently added to the vial. Anhydrous magnesium sulfate (150 mg) was placed on top of the emulsion to cover the droplets, followed by addition of CAL-B (2.0 mg). The vial was stood in an incubator at 50°C without stirring. The reaction was monitored by taking aliquot samples from the supernatant, which were analyzed to determine the yield of **3ab** by gas chromatography (SHIMADZU GC-2014 Gas chromatograph system) equipped with an Inert Cap 17 capillary column (0.18 mm x 20 m, GL Science) using *n*-dodecane as an internal standard.

Water content measurement (Figure S4): The water content in the organic phase in a Pickering emulsion was measured by Karl-Fischer titration using a DL32 Karl Fisher coulometer (Mettler Toledo). The water content of the organic phase immediately after emulsification was 109 ppm, indicating that the organic phase was saturated with water. The supernatant was then removed, an anhydrous organic solvent was added to the remaining emulsion, and the water content of the organic phase was measured again after 1 h incubation at room temperature. This process was repeated three times, and the water content in each measurement was 82, 86, and 78 ppm. This result suggests that when water is consumed in the organic phase, it was constantly supplied from the emulsion droplets due to the equilibrium. When magnesium sulfate was added as a dehydrating reagent on the emulsion, the water content in the organic phase was significantly dropped and kept below 25 ppm even after 12 h.

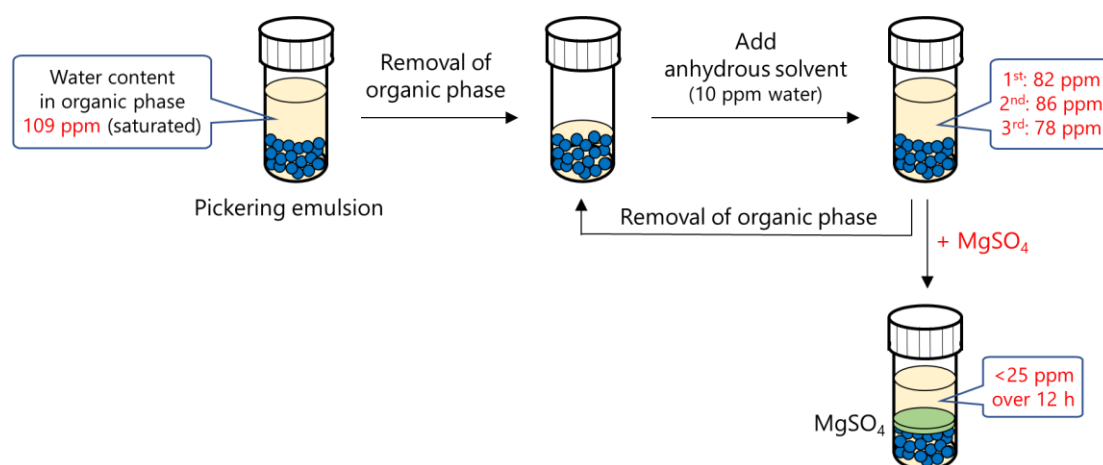
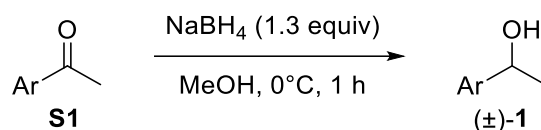


Figure S4. Water content in the supernatant of a Pickering emulsion.

7. Substrate synthesis

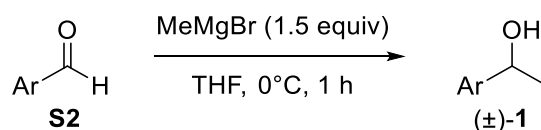
Alcohols **1a**, **1c**, **1d**, **1e**, **1k**, **1m**, **1n**, **1o**, and **1r** were commercially available. Alcohols **1f** and **1l** were synthesized by reduction of the corresponding ketones (General procedure A). Alcohols **1b**, **1g**, **1h**, **1i**, **1j**, **1p**, and **1q** were synthesized by methylation of the corresponding aldehydes (General procedure B). Deuterated compound **1e-d** was prepared by a modified General procedure A using NaBD₄. The ¹H NMR data of all the synthesized compounds matched with the literature data.

General procedure A:



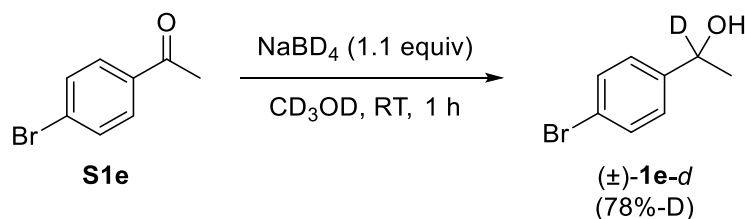
In a 100 mL two neck flask, ketone **S1** (10 mmol) was dissolved in methanol (50 mL), and sodium borohydride (13 mmol) was added to the mixture at 0°C. After stirring at room temperature for 1h, the reaction was quenched with saturated aq. NH₄Cl, and the resulting mixture was extracted with ethyl acetate (x3). The combined organic layer was dried over anhydrous sodium sulfate and evaporated in vacuo. The residue was purified by silica gel column chromatography to give (±)-**1**.

General procedure B:



In a 100 mL two neck flask, aldehyde **S2** (10 mmol) was dissolved in THF (50 mL), and methyl magnesium bromide (3.0 M in THF, 5 mL, 15 mmol) was added to the mixture at 0°C. After stirring at room temperature for 1h, the reaction was quenched with saturated aq. NH₄Cl, and the mixture was extracted with ethyl acetate (x3). The combined organic layer was dried over anhydrous sodium sulfate and evaporated in vacuo. The residue was purified by silica gel column chromatography to give (±)-**1**.

Preparation of (±)-**1e-d**:



In a 10-mL round-bottom flask, sodium borohydride-*d*₄ (1.1 mmol) was added to methanol-*d*₄ (3 mL) and the mixture was stirred at 0°C. After 15 min, ketone **S1e** (1.0 mmol) was added to the mixture at 0°C, and the resultant mixture was stirred at room temperature for 1 h. The reaction was quenched with saturated aq. NH₄Cl, and the reaction mixture was extracted with ethyl acetate (x3). The combined

organic layers were dried over anhydrous sodium sulfate, filtrated, and evaporated in vacuo. The residue was purified by silica gel column chromatography to give (\pm)-**1e-d** (95% yield, 78%-D content).

8. Dynamic kinetic resolution in Pickering emulsions

Large scale experiment (Figure S5): A Pickering emulsion was prepared in a 300-mL beaker by mixing methyl-modified silica nanoparticles (1.1 g), aqueous sulfuric acid (0.05 M, 11 mL), and *n*-octane (22 mL) at 20,000 rpm for 90 sec using a T10 basic ULTRA-TURRAX homogenizer (IKA) equipped with a S10N-8G Dispersing tool ($\phi = 8$ mm). After the supernatant organic layer was removed, *n*-octane (22 mL) containing (\pm)-**1j** (3.73 mmol, 500 mg) and vinyl decanoate (**2b**; 11.2 mmol, 2.4 mL, 3.0 eq) was gently added to the beaker. Anhydrous magnesium sulfate (5.5 g) was placed on top of the emulsion to cover the droplets, followed by addition of CAL-B (70.0 mg). The beaker was stood in an incubator at 50°C without stirring. After 21 h, the reaction mixture was diluted with diethyl ether and naturized by solid sodium hydrogen carbonate. The resulting mixture was dried over anhydrous magnesium sulfate, filtrated, and evaporated. The residue containing was purified by silica gel column chromatography to remove unreacted **1j**. The purified ester **3jb** was then subjected to methanolysis by adding methanol (60 mL) and sodium hydroxide (10 mmol, 0.40 g). After stirring for 1 h at room temperature, the reaction was quenched by adding saturated aq. NH_4Cl , and the mixture was extracted with diethyl ether (x 3 times). The combined organic layer was dried over anhydrous sodium sulfate, filtrated, and evaporated in vacuo. The residue was purified by silica gel column chromatography to give enantiomerically enriched alcohol (*R*)-**1j** (460 mg, 92% isolated yield, 98% ee).

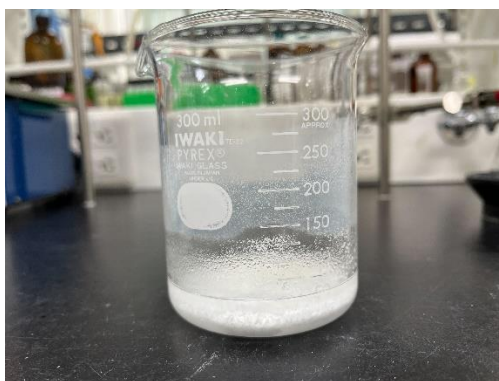
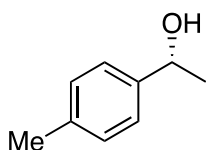
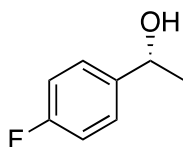


Figure S5. Large scale DKR of (\pm)-**1j** (3.7 mmol) in a Pickering emulsion

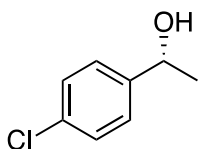


(*R*)-1-(*p*-Tolyl)ethanol (1b**)^[3]:** a colorless oil; HPLC analysis DAICEL CHIRALPAK IJ-3 (Hexane/*i*-PrOH = 98/2, 1.0 mL/min, 220 nm, 30°C), 13.71 min (*minor*), 15.06 min (*major*); >99% ee;

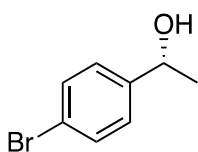
optical rotation $[\alpha]_{\text{D}}^{25} = +53.3$ (c 0.6, CHCl_3) (lit.^[3] $[\alpha]_{\text{D}}^{25} = +41.00$ (c 1.0, CHCl_3), 90% ee, *R*); ^1H NMR (300 MHz, CDCl_3) δ 7.27 (d, $J = 7.9$ Hz, 2H), 7.16 (d, $J = 7.9$ Hz, 2H), 4.88 (qd, $J = 6.3, 2.5$ Hz, 1H), 2.35 (s, 3H), 1.74 (brs, 1H), 1.49 (d, $J = 6.3$ Hz, 3H); ^{13}C NMR (75 MHz, CDCl_3) δ 143.0, 137.3, 129.3, 125.5, 70.4, 25.2, 21.2.



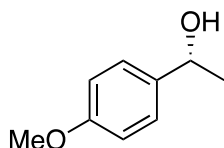
(*R*)-1-(*p*-Fluorophenyl)ethanol (1c)^[3]: a colorless oil; HPLC analysis DAICEL CHIRALPAK IJ-3 (Hexane/*i*-PrOH = 98/2, 1.0 mL/min, 220 nm, 30°C), 14.01 min (*minor*), 15.03 min (*major*); >99% ee; optical rotation $[\alpha]_{\text{D}}^{25} = +53.4$ (c 0.7 CHCl_3) (lit.^[3] $[\alpha]_{\text{D}}^{25} = +39.97$ (c 1.0, CHCl_3), 86% ee, *R*); ^1H NMR (300 MHz, CDCl_3) δ 7.38-7.31 (m, 2H), 7.07-6.99 (m, 2H), 4.90 (q, $J = 6.5$ Hz, 1H), 1.78 (s, 1H), 1.48 (d, $J = 6.5$ Hz, 3H); ^{13}C NMR (75 MHz, CDCl_3) δ 162.2 (d, $J = 245.6$ Hz), 141.6, 127.2 (d, $J = 8.0$ Hz), 115.3 (d, $J = 21.7$ Hz), 69.9, 25.4.



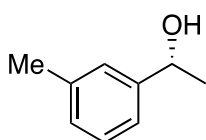
(*R*)-1-(*p*-Chlorophenyl)ethanol (1d)^[4]: a colorless oil; HPLC analysis DAICEL CHIRALPAK IJ-3 (Hexane/*i*-PrOH = 98/2, 1.0 mL/min, 220 nm, 30°C), 15.75 min (*minor*), 16.99 min (*major*); 96% ee; optical rotation $[\alpha]_{\text{D}}^{25} = +35.9$ (c 0.7, CHCl_3) (lit.^[4] $[\alpha]_{\text{D}}^{28} = +36.1$ (c 0.93, CHCl_3), 76% ee, *R*); ^1H NMR (300 MHz, CDCl_3) δ 7.31 (s, 4H), 4.89 (q, $J = 6.3$ Hz, 1H), 1.84 (brs, 1H), 1.48 (d, $J = 6.3$ Hz, 3H); ^{13}C NMR (75 MHz, CDCl_3) δ 144.4, 133.2, 128.7, 126.9, 69.9, 25.4.



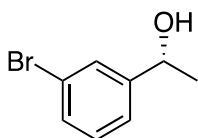
(*R*)-1-(*p*-Bromophenyl)ethanol (1e)^[4]: a pale-yellow solid; HPLC analysis DAICEL CHIRALPAK IJ-3 (Hexane/*i*-PrOH = 98/2, 1.0 mL/min, 220 nm, 30°C), 17.89 min (*minor*), 19.30 min (*major*); 99% ee; optical rotation $[\alpha]_{\text{D}}^{25} = +29.0$ (c 1.0, CHCl_3) (lit.^[4] $[\alpha]_{\text{D}}^{27} = +28.2$ (c 0.88, CHCl_3), 78% ee, *R*); ^1H NMR (300 MHz, CDCl_3) δ 7.47 (d, $J = 8.6$ Hz, 2H), 7.25 (d, $J = 8.6$ Hz, 2H), 4.87 (q, $J = 6.3$ Hz, 1H), 1.85 (brs, 1H), 1.47 (d, $J = 6.3$ Hz, 3H); ^{13}C NMR (75 MHz, CDCl_3) δ 144.9, 131.7, 127.3, 121.3, 69.9, 25.4.



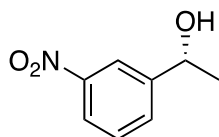
(R)-1-(*p*-Methoxyphenyl)ethanol (1f)^[31]: a colorless oil; HPLC analysis DAICEL CHIRALPAK IJ-3 (Hexane/*i*-PrOH = 95/5, 1.0 mL/min, 220 nm, 30°C), 16.01 min (*minor*), 17.04 min (*major*); >99% ee; optical rotation $[\alpha]_{\text{D}}^{25} = +46.2$ (*c* 1.4, CHCl₃) (lit.^[31] $[\alpha]_{\text{D}}^{25} = +40.00$ (*c* 1.0, CHCl₃), 96% ee, *R*); ¹H NMR (300 MHz, CDCl₃) δ 7.30 (d, *J* = 8.6 Hz, 2H), 6.89 (d, *J* = 8.6 Hz, 2H), 4.86 (qd, *J* = 6.4, 3.2 Hz, 1H), 3.81 (s, 3H), 1.72 (d, *J* = 3.2 Hz, 1H), 1.48 (d, *J* = 6.4 Hz, 3H); ¹³C NMR (75 MHz, CDCl₃) δ 159.1, 138.1, 126.8, 114.0, 70.1, 55.4, 25.1.



(R)-1-(*m*-Tolyl)ethanol (1g)^[31]: a colorless oil; HPLC analysis DAICEL CHIRALPAK IJ-3 (Hexane/*i*-PrOH = 98/2, 1.0 mL/min, 220 nm, 30°C), 11.77 min (*minor*), 13.15 min (*major*); 98% ee; optical rotation $[\alpha]_{\text{D}}^{25} = +2.7$ (*c* 0.1, CHCl₃) (lit.^[31] $[\alpha]_{\text{D}}^{25} = +38.70$ (*c* 1.0, CHCl₃), 92% ee, *R*); ¹H NMR (300 MHz, CDCl₃) δ 7.27-7.16 (m, 3H), 7.10 (d, *J* = 7.6 Hz, 1H), 4.87 (qd, *J* = 6.4, 3.0 Hz, 1H), 2.37 (s, 3H), 1.83 (d, *J* = 3.0 Hz, 1H), 1.49 (d, *J* = 6.4 Hz, 3H); ¹³C NMR (75 MHz, CDCl₃) δ 145.9, 138.2, 128.5, 128.3, 126.2, 122.5, 70.5, 25.2, 21.6.

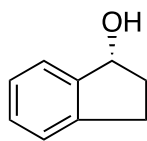


(R)-1-(*m*-Bromophenyl)ethanol (1h)^[31]: a colorless oil; HPLC analysis DAICEL CHIRALPAK IJ-3 (Hexane/*i*-PrOH = 95/5, 1.0 mL/min, 220 nm, 30°C), 8.44 min (*minor*), 9.84 min (*major*); 98% ee; optical rotation $[\alpha]_{\text{D}}^{25} = +36.8$ (*c* 0.7, CHCl₃) (lit.^[31] $[\alpha]_{\text{D}}^{25} = +25.23$ (*c* 1.0, CHCl₃), 86% ee, *R*); ¹H NMR (300 MHz, CDCl₃) δ 7.54 (t, *J* = 1.8 Hz, 1H), 7.40 (dt, *J* = 7.7, 1.8 Hz, 1H), 7.29 (dt, *J* = 7.7, 1.8 Hz, 1H), 7.22 (t, *J* = 7.7 Hz, 1H), 4.88 (qd, *J* = 6.4, 3.4 Hz, 1H), 1.84 (d, *J* = 3.4 Hz, 1H), 1.49 (d, *J* = 6.4 Hz, 3H); ¹³C NMR (75 MHz, CDCl₃) δ 148.2, 130.6, 130.3, 128.7, 124.2, 122.8, 69.9, 25.4.

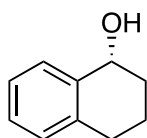


(R)-1-(*m*-Nitrophenyl)ethanol (1i)^[41]: a colorless solid; HPLC analysis DAICEL CHIRALPAK IE-3 (Hexane/*i*-PrOH = 95/5, 1.0 mL/min, 220 nm, 30°C), 17.88 min (*minor*), 18.88 min (*major*); 97% ee; optical rotation $[\alpha]_{\text{D}}^{25} = +37.0$ (*c* 1.1, CHCl₃) (lit.^[41] $[\alpha]_{\text{D}}^{27} = +26.3$ (*c* 0.6, CHCl₃), 79% ee, *R*); ¹H NMR (300 MHz, CDCl₃) δ 8.26 (t, *J* = 1.9 Hz, 1H), 8.15-8.12 (m, 1H), 7.72 (d, *J* = 7.9 Hz, 1H), 7.53 (t, *J* = 7.9 Hz, 1H), 5.03 (qd, *J* = 6.4, 3.9 Hz, 1H), 1.95 (d, *J* = 3.9 Hz, 1H), 1.55 (d, *J* = 5.4 Hz, 3H);

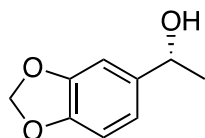
^{13}C NMR (75 MHz, CDCl_3) δ 148.4, 148.0, 131.7, 129.6, 122.5, 120.5, 69.5, 25.6.



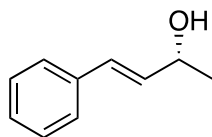
(R)-1-Indanol (1j)^[31]: a colorless solid; HPLC analysis DAICEL CHIRALPAK IC-3 (Hexane/*i*-PrOH = 98/2, 1.0 mL/min, 220 nm, 30°C), 15.04 min (*minor*), 17.67 min (*major*); >99% ee; optical rotation $[\alpha]_{\text{D}}^{25} = -22.0$ (*c* 0.6, CHCl_3) (lit.^[31] $[\alpha]_{\text{D}}^{25} = -23.97$ (*c* 1.0, CHCl_3), 96% ee, *R*); ^1H NMR (300 MHz, CDCl_3) δ 7.44-7.41 (m, 1H), 7.31-7.21 (m, 3H), 5.26 (q, *J* = 6.1 Hz, 1H), 3.07 (dq, *J* = 15.8, 4.5 Hz, 1H), 2.88-2.78 (m, 1H), 2.56-2.45 (m, 1H), 2.01-1.90 (m, 1H), 1.71 (brs, 1H); ^{13}C NMR (75 MHz, CDCl_3) δ 145.1, 143.5, 128.5, 126.9, 125.0, 124.3, 76.6, 36.1, 29.9.



(R)-1-Tetralol (1k)^[31]: a colorless solid; HPLC analysis DAICEL CHIRALPAK IJ-3 (Hexane/*i*-PrOH = 98/2, 1.0 mL/min, 220 nm, 30°C), 13.08 min (*minor*), 14.43 min (*major*); >99% ee; optical rotation $[\alpha]_{\text{D}}^{25} = -27.7$ (*c* 0.7, CHCl_3) (lit.^[31] $[\alpha]_{\text{D}}^{25} = -25.77$ (*c* 1.0, CHCl_3), 96% ee, *R*); ^1H NMR (300 MHz, CDCl_3) δ 7.46-7.41 (m, 1H), 7.25-7.17 (m, 2H), 7.13-7.08 (m, 1H), 4.79 (dd, *J* = 9.5, 5.3 Hz, 1H), 2.89-2.67 (m, 2H), 2.07-1.86 (m, 3H), 1.84-1.75 (m, 1H), 1.72 (d, *J* = 6.2 Hz, 1H); ^{13}C NMR (75 MHz, CDCl_3) δ 138.9, 137.2, 129.2, 128.8, 127.7, 126.3, 68.3, 32.4, 29.4, 18.9.

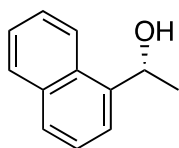


(R)-1-(Benzo[d][1,3]dioxol-5-yl)ethanol (1l)^[31]: a pale-yellow oil; HPLC analysis DAICEL CHIRAL-PAK IJ-3 (Hexane/*i*-PrOH = 95/5, 1.0 mL/min, 220 nm, 30°C), 15.98 min (*minor*), 17.31 min (*major*); 97% ee; optical rotation $[\alpha]_{\text{D}}^{25} = +31.2$ (*c* 1.5, CHCl_3) (lit.^[31] $[\alpha]_{\text{D}}^{25} = +38.70$ (*c* 1.0, CHCl_3), 93% ee, *R*); ^1H NMR (300 MHz, CDCl_3) δ 6.90 (d, *J* = 1.7 Hz, 1H), 6.84-6.75 (m, 2H), 5.95 (s, 2H), 4.82 (q, *J* = 6.4 Hz, 1H), 1.77 (s, 1H), 1.46 (d, *J* = 6.4 Hz, 3H); ^{13}C NMR (75 MHz, CDCl_3) δ 147.9, 147.0, 140.1, 118.8, 108.2, 106.2, 101.1, 70.4, 25.3.

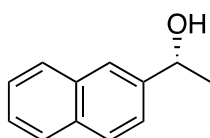


(R)-4-Phenyl-3-buten-2-ol (1m)^[51]: a colorless solid; HPLC analysis DAICEL CHIRALPAK IB N-3 (Hexane/*i*-PrOH = 90/10, 1.0 mL/min, 220 nm, 30°C), 8.34 min (*major*), 11.53 min (*minor*); 98% ee; optical rotation $[\alpha]_{\text{D}}^{25} = +20.0$ (*c* 0.6, CHCl_3) (lit.^[51] $[\alpha]_{\text{D}}^{25} = +31.8$ (*c* 0.5, CHCl_3), 94% ee, *R*); ^1H NMR (300 MHz, CDCl_3) δ 7.40-7.29 (m, 4H), 7.26-7.22 (m, 1H), 6.57 (d, *J* = 16.1 Hz, 1H), 6.27 (dd,

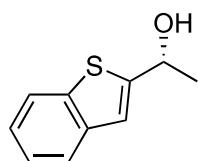
$J = 16.1, 6.3$ Hz, 1H), 4.55-4.45 (m, 1H), 1.57 (s, 1H), 1.38 (d, $J = 6.2$ Hz, 3H); ^{13}C NMR (75 MHz, CDCl_3) δ 136.8, 133.6, 129.6, 128.7, 127.8, 126.6, 69.1, 23.6.



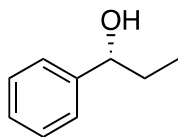
(R)-1-(1-Naphthyl)ethanol (1n)^[3]: a colorless solid; HPLC analysis DAICEL CHIRALPAK IC-3 (Hexane/*i*-PrOH = 95/5, 1.0 mL/min, 220 nm, 30°C), 8.67 min (*minor*), 10.35 min (*major*); 95% ee; optical rotation $[\alpha]_{\text{D}}^{25} = +24.6$ (c 1.0, CHCl_3) (lit.^[3] $[\alpha]_{\text{D}}^{25} = +58.63$ (c 1.0, CHCl_3), 90% ee, *R*); ^1H NMR (300 MHz, CDCl_3) δ 8.13 (d, $J = 7.6$ Hz, 1H), 7.90-7.87 (m, 1H), 7.79 (d, $J = 7.9$ Hz, 1H), 7.69 (d, $J = 6.9$ Hz, 1H), 7.56-7.46 (m, 3H), 5.70 (qd, $J = 6.4, 3.7$ Hz, 1H), 1.91 (d, $J = 3.7$ Hz, 1H), 1.68 (d, $J = 6.4$ Hz, 3H); ^{13}C NMR (75 MHz, CDCl_3) δ 141.5, 133.9, 130.4, 129.0, 128.1, 126.2, 125.7, 125.6, 123.3, 122.1, 67.3, 24.5.



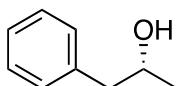
(R)-1-(2-Naphthyl)ethanol (1o)^[3]: a colorless solid; HPLC analysis DAICEL CHIRALPAK IJ-3 (Hexane/*i*-PrOH = 90/10, 1.0 mL/min, 220 nm, 30°C), 11.58 min (*minor*), 14.53 min (*major*); 87% ee; optical rotation $[\alpha]_{\text{D}}^{25} = +31.9$ (c 1.4, CHCl_3) (lit.^[3] $[\alpha]_{\text{D}}^{25} = +38.00$ (c 1.0, CHCl_3), 92% ee, *R*); ^1H NMR (300 MHz, CDCl_3) δ 7.86-7.82 (m, 4H), 7.53-7.44 (m, 3H), 5.08 (qd, $J = 6.5, 3.4$ Hz, 1H), 1.89 (d, $J = 3.4$ Hz, 1H), 1.59 (d, $J = 6.5$ Hz, 3H); ^{13}C NMR (75 MHz, CDCl_3) δ 143.3, 133.4, 133.0, 128.5, 128.1, 127.8, 126.3, 125.9, 123.94, 123.92, 70.7, 25.3.



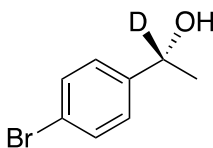
(R)-1-(benzo[*b*]thiophen-2-yl)ethanol (1p)^[6]: a colorless solid; HPLC analysis DAICEL CHIRALPAK IJ-3 (Hexane/*i*-PrOH = 90/10, 1.0 mL/min, 220 nm, 30°C), 12.96 min (*minor*), 14.91 min (*major*); 98% ee; optical rotation $[\alpha]_{\text{D}}^{25} = +30.5$ (c 1.0, CHCl_3) (lit.^[6] $[\alpha]_{\text{D}}^{24} = +22.9$ (c 2.89, CHCl_3), 93% ee, *R*); ^1H NMR (300 MHz, CDCl_3) δ 7.83-7.80 (m, 1H), 7.72 (dd, $J = 6.5, 2.1$ Hz, 1H), 7.37-7.27 (m, 2H), 7.20 (s, 1H), 5.25-5.18 (m, 1H), 2.06 (d, $J = 4.8$ Hz, 1H), 1.66 (d, $J = 6.2$ Hz, 3H); ^{13}C NMR (75 MHz, CDCl_3) δ 150.6, 139.7, 139.4, 124.4, 124.3, 123.6, 122.6, 119.6, 67.0, 25.2.



(R)-1-Phenyl-1-propanol (1q)^[3]: a colorless oil; HPLC analysis DAICEL CHIRALPAK IJ-3 (Hexane/*i*-PrOH = 98/2, 1.0 mL/min, 220 nm, 30°C), 11.41 min (*minor*), 12.17 min (*major*); 98% ee; optical rotation $[\alpha]_{\text{D}}^{25} = +7.3$ (*c* 0.1, CHCl₃) (lit.^[3] $[\alpha]_{\text{D}}^{25} = +38.07$ (*c* 0.5, CHCl₃), 89% ee, *R*); ¹H NMR (300 MHz, CDCl₃) δ 7.38-7.25 (m, 5H), 4.60 (td, *J* = 6.7, 3.4 Hz, 1H), 1.91-1.68 (m, 3H), 0.92 (t, *J* = 7.4 Hz, 3H); ¹³C NMR (75 MHz, CDCl₃) δ 144.7, 128.5, 127.6, 126.1, 76.2, 32.0, 10.3.



(R)-1-Phenyl-2-propanol (1r)^[4]: a colorless oil; HPLC analysis DAICEL CHIRALPAK IE-3 (Hexane/*i*-PrOH = 98/2, 1.0 mL/min, 220 nm, 30°C), 10.77 min (*minor*), 11.97 min (*major*); 97% ee; optical rotation $[\alpha]_{\text{D}}^{25} = -24.0$ (*c* 0.8, CHCl₃) (lit.^[4] $[\alpha]_{\text{D}}^{26} = -25.7$ (*c* 0.74, CHCl₃), 64% ee, *R*); ¹H NMR (300 MHz, CDCl₃) δ 7.35-7.29 (m, 2H), 7.27-7.21 (m, 3H), 4.13-4.00 (m, 1H), 2.80 (dd, *J* = 13.4, 4.8 Hz, 1H), 2.69 (dd, *J* = 13.4, 7.9 Hz, 1H), 1.54 (s, 1H), 1.25 (d, *J* = 6.2 Hz, 3H); ¹³C NMR (75 MHz, CDCl₃) δ 138.6, 129.5, 128.6, 126.5, 68.9, 45.8, 22.8.



(R)-1-(*p*-Bromophenyl)ethan-1-d-1-ol (1e-d) [79%-D]: a pale-yellow solid; HPLC analysis DAICEL CHIRALPAK IJ-3 (Hexane/*i*-PrOH = 95/5, 1.0 mL/min, 220 nm, 30°C), 9.68 min (*minor*), 10.50 min (*major*); 99% ee; optical rotation $[\alpha]_{\text{D}}^{25} = +16.3$ (*c* 0.6, CHCl₃); ¹H NMR (300 MHz, CDCl₃) δ 7.49-7.46 (m, 2H), 7.28-7.24 (m, 2H), 4.91-4.84 (m, 0.21H), 1.80-1.78 (m, 1H), 1.49-1.46 (m, 3H); ¹³C NMR (75 MHz, CDCl₃) δ 144.8, 131.7, 127.3, 121.3, 69.9 (CHOH), 69.5 (t, *J* = 22.0 Hz, CDOH), 25.4 (CH(OH)CH₃), 25.2 (CD(OH)CH₃); ²H NMR (77 MHz, CHCl₃) δ 4.83 (brs); HRMS (EI) *m/z* calcd for C₈H₈DOBr [M⁺]: 200.9895; found 200.9897.

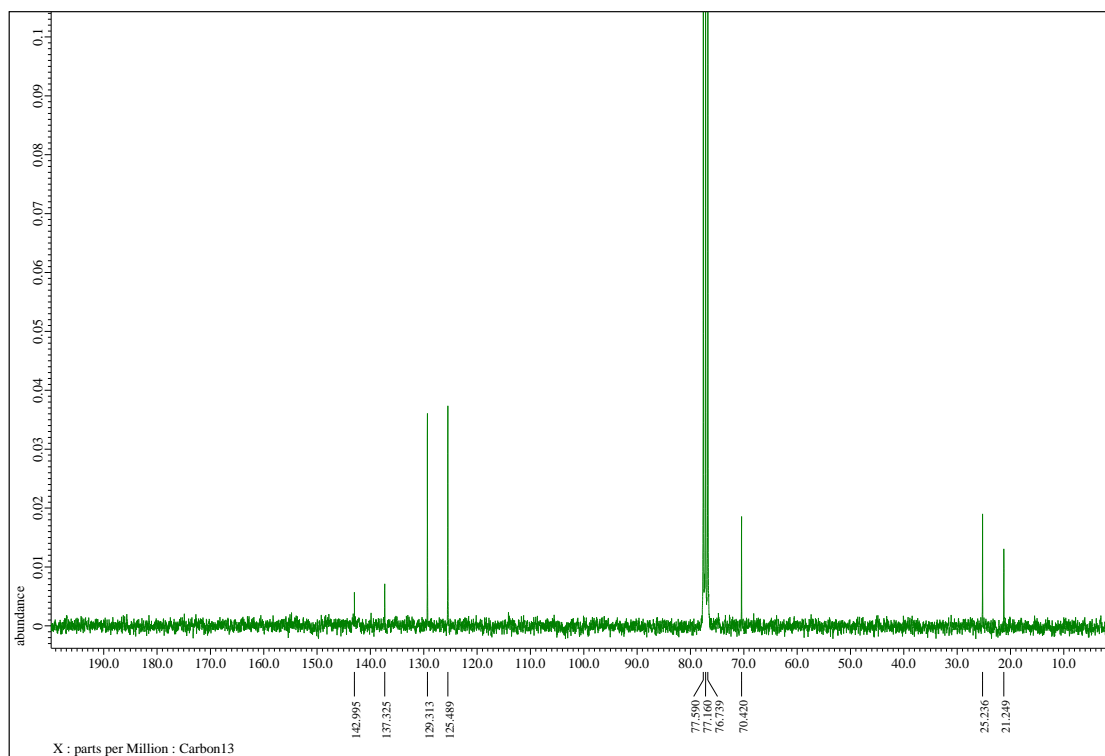
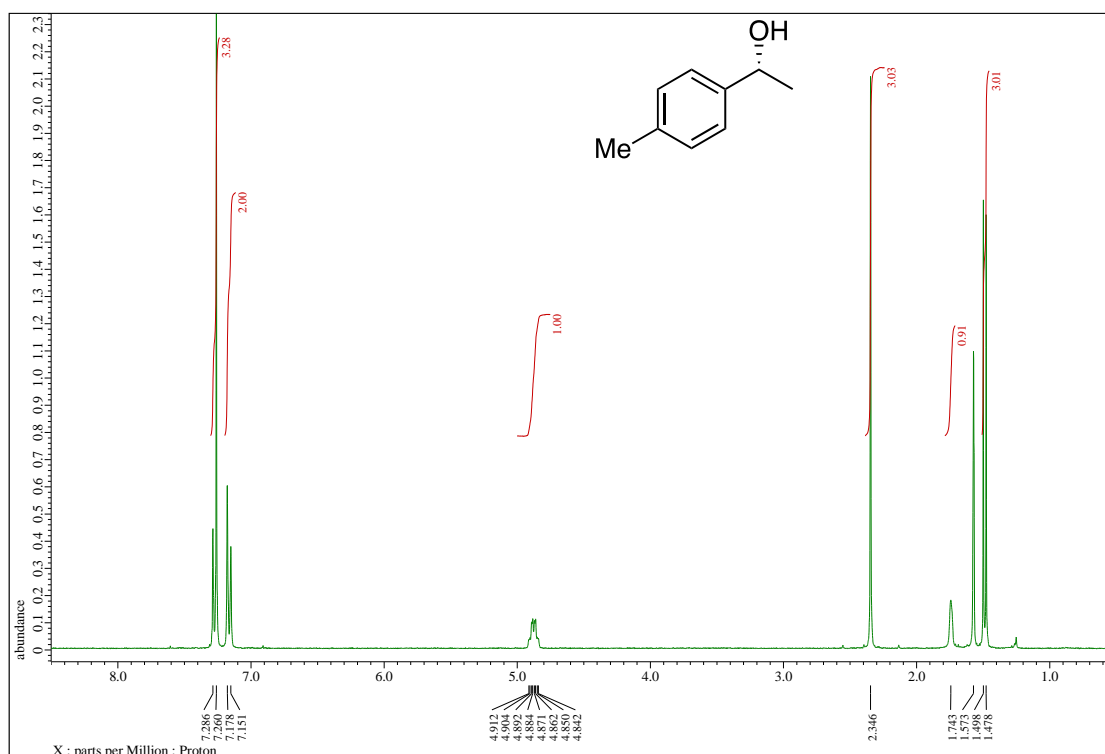
References

- [1] H. Yang, L. Fu, L. Wei, J. Liang, B. P. Binks, *J. Am. Chem. Soc.* **2015**, *137*, 1362–1371.
- [2] W. Stöber, A. Fink, E. Bohn, *J. Colloid Interface Sci.* **1968**, *26*, 62–69.
- [3] L. Zhang, Y. Tang, Z. Han, K. Ding, *Angew. Chem. Int. Ed.* **2019**, *58*, 4973–4977.
- [4] B. Gao, X. Feng, W. Meng, H. Du, *Angew. Chem. Int. Ed.* **2020**, *59*, 4498 – 4504.
- [5] S.-Q. Yang, A.-J. Han, Y. Liu, X.-Y. Tang, G.-Q. Lin, Z.-T. He, *J. Am. Chem. Soc.* **2023**, *145*, 3915–3925.

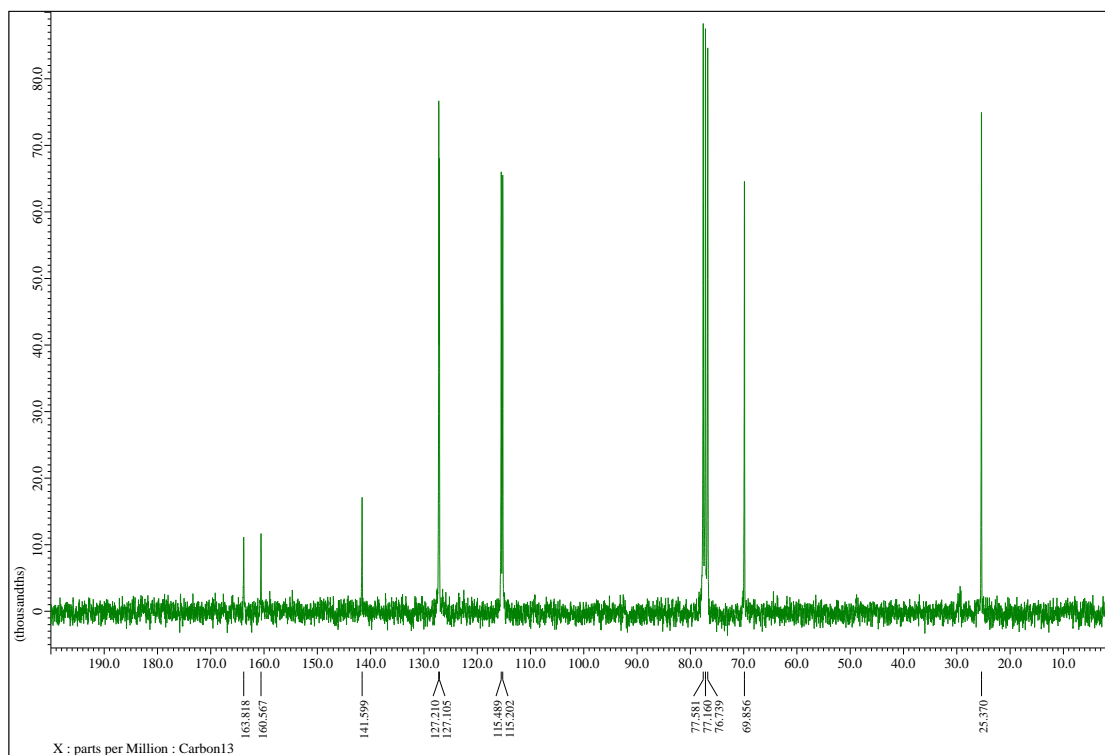
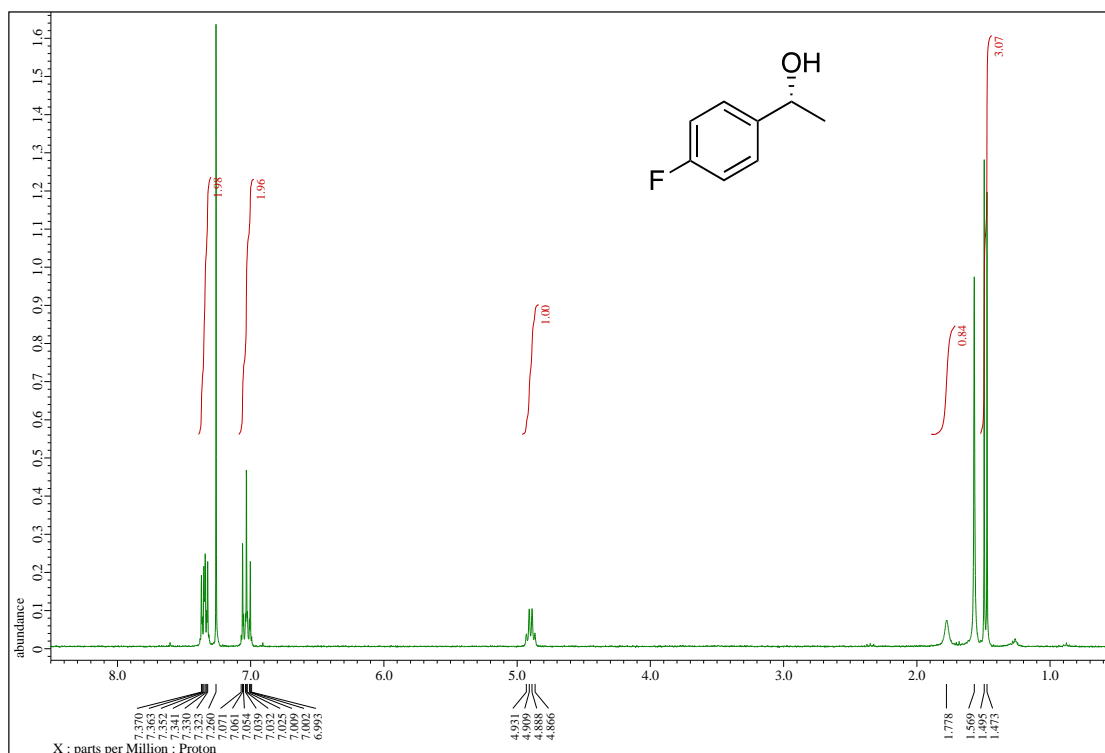
[6] X. Ren, G. Li, S. Wei, H. Du, *Org. Lett.* **2015**, *17*, 990–993.

9. NMR spectra

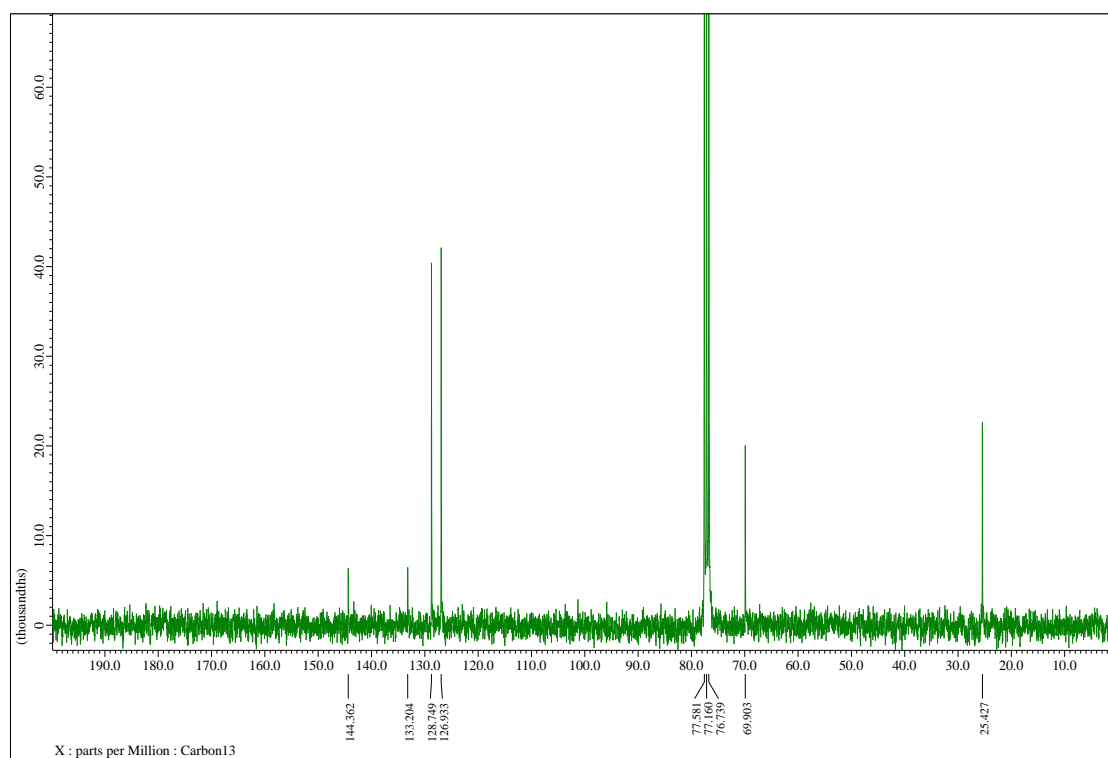
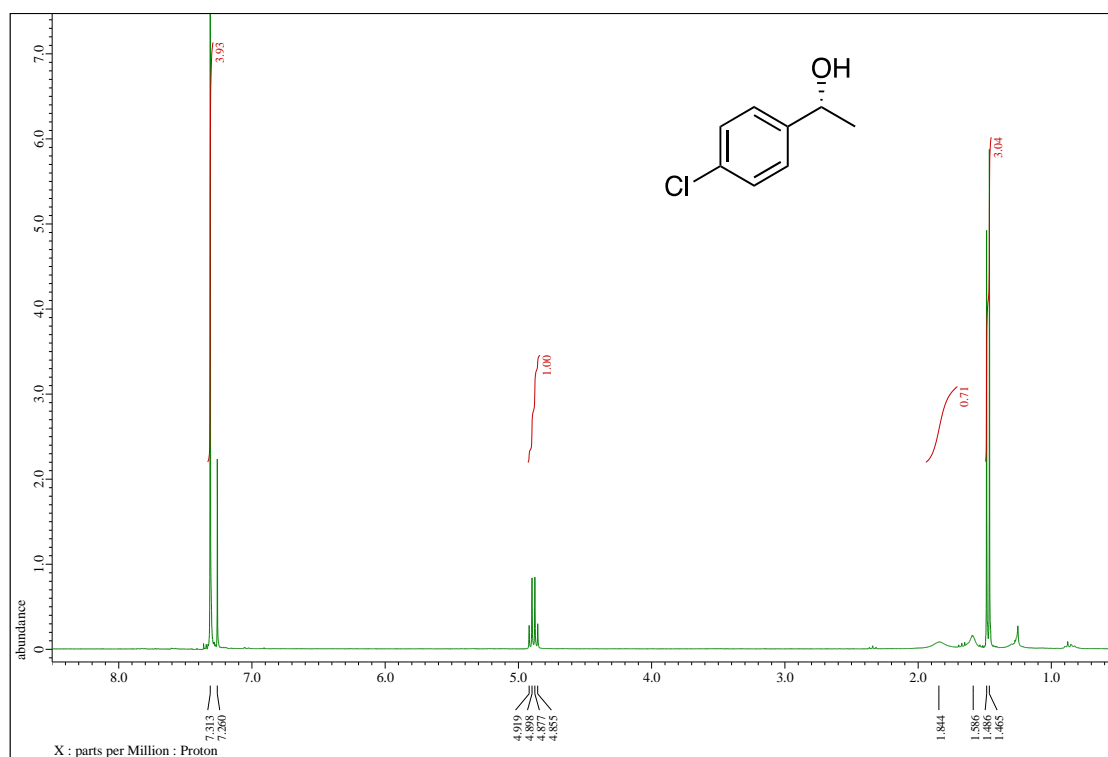
(*R*)-1-(*p*-Tolyl)ethanol (1b)



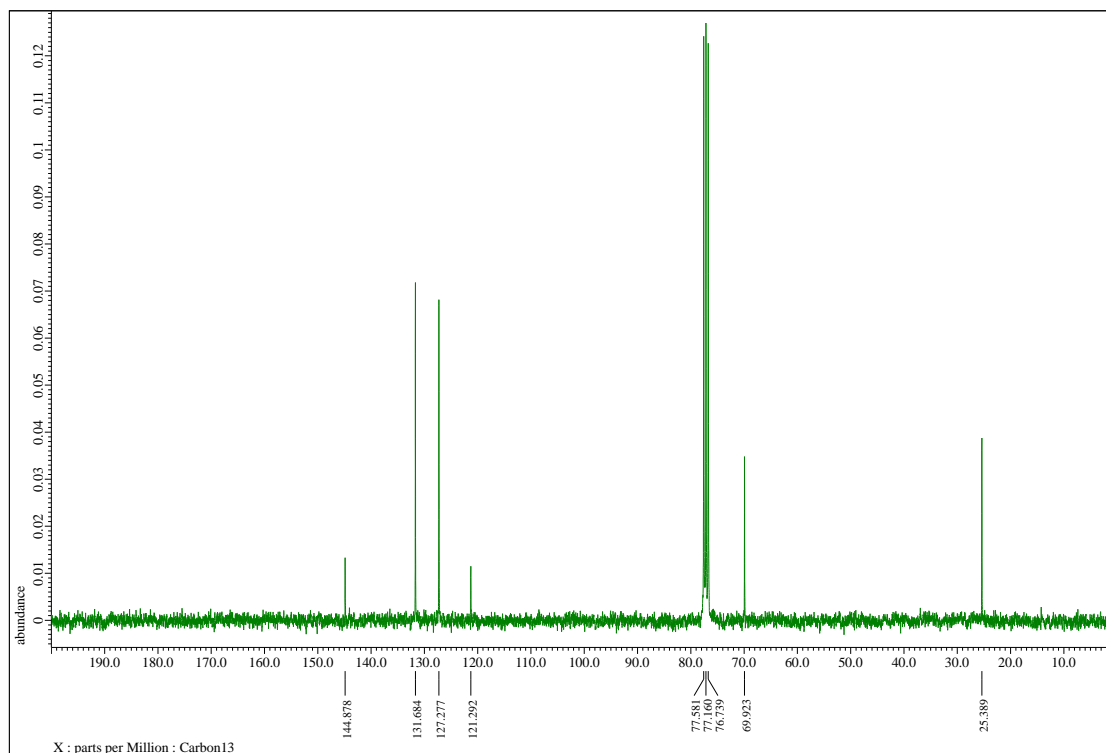
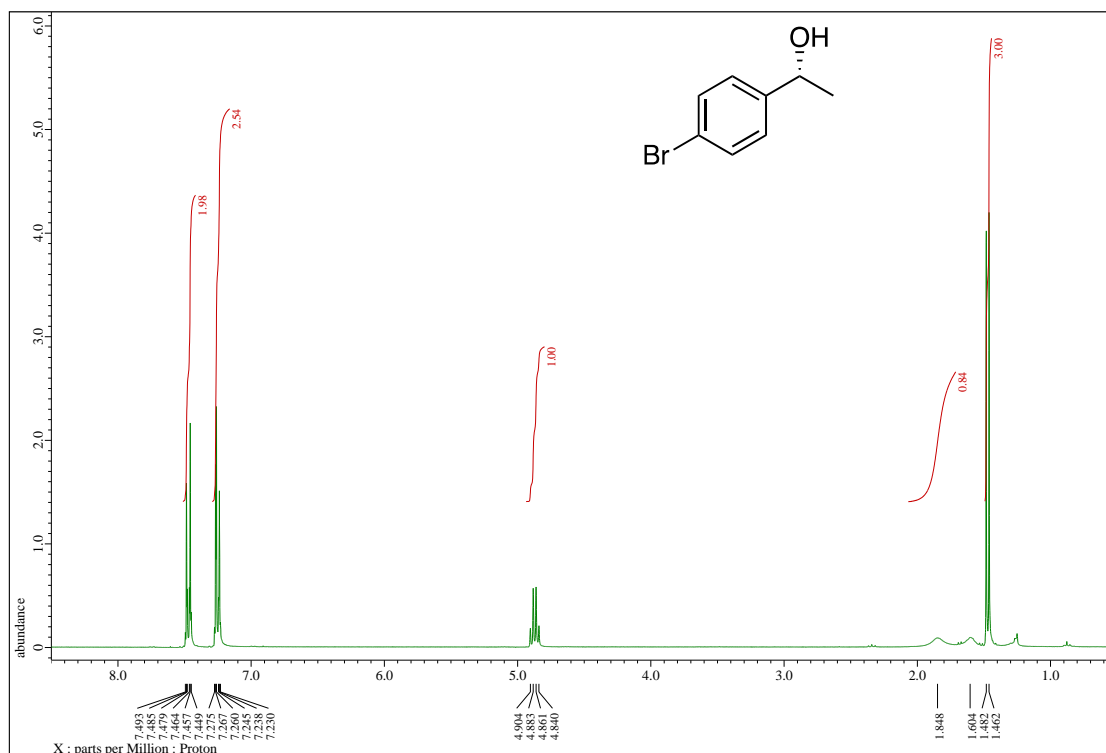
(R)-1-(p-Fluorophenyl)ethanol (1c)



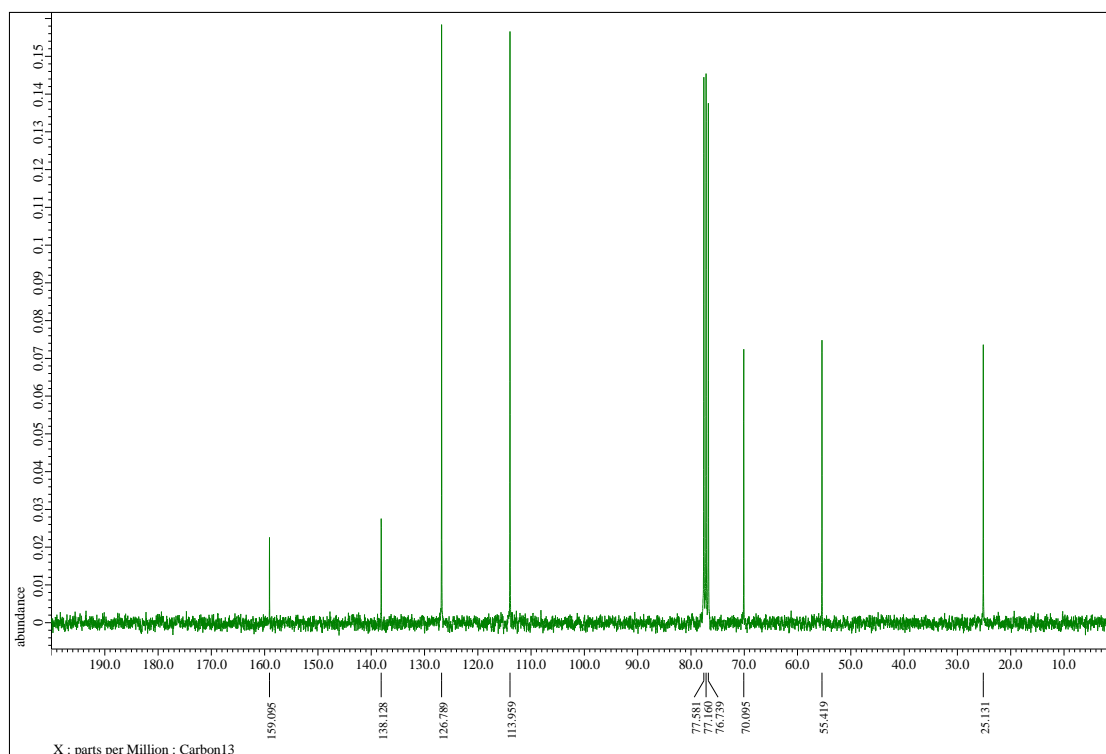
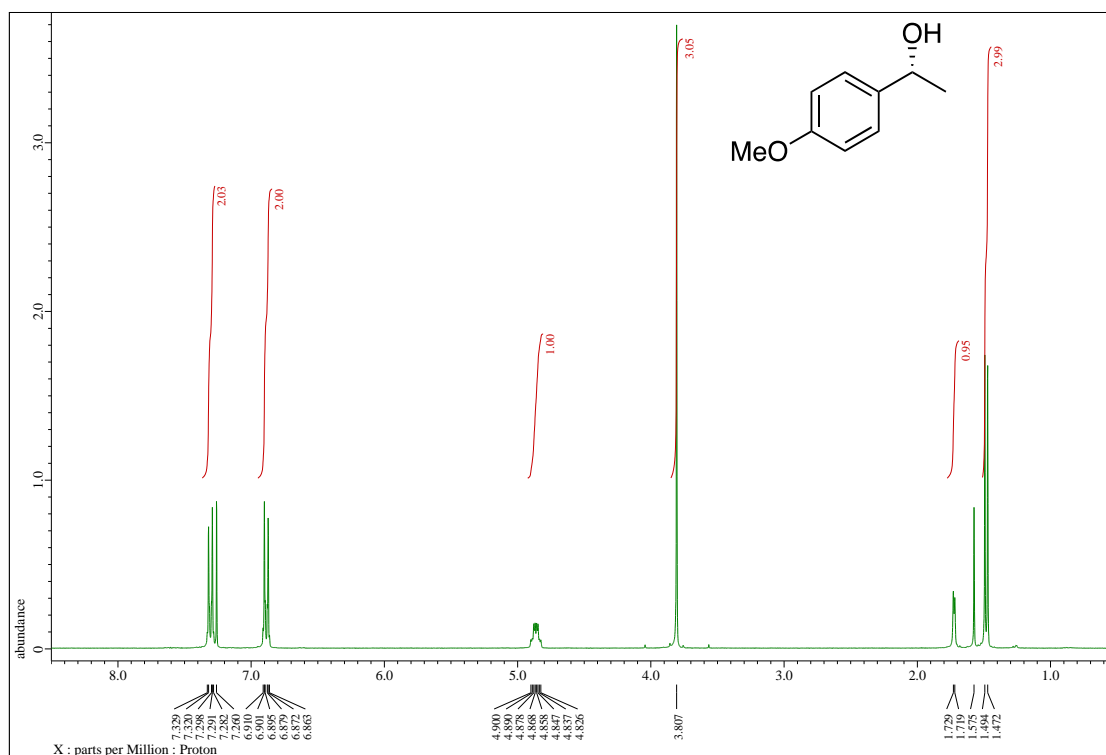
(R)-1-(p-Chlorophenyl)ethanol (1d)



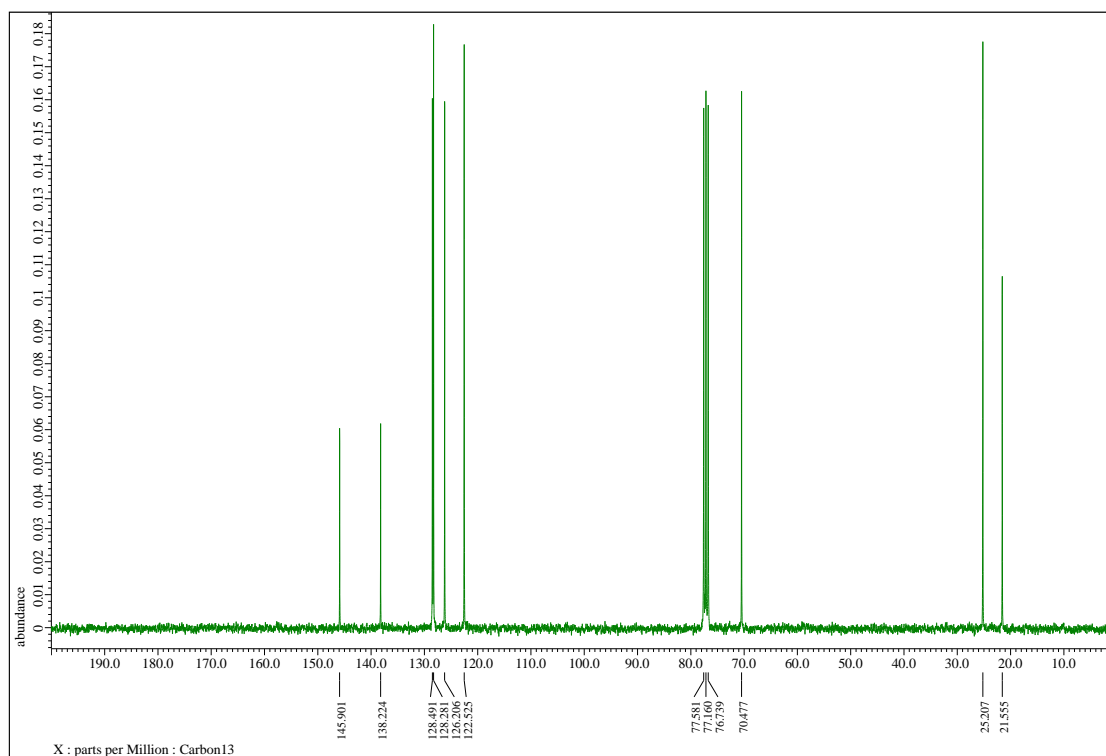
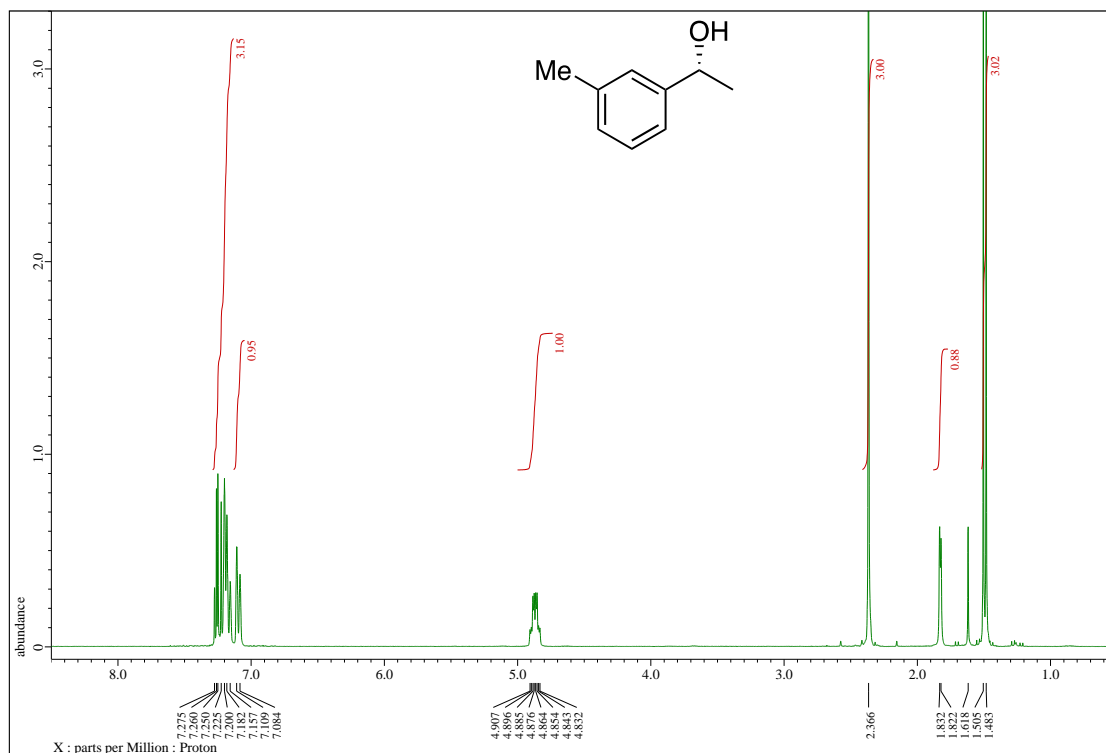
(R)-1-(p-Bromophenyl)ethanol (1e)



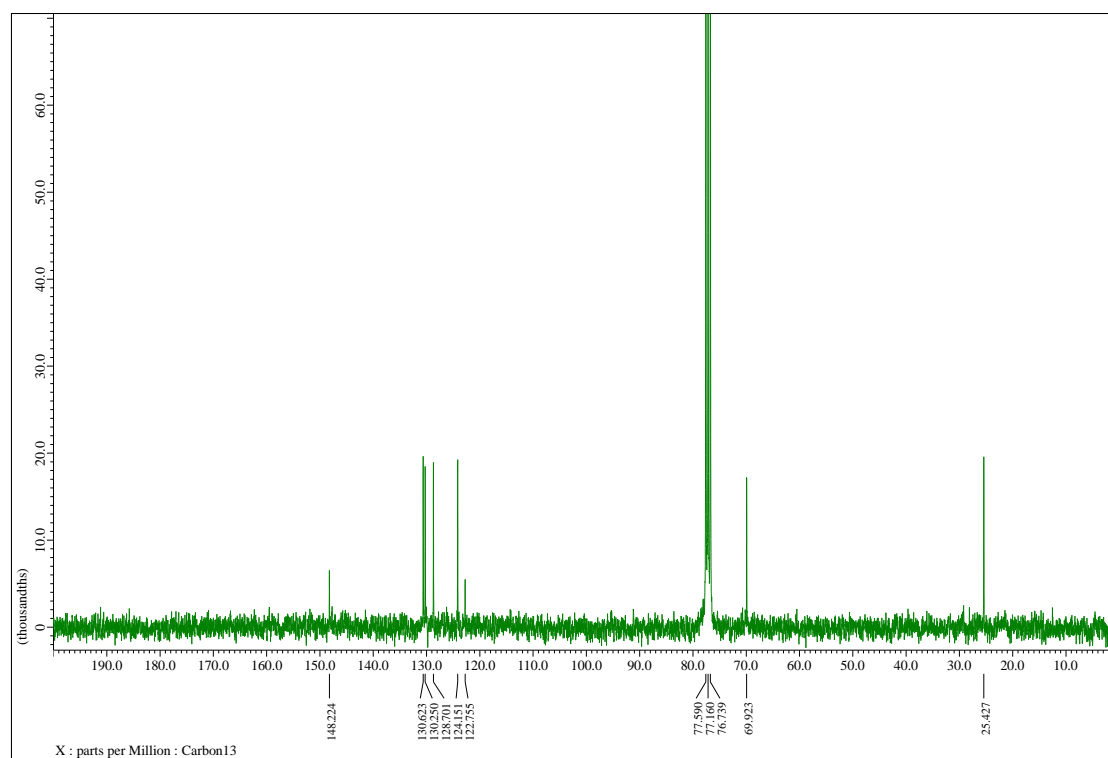
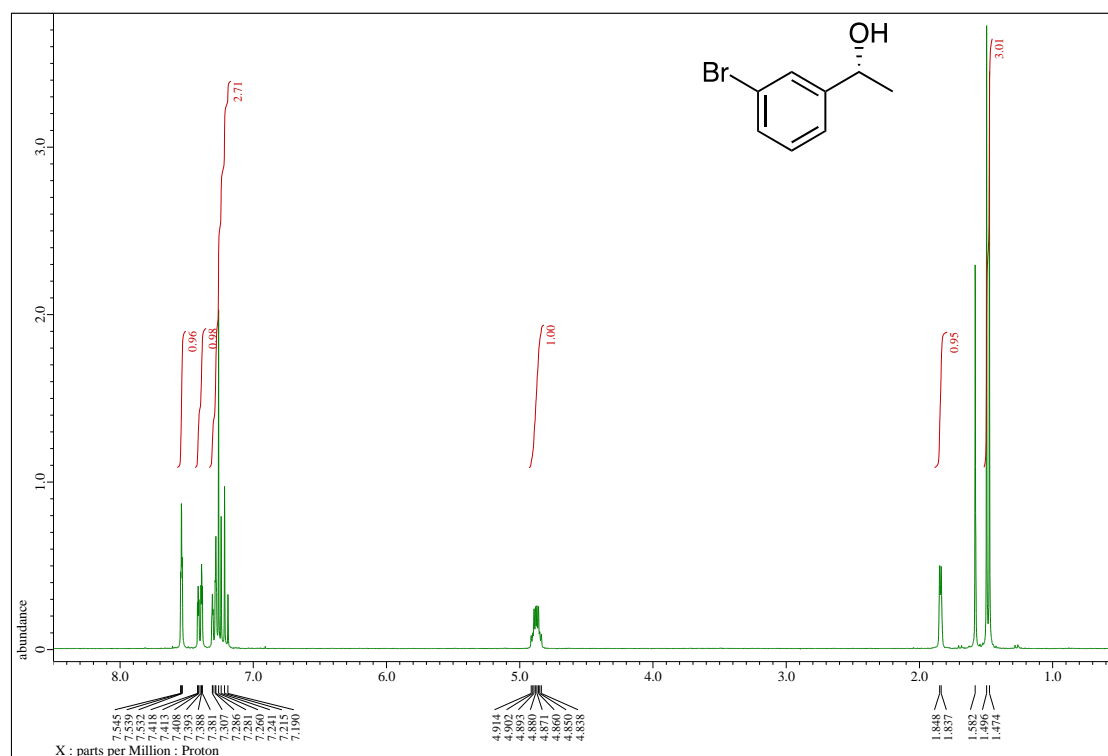
(R)-1-(p-Methoxyphenyl)ethanol (1f)



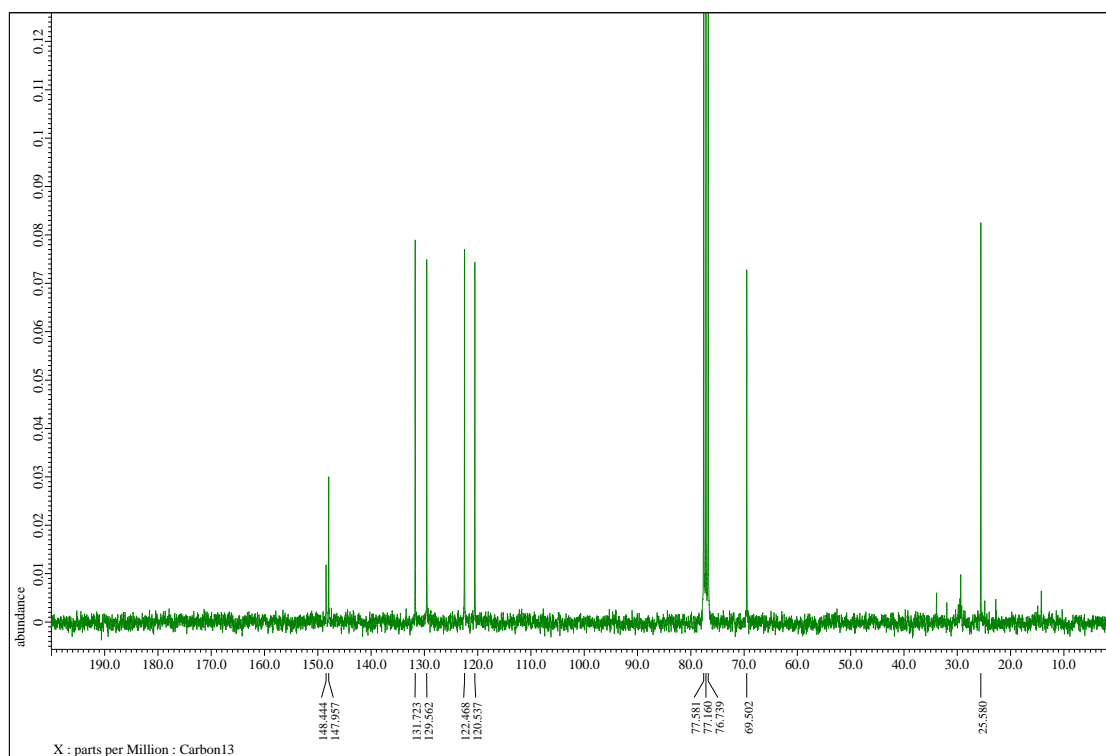
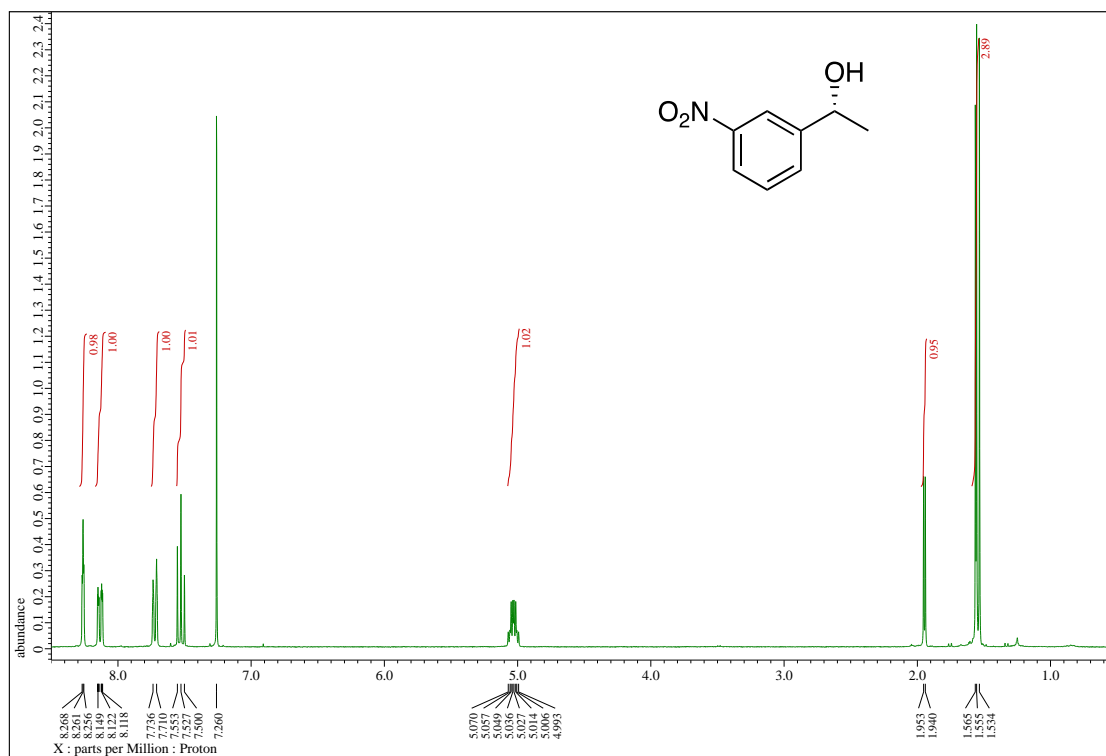
(R)-1-(*m*-Tolyl)ethanol (1g)



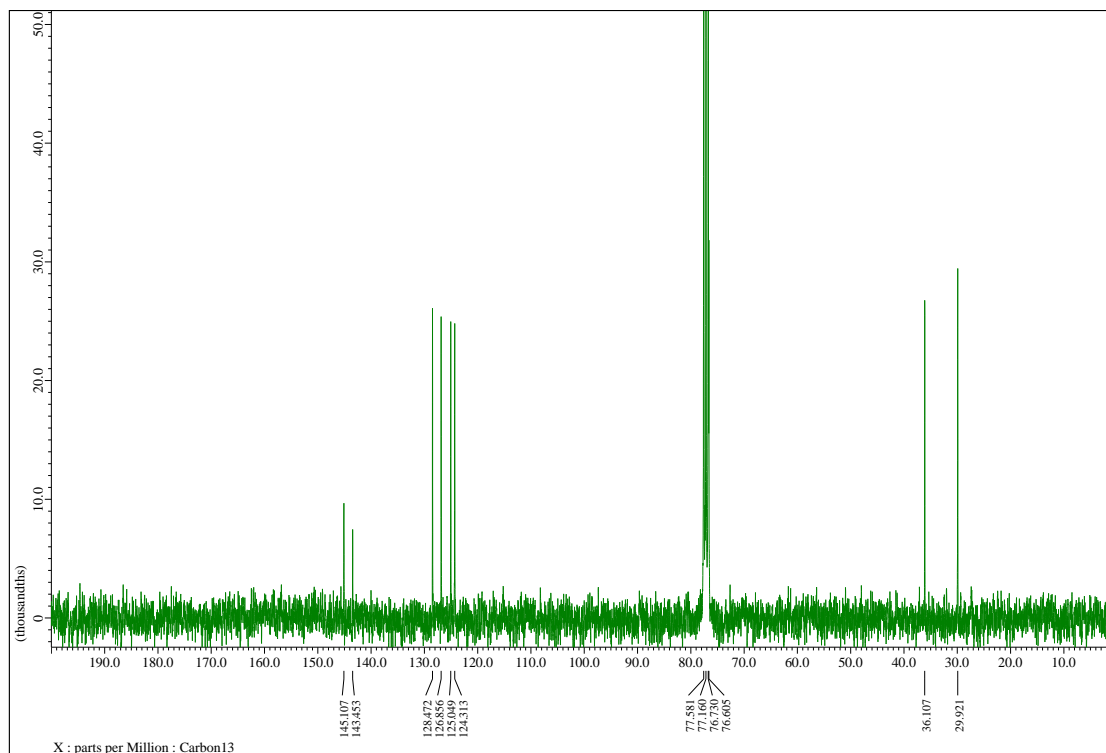
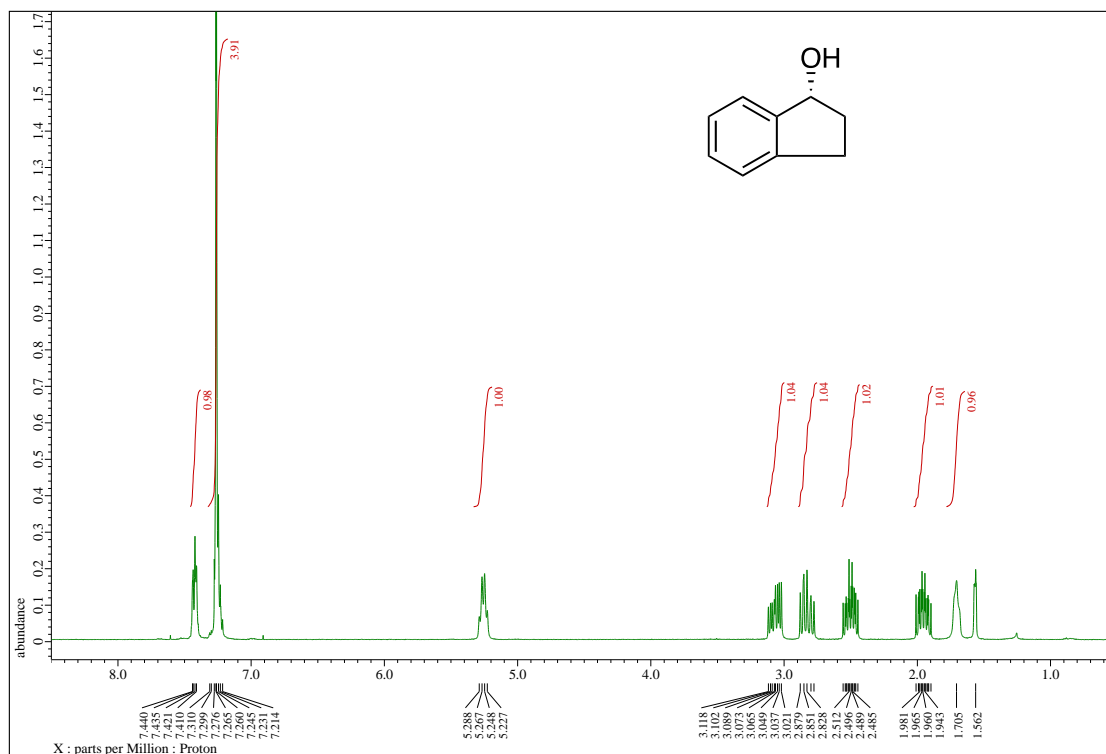
(R)-1-(*m*-Bromophenyl)ethanol (1h)



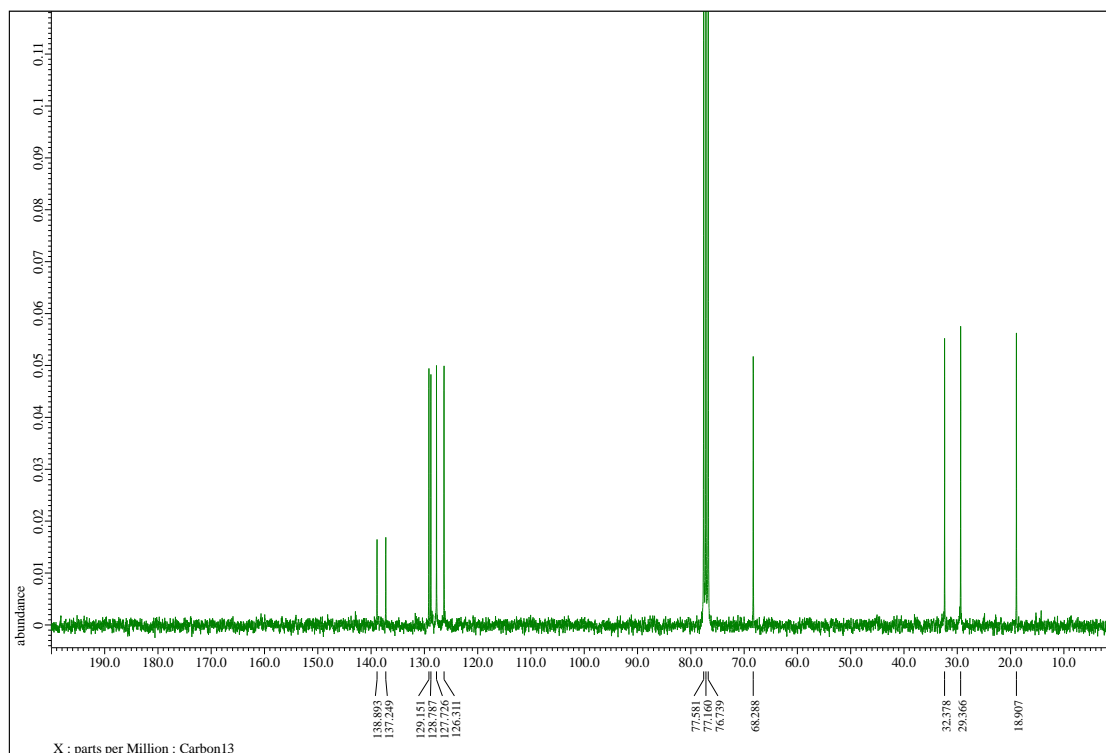
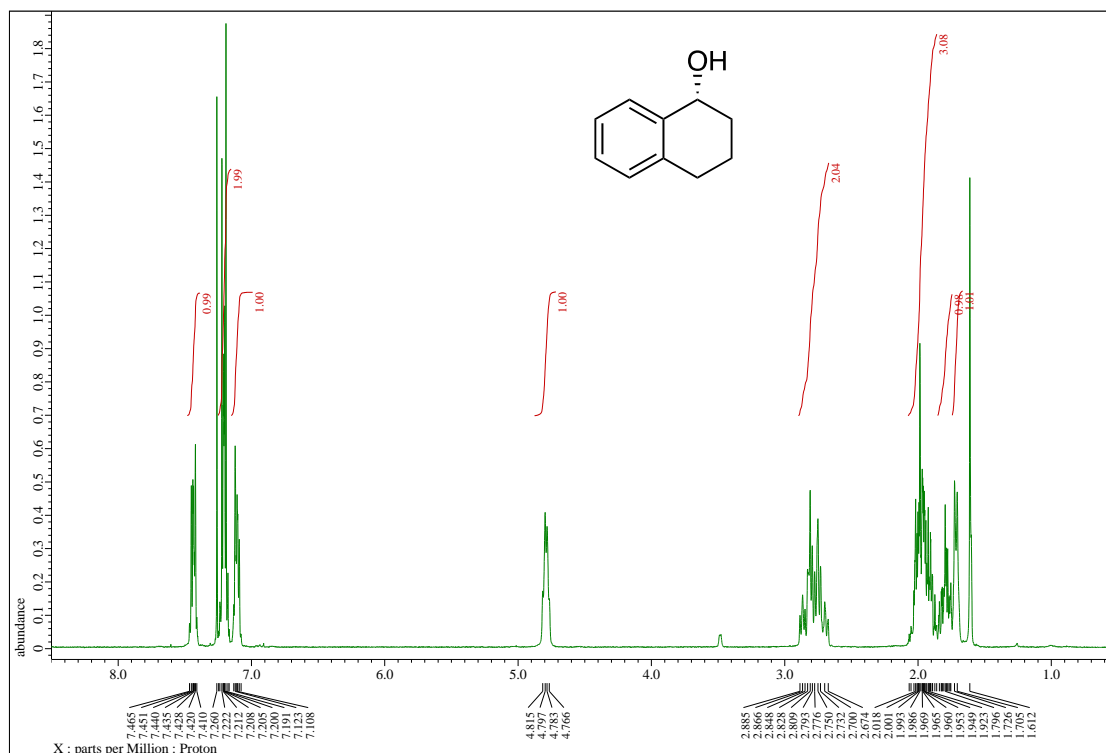
(R)-1-(*m*-Nitrophenyl)ethanol (1i)



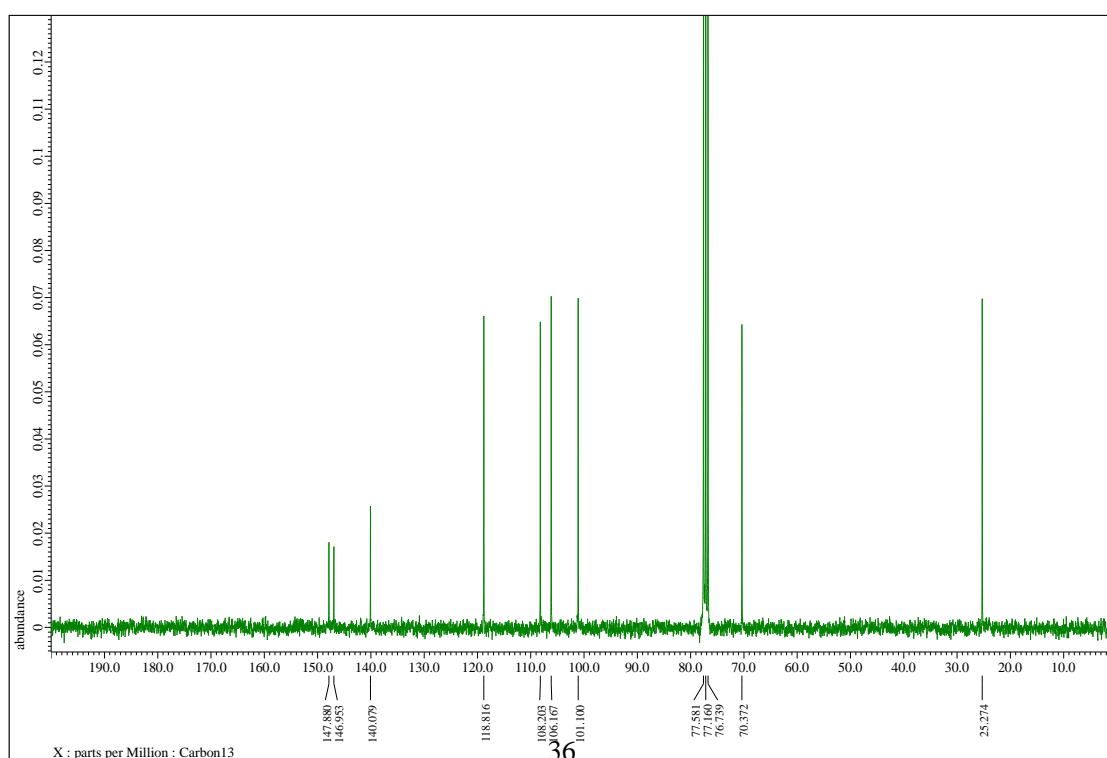
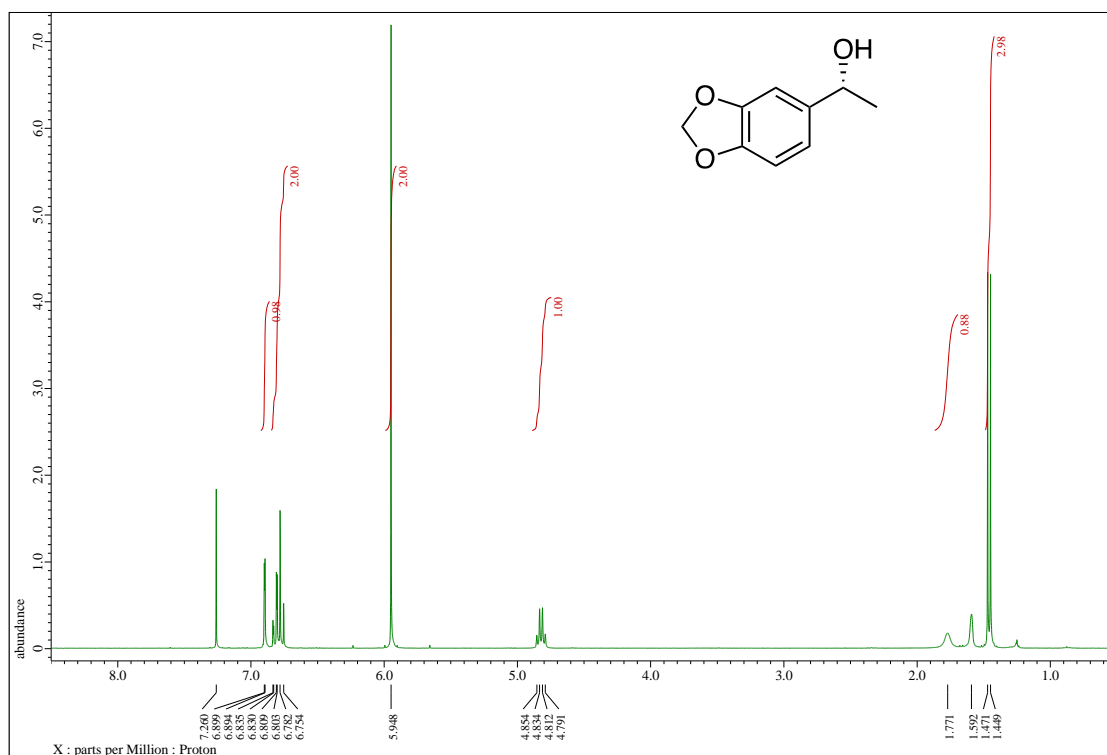
(R)-1-Indanol (1j)



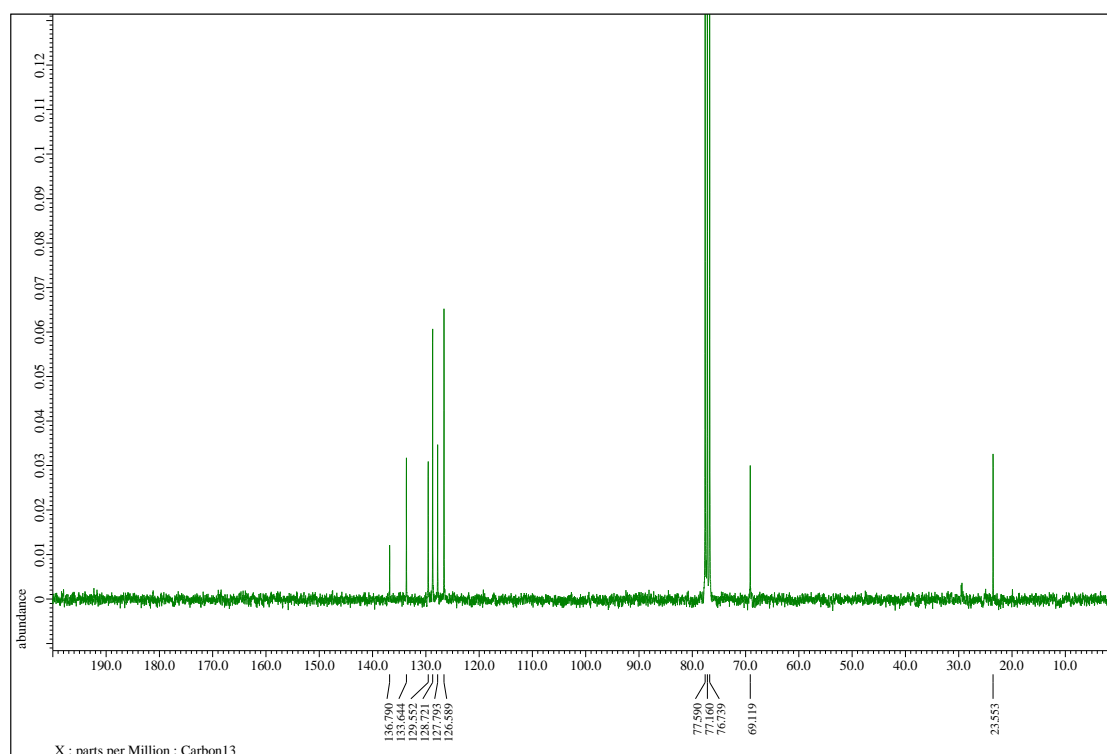
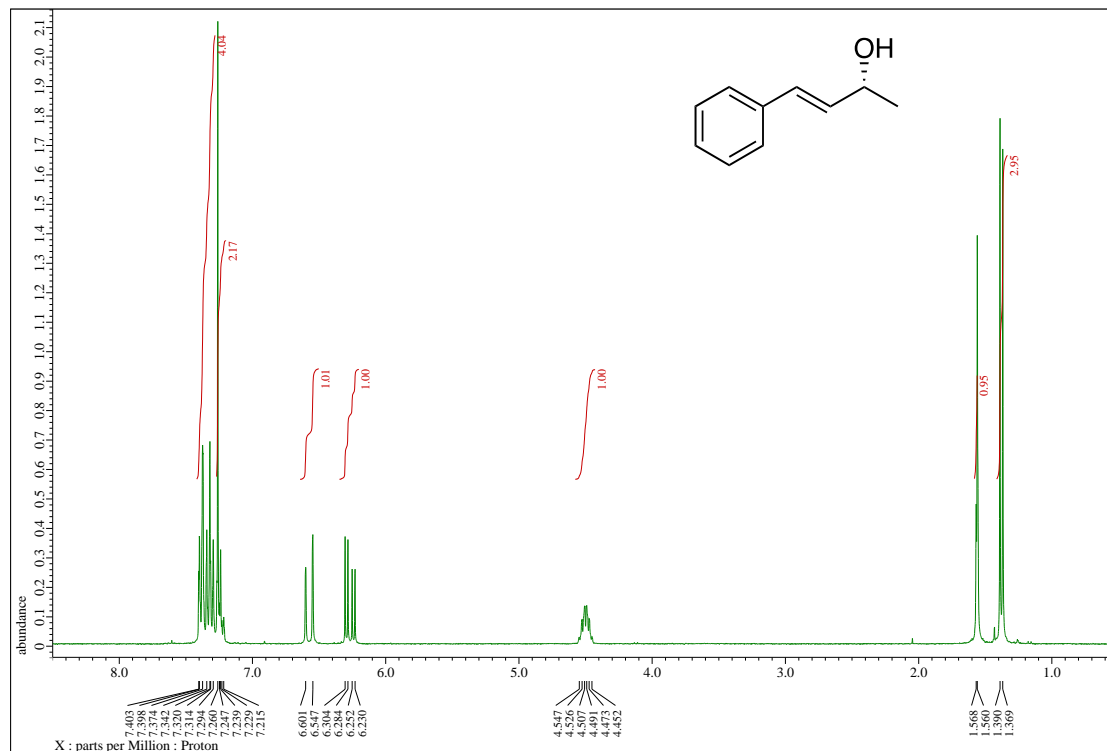
(R)-1-Tetralol (1k)



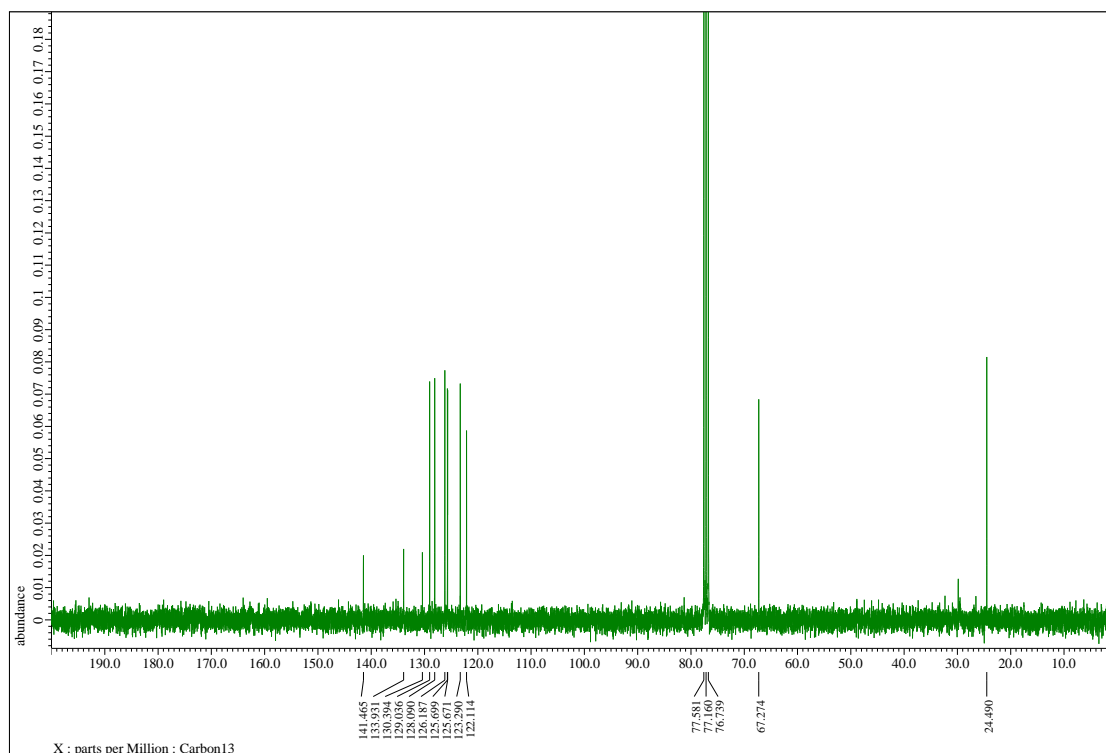
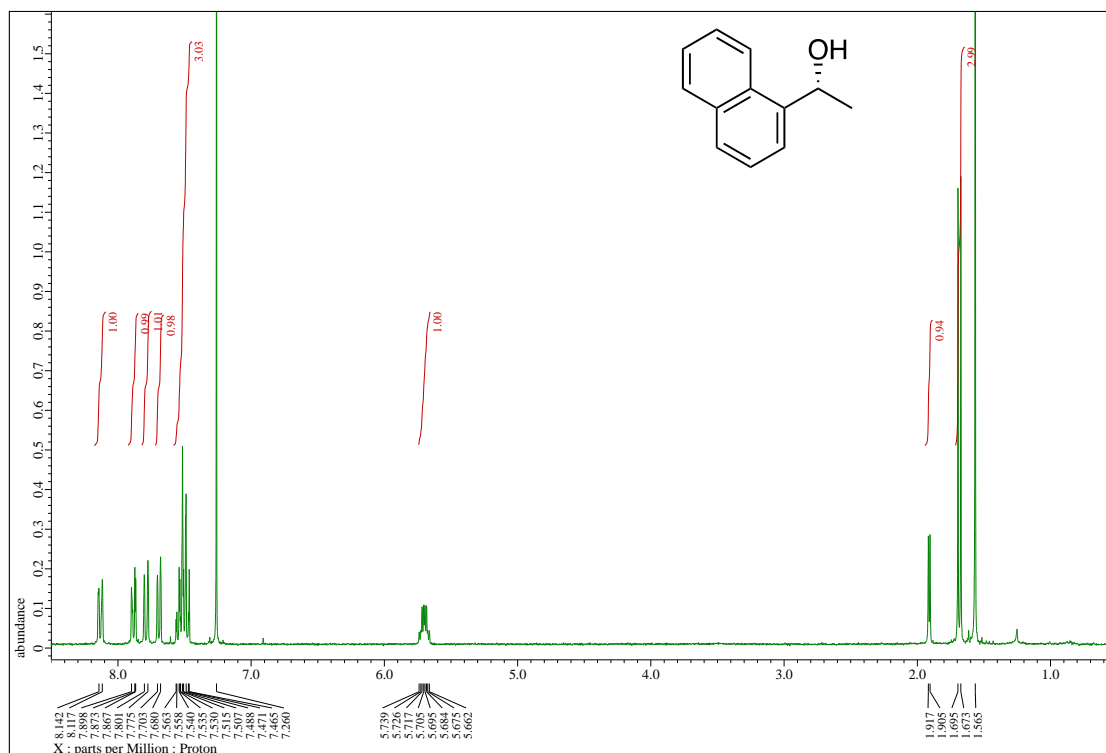
(R)-1-(Benzo[d][1,3]dioxol-5-yl)ethanol (11)



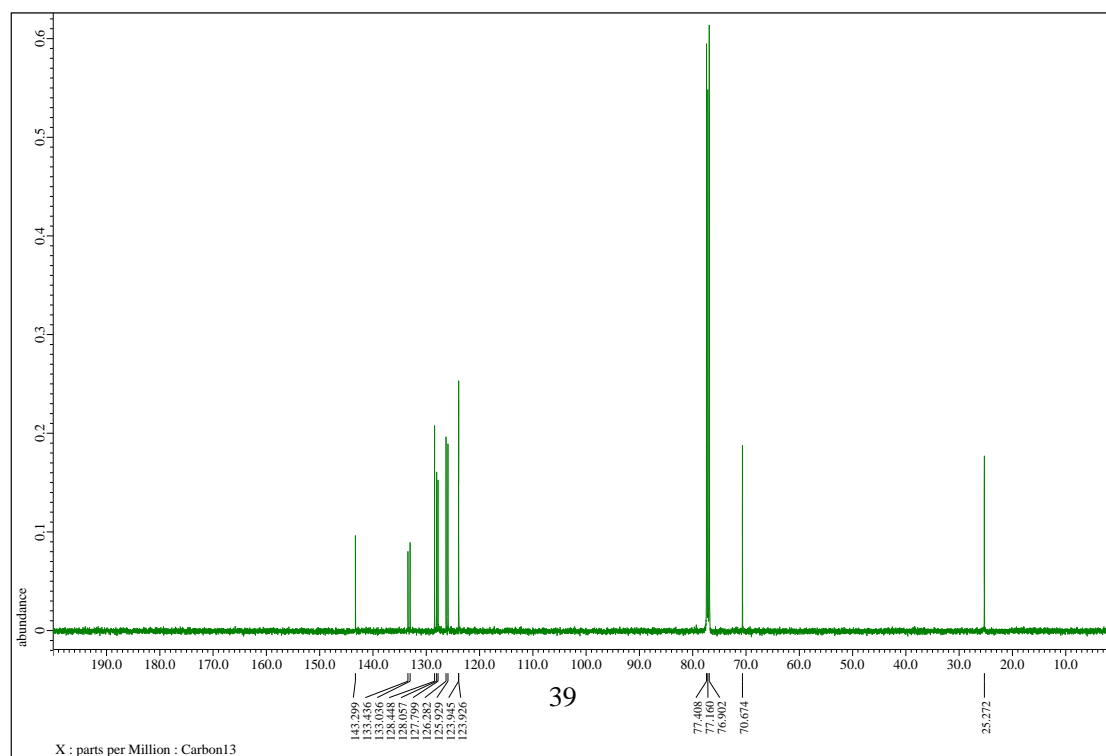
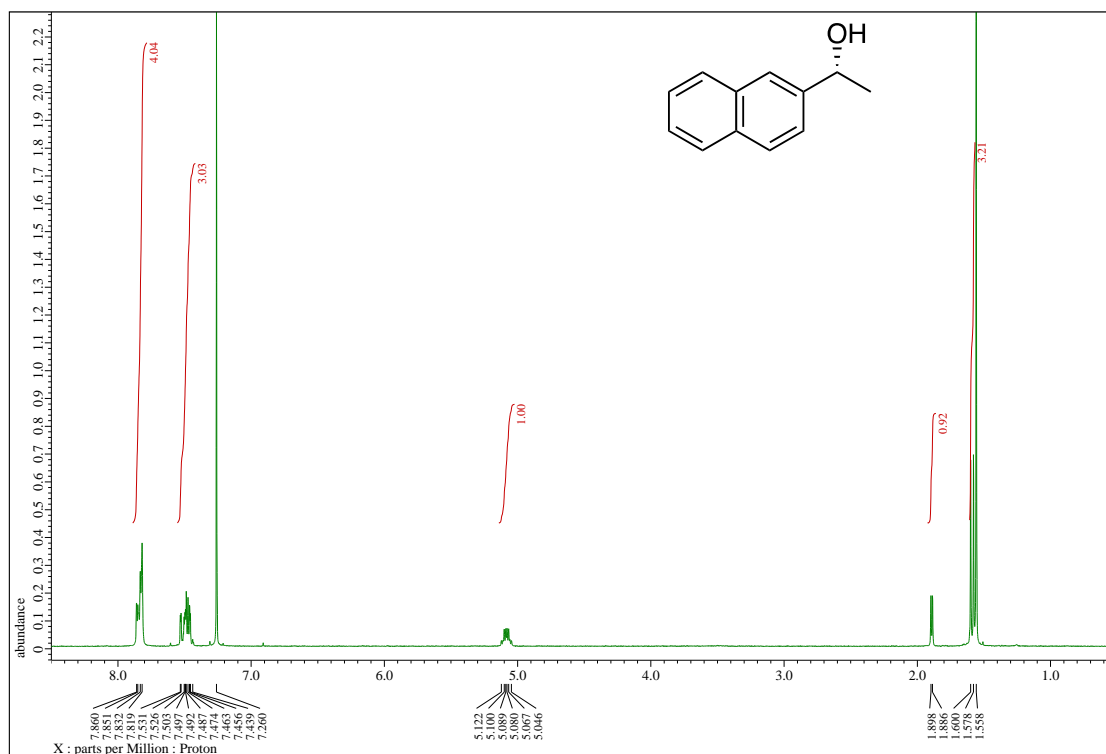
(R)- 4-Phenyl-3-buten-2-ol (1m)



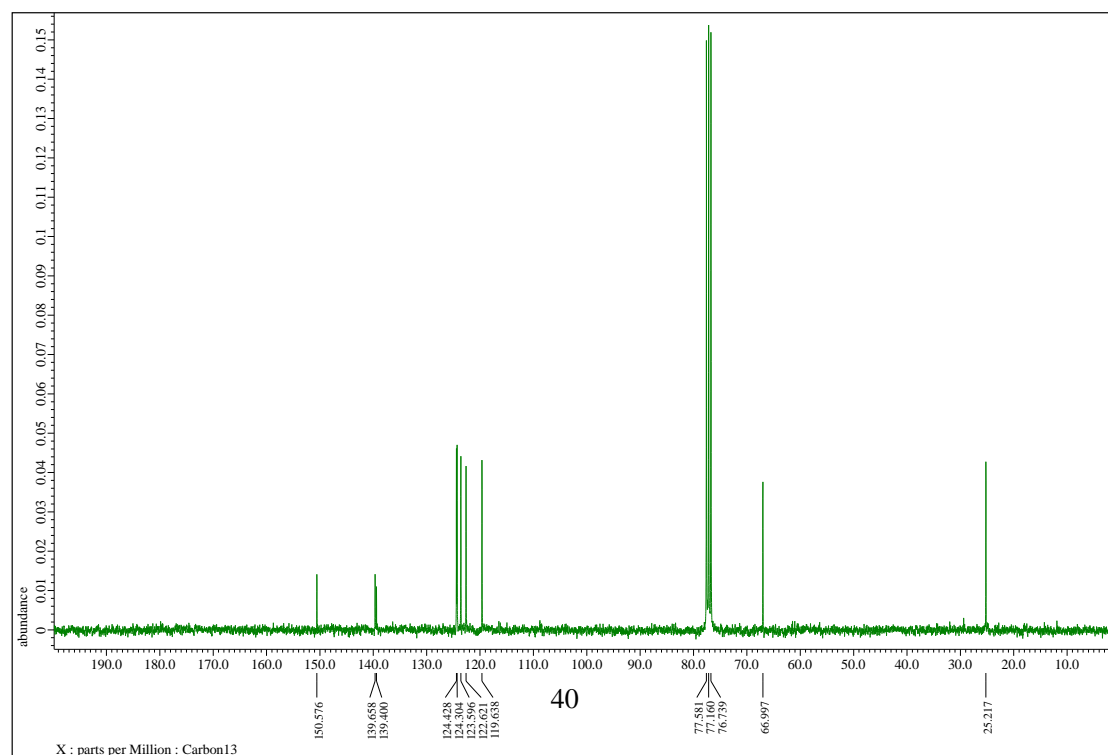
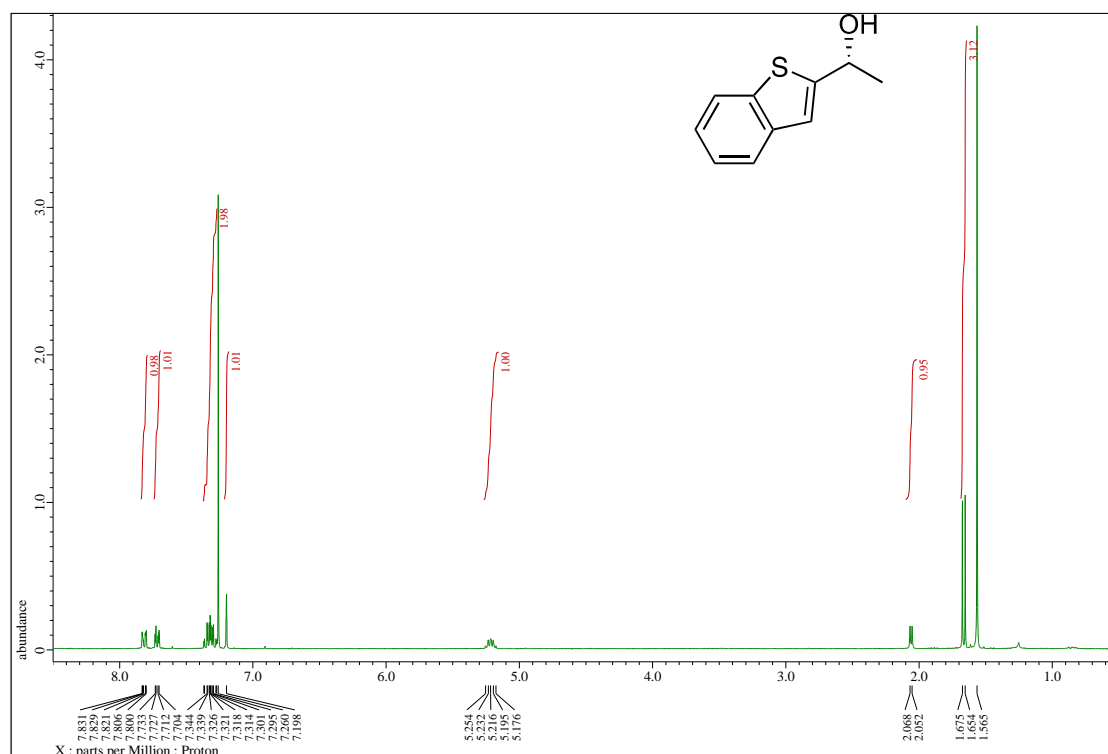
(R)-1-(1-Naphthyl)ethanol (1n)



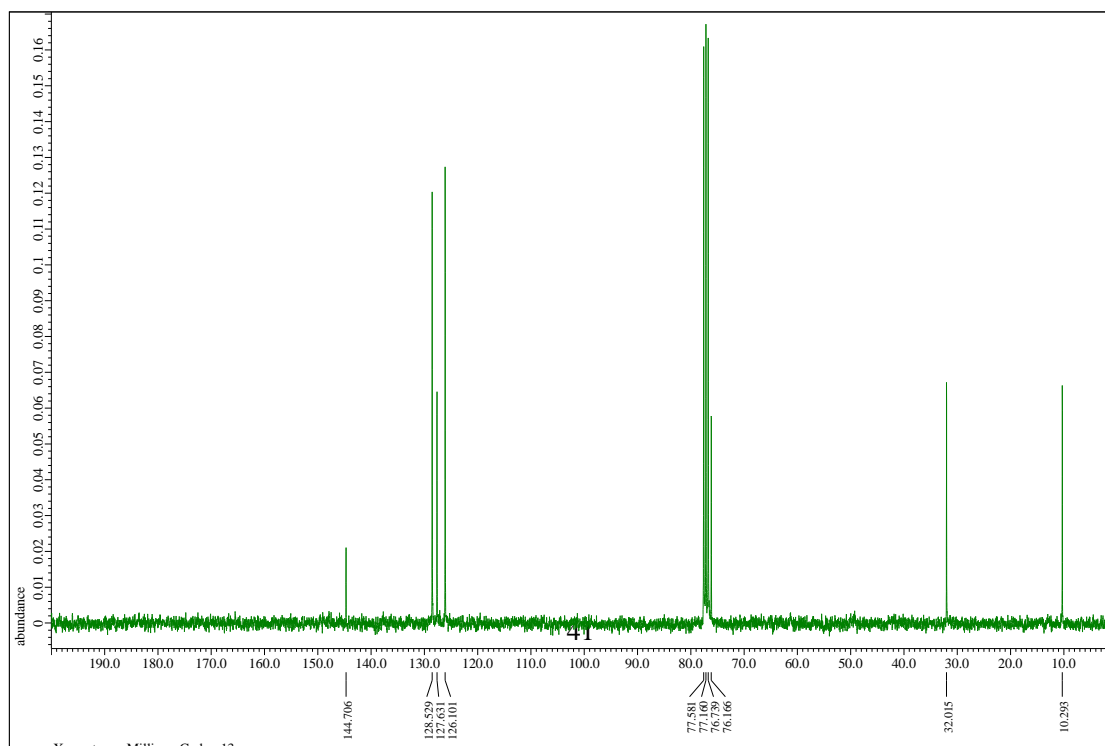
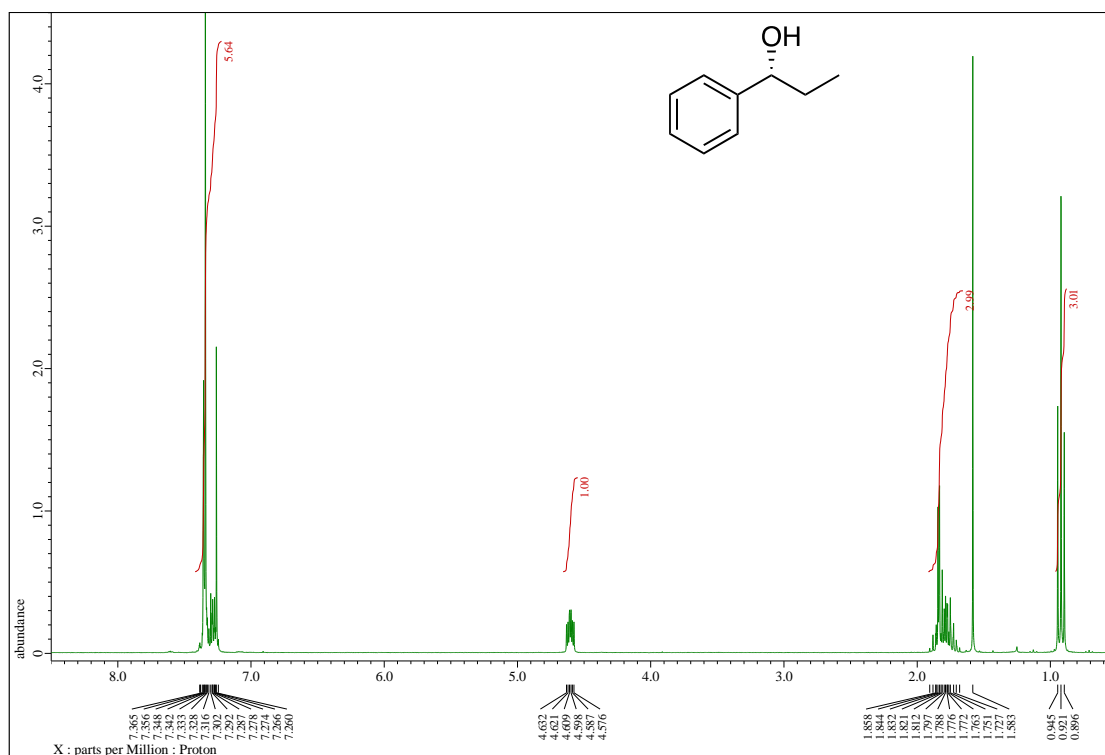
(R)-1-(2-Naphthyl)ethanol (1o)



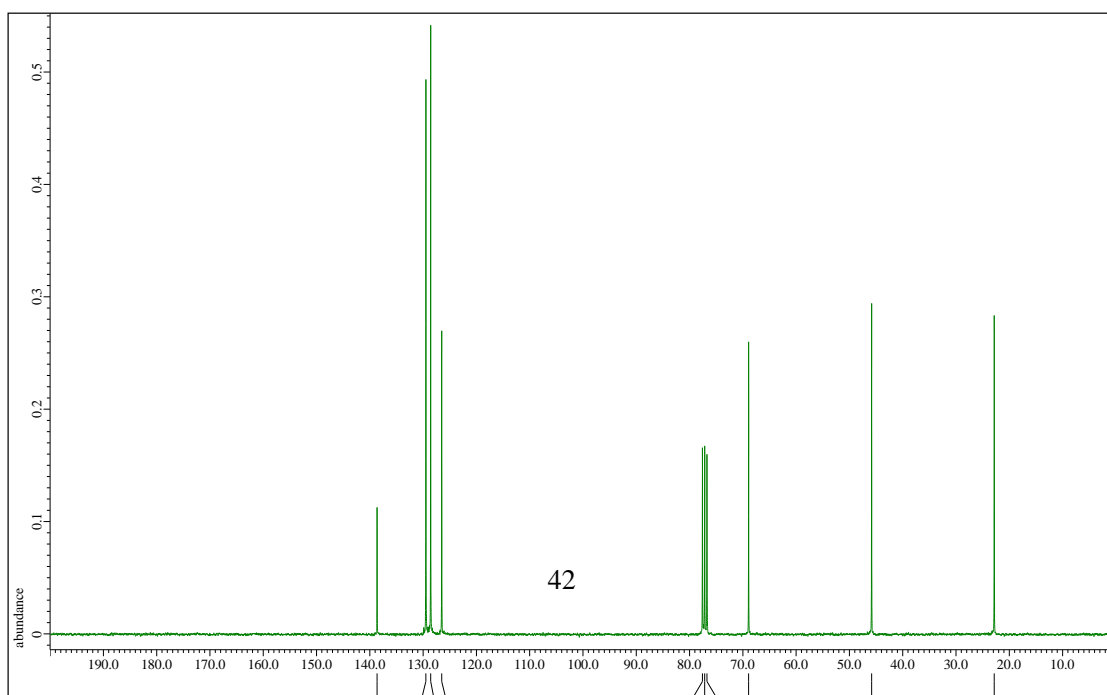
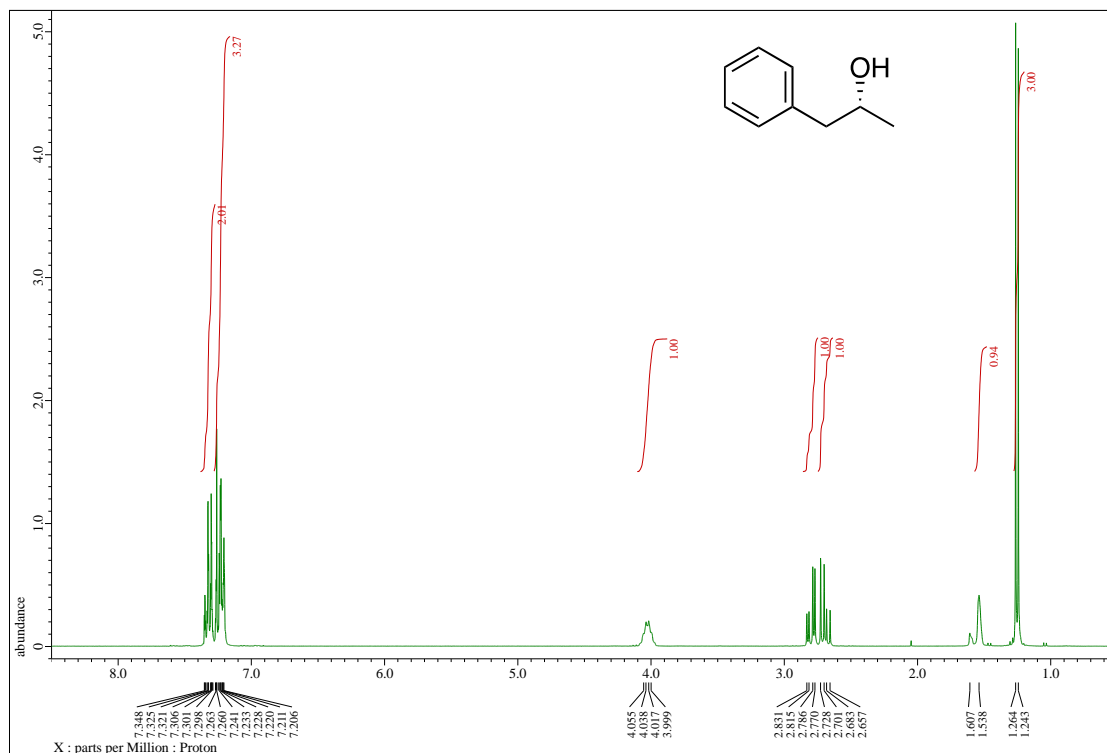
(R)-1-(Benzo[b]thiophen-2-yl)ethanol (1p)



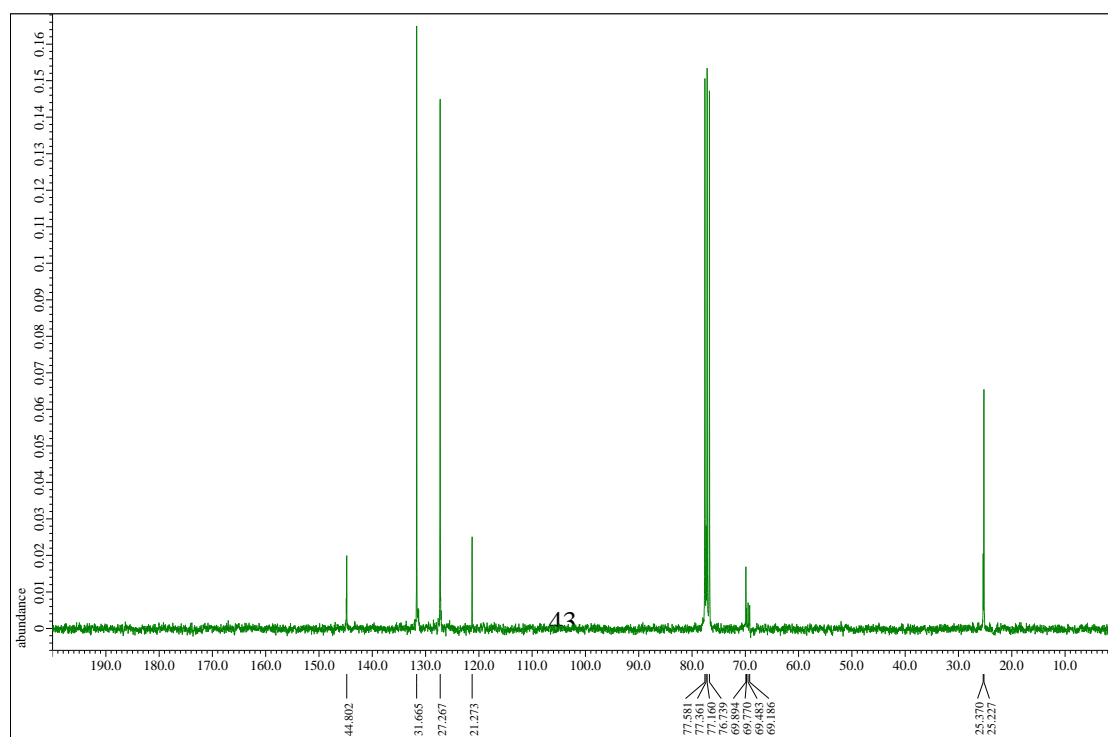
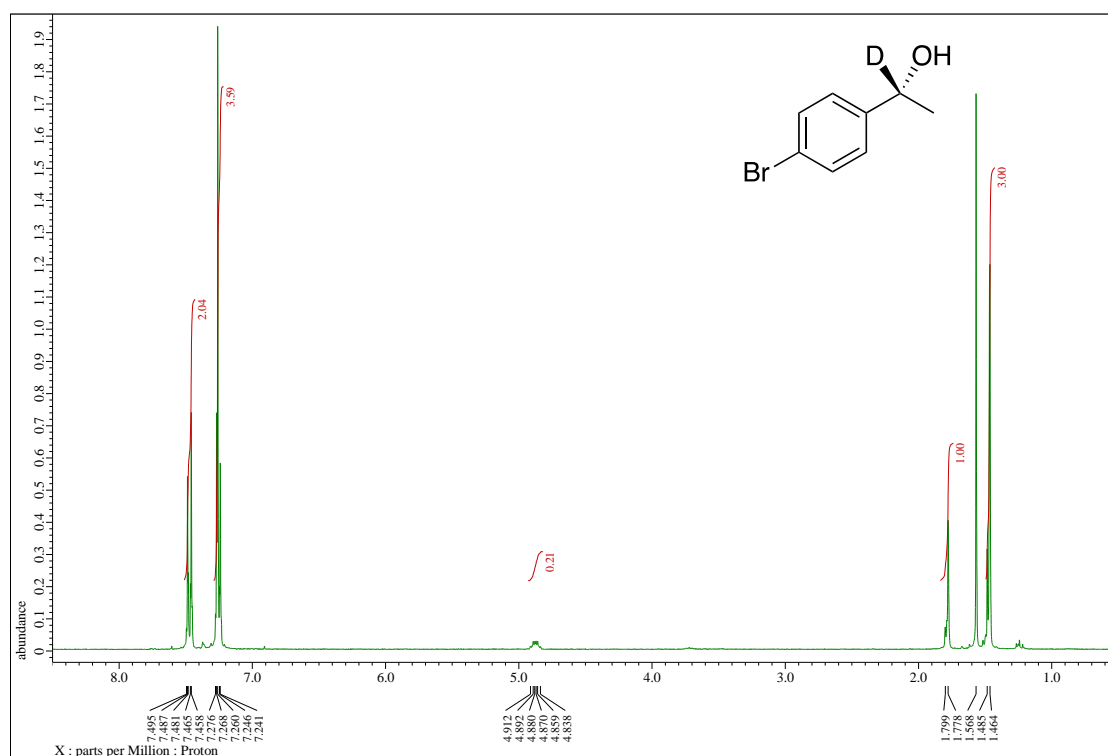
(R)-1-Phenyl-1-propanol (1q)

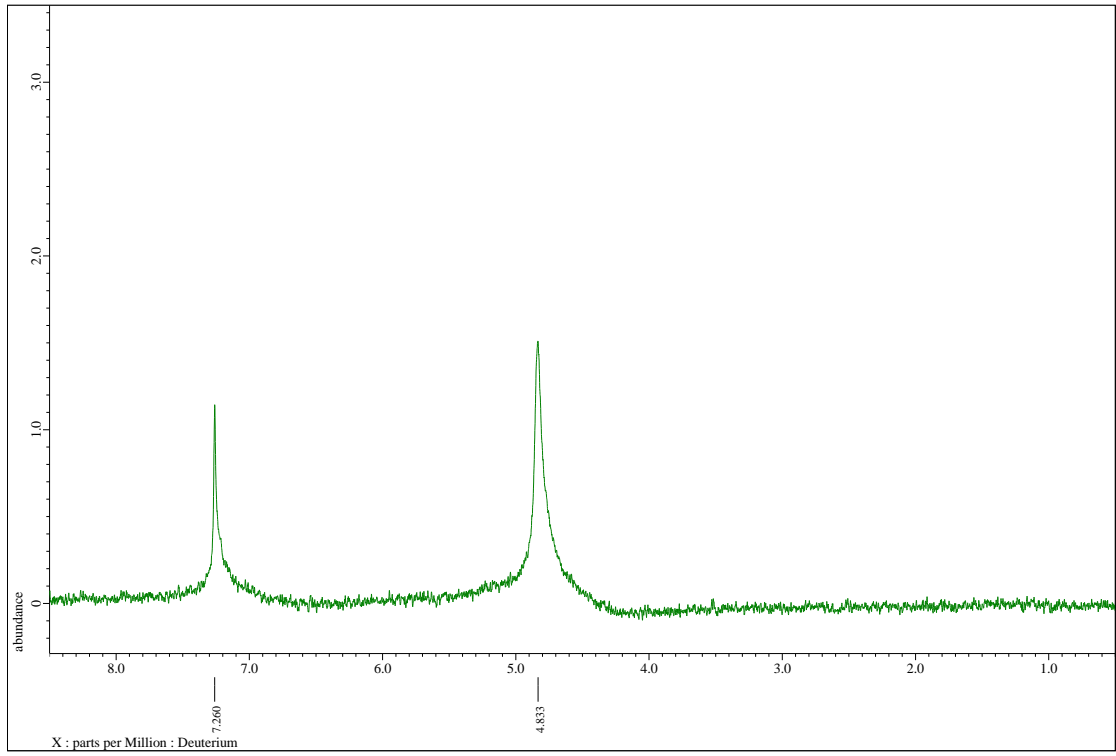


(R)-1-Phenyl-2-propanol (1r)



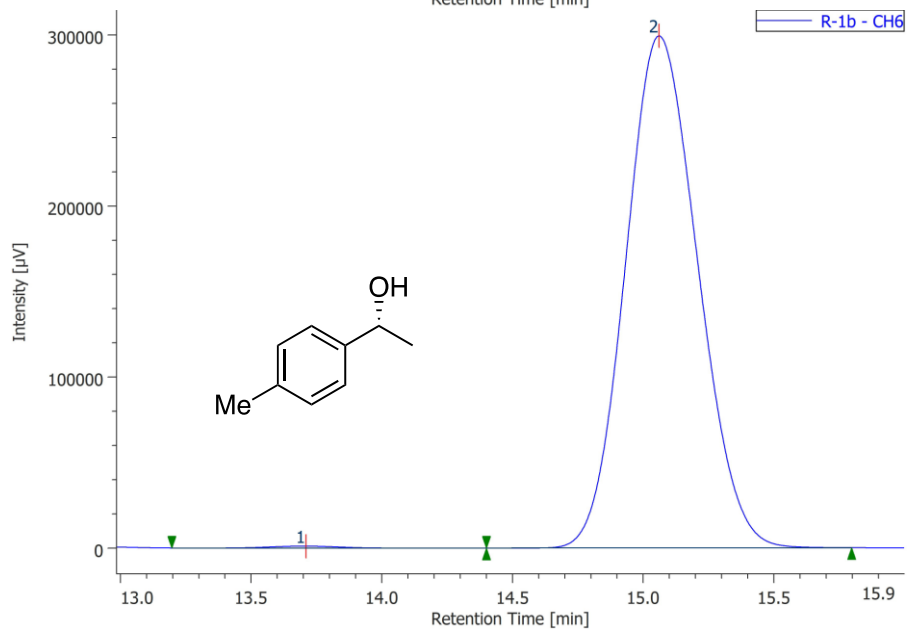
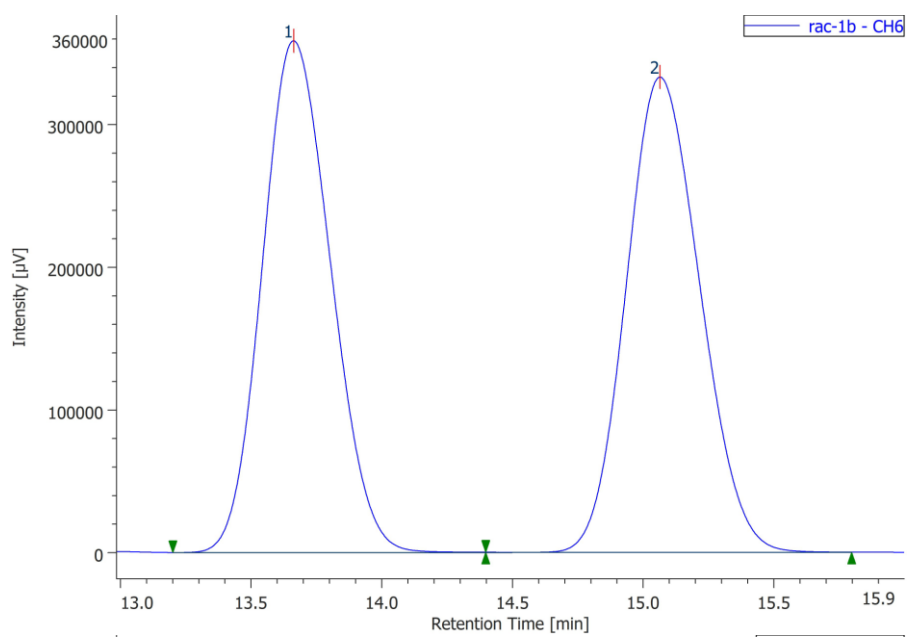
(R)-1-(p-Bromophenyl)ethan-1-d-1-ol (1e-d)





10. HPLC spectra

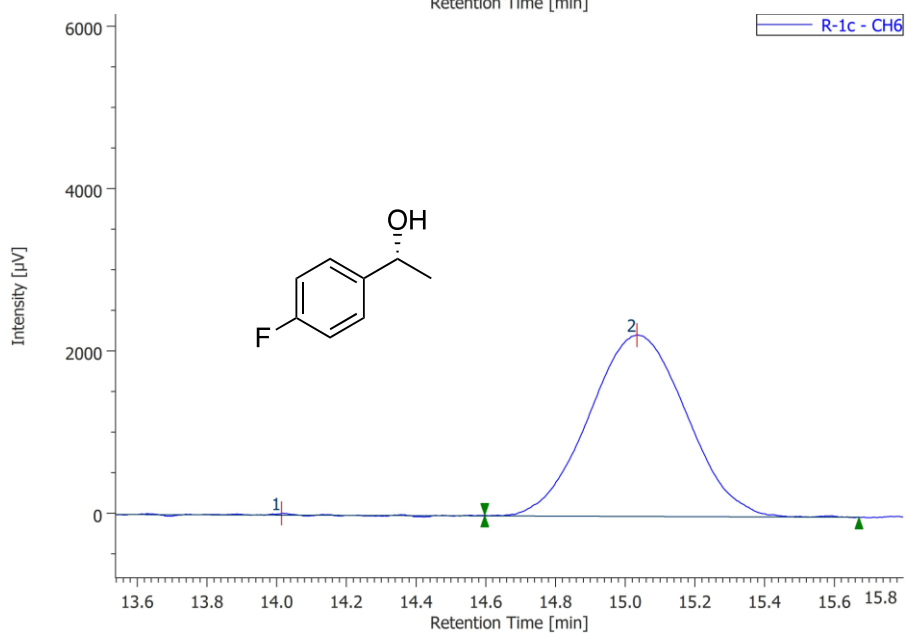
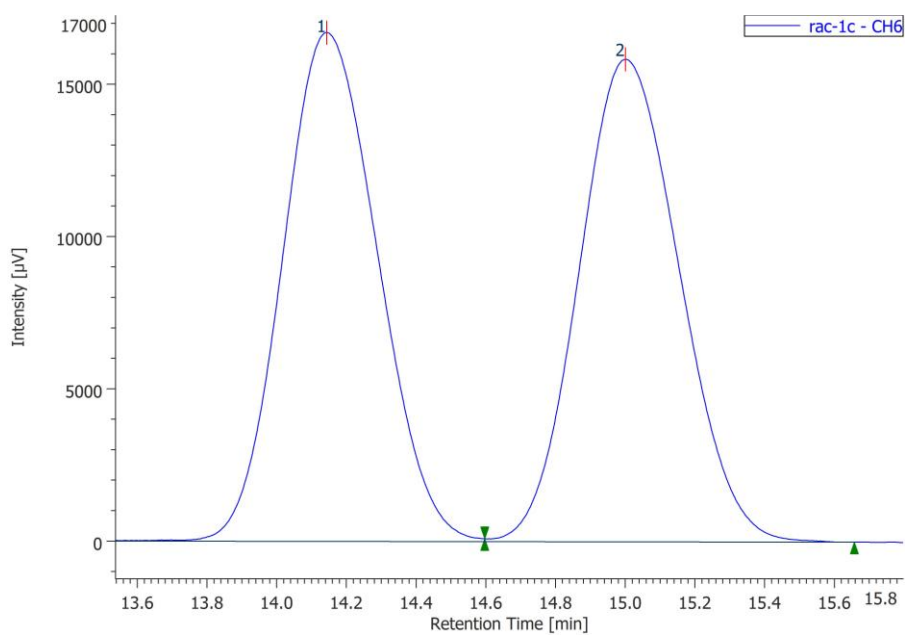
(*R*)-1-(*p*-Tolyl)ethanol (1b)



#	Peak Name	CH	tR [min]	Area [$\mu\text{V}\cdot\text{sec}$]	Height [μV]	Area%	Height%	Quantity	NTP	Resolution	Symmetry Factor	Warning
1	Unknown	6	13.710	17646	1075	0.307	0.358	N/A	14362	2.793	0.938	
2	Unknown	6	15.060	5733846	299368	99.693	99.642	N/A	13862	N/A	1.108	

IJ-3, Hexane:2-Propanol =98:2

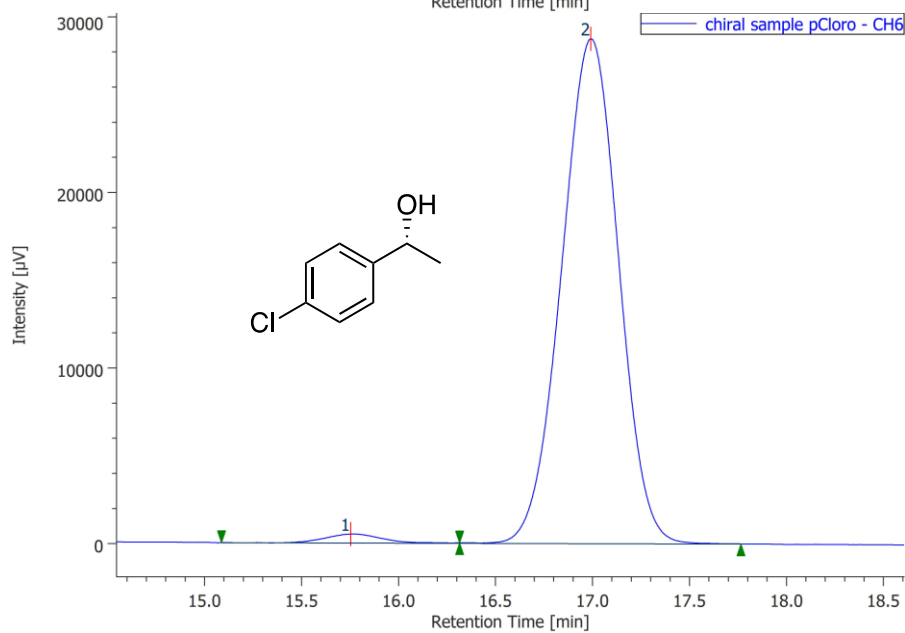
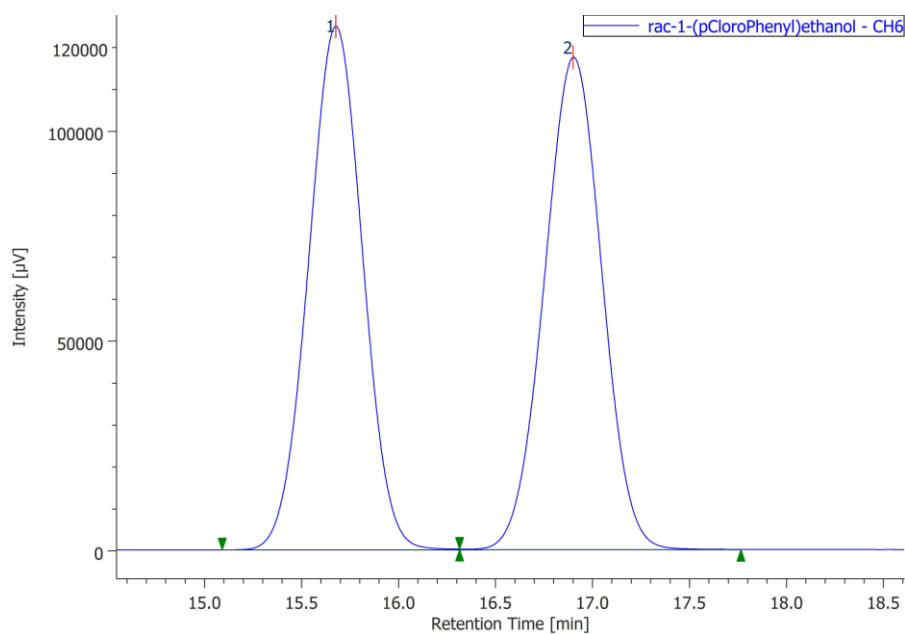
(R)-1-(p-Fluorophenyl)ethanol (1c)



#	Peak Name	CH	tR [min]	Area [μ V-sec]	Height [μ V]	Area%	Height%	Quantity	NTP	Resolution	Symmetry Factor	Warning
1	Unknown	6	14.013	169	21	0.389	0.923	N/A	4707	1.529	N/A	
2	Unknown	6	15.033	43308	2235	99.611	99.077	N/A	13341	N/A	1.031	

IJ-3, Hexane:2-Propanol =98:2

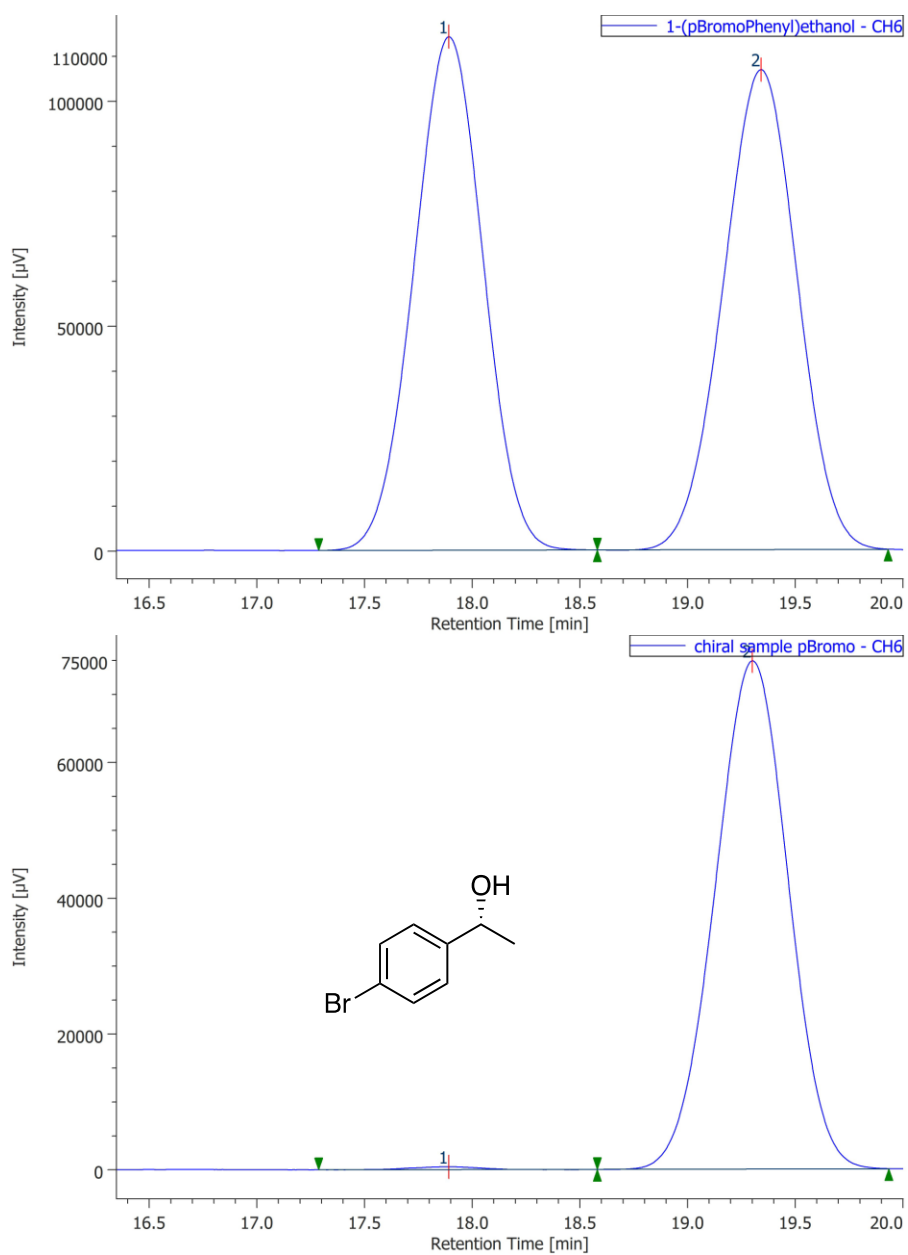
(R)-1-(p-Chlorophenyl)ethanol (1d)



#	Peak Name	CH	tR [min]	Area [μV·sec]	Height [μV]	Area%	Height%	Quantity	NTP	Resolution	Symmetry Factor	Warning
1	Unknown	6	15.753	10458	510	1.752	1.743	N/A	14337	2.321	1.284	
2	Unknown	6	16.990	586506	28743	98.248	98.257	N/A	15714	N/A	0.984	

IJ-3, Hexane:2-Propanol =98:2

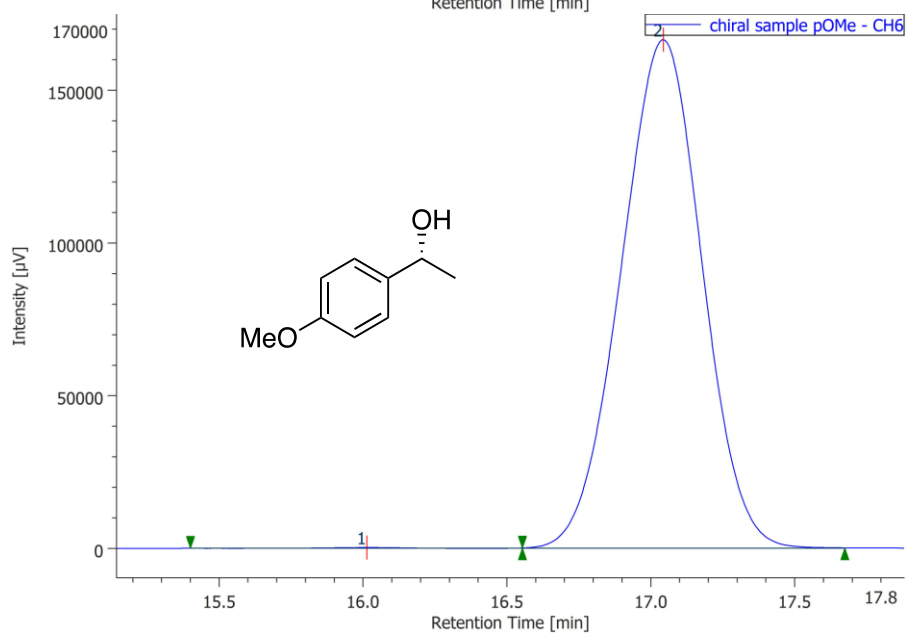
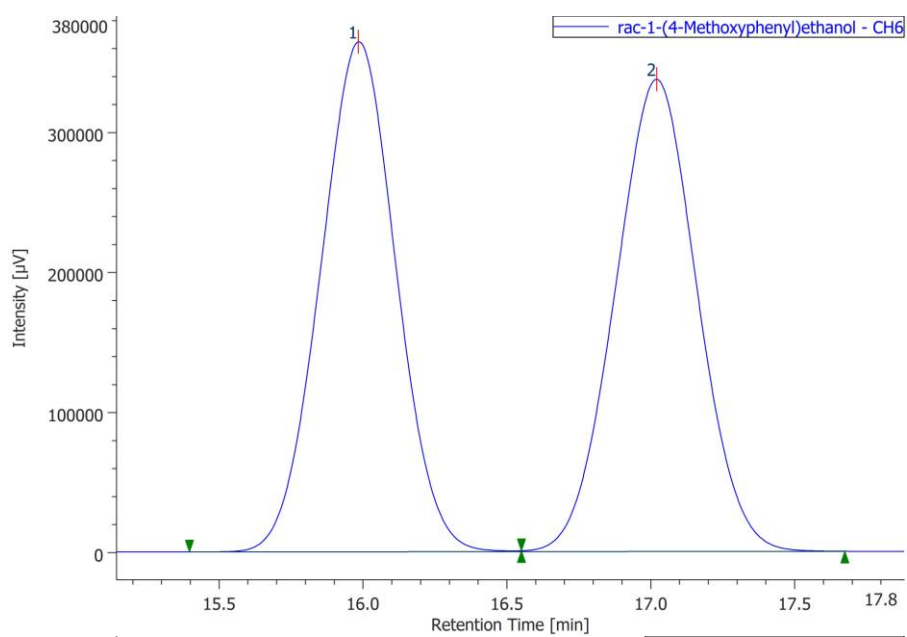
(R)-1-(p-Bromophenyl)ethanol (1e)



#	Peak Name	CH	tR [min]	Area [$\mu\text{V}\cdot\text{sec}$]	Height [μV]	Area%	Height%	Quantity	NTP	Resolution	Symmetry Factor	Warning
1	Unknown	6	17.890	8477	412	0.476	0.548	N/A	14659	2.311	0.845	
2	Unknown	6	19.300	1771208	74827	99.524	99.452	N/A	14898	N/A	0.987	

IJ-3, Hexane:2-Propanol =98:2

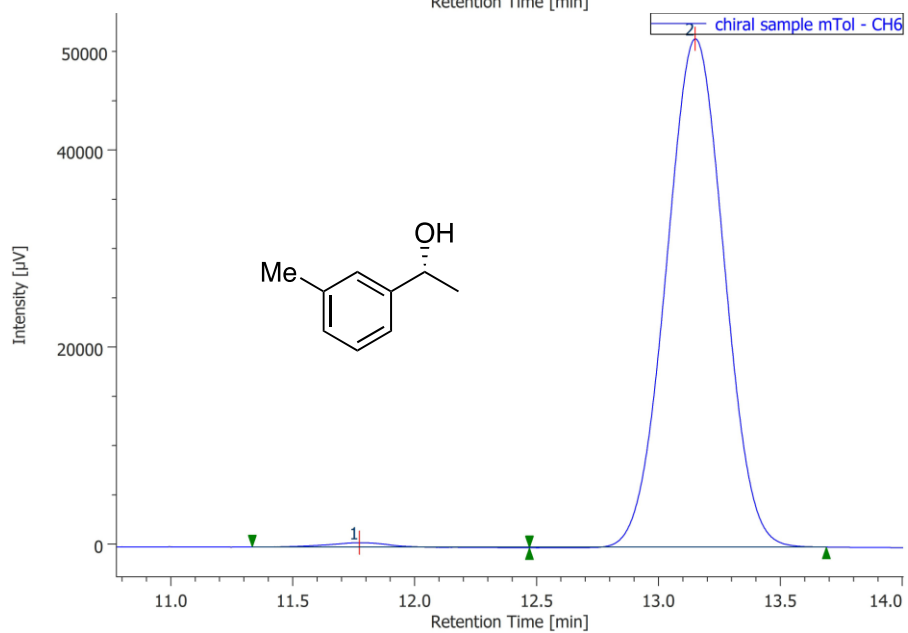
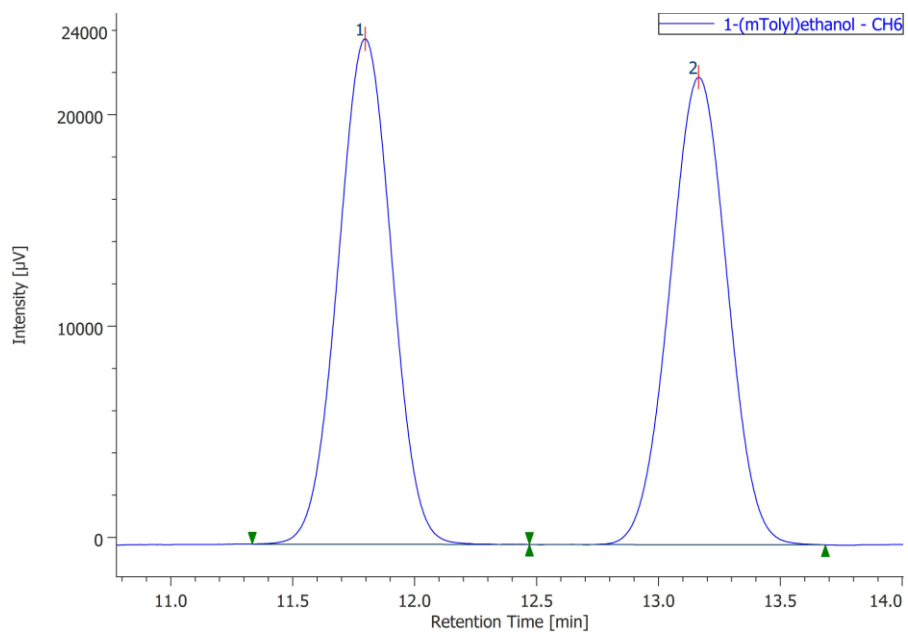
(R)-1-(*p*-Methoxyphenyl)ethanol (1f)



#	Peak Name	CH	tR [min]	Area [μ V-sec]	Height [μ V]	Area%	Height%	Quantity	NTP	Resolution	Symmetry Factor	Warning
1	Unknown	6	16.013	3013	213	0.093	0.128	N/A	25354	2.239	N/A	
2	Unknown	6	17.043	3253306	166376	99.907	99.872	N/A	17166	N/A	0.980	

IJ-3, Hexane:2-Propanol =95:5

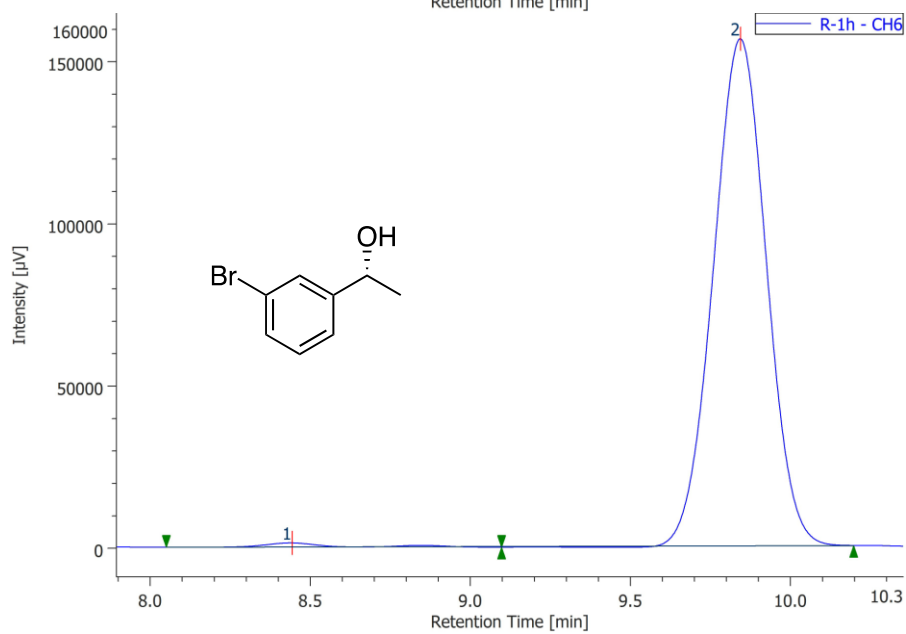
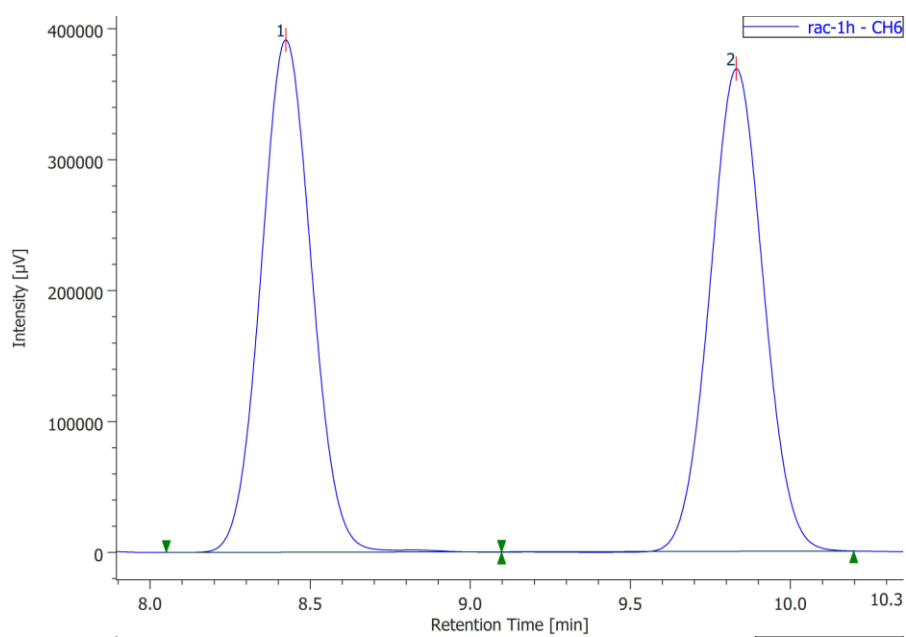
(R)-1-(*m*-Tolyl)ethanol (1g)



#	Peak Name	CH	tR [min]	Area [$\mu\text{V}\cdot\text{sec}$]	Height [μV]	Area%	Height%	Quantity	NTP	Resolution	Symmetry Factor	Warning
1	Unknown	6	11.773	7666	446	0.893	0.857	N/A	11124	3.115	0.842	
2	Unknown	6	13.150	850937	51591	99.107	99.143	N/A	14301	N/A	1.012	

IJ-3, Hexane:2-Propanol =98:2

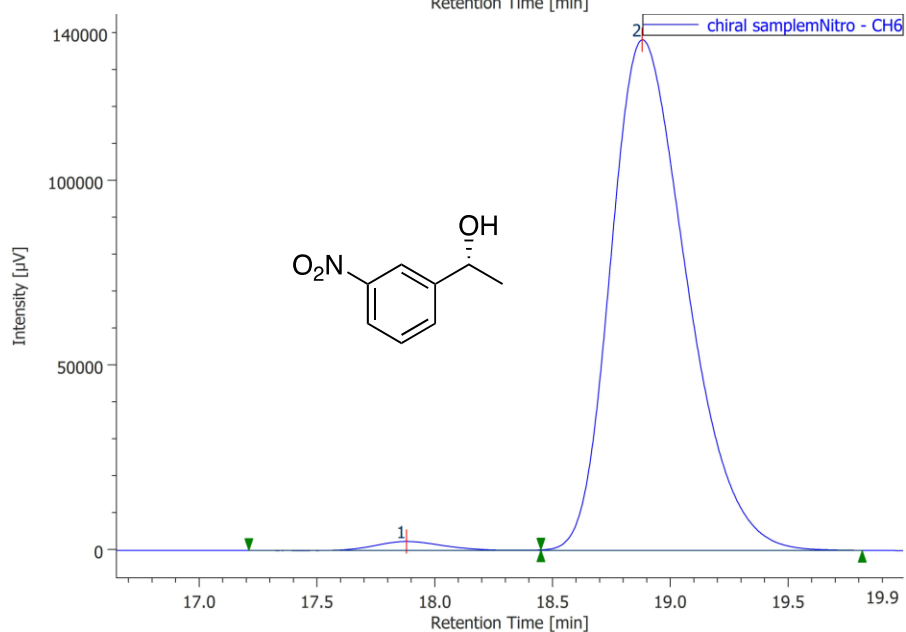
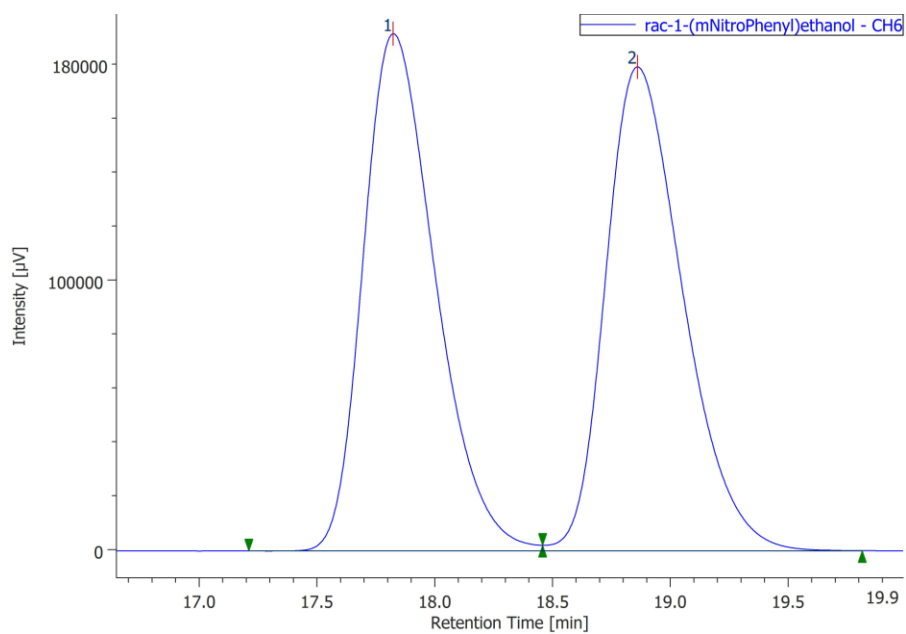
(R)-1-(*m*-Bromophenyl)ethanol (1h)



#	Peak Name	CH	tR [min]	Area [$\mu\text{V}\cdot\text{sec}$]	Height [μV]	Area%	Height%	Quantity	NTP	Resolution	Symmetry Factor	Warning
1	Unknown	6	8.443	14394	1205	0.794	0.765	N/A	15485	4.864	2.004	
2	Unknown	6	9.843	1799283	156276	99.206	99.235	N/A	16585	N/A	0.999	

IJ-3, Hexane:2-Propanol =95:5

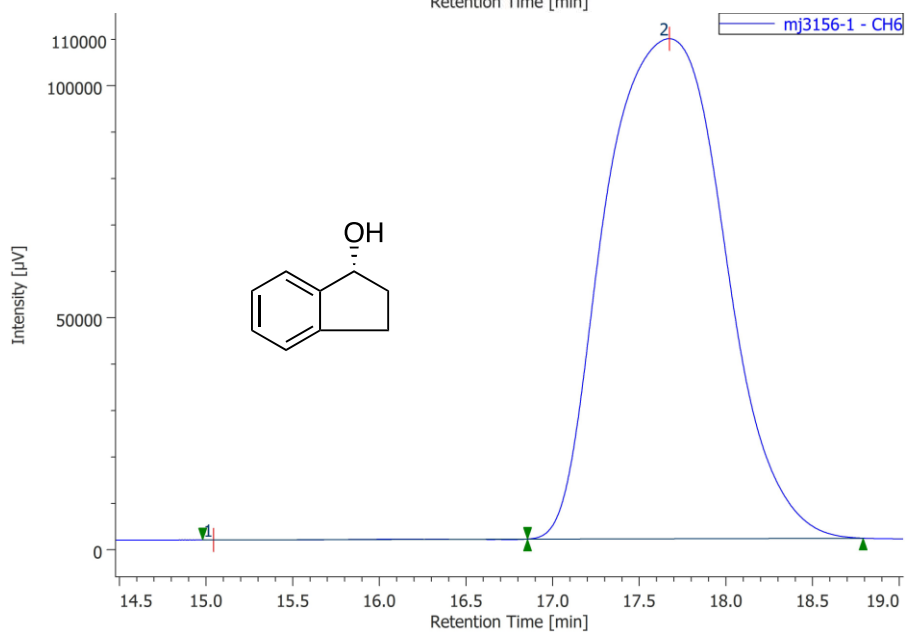
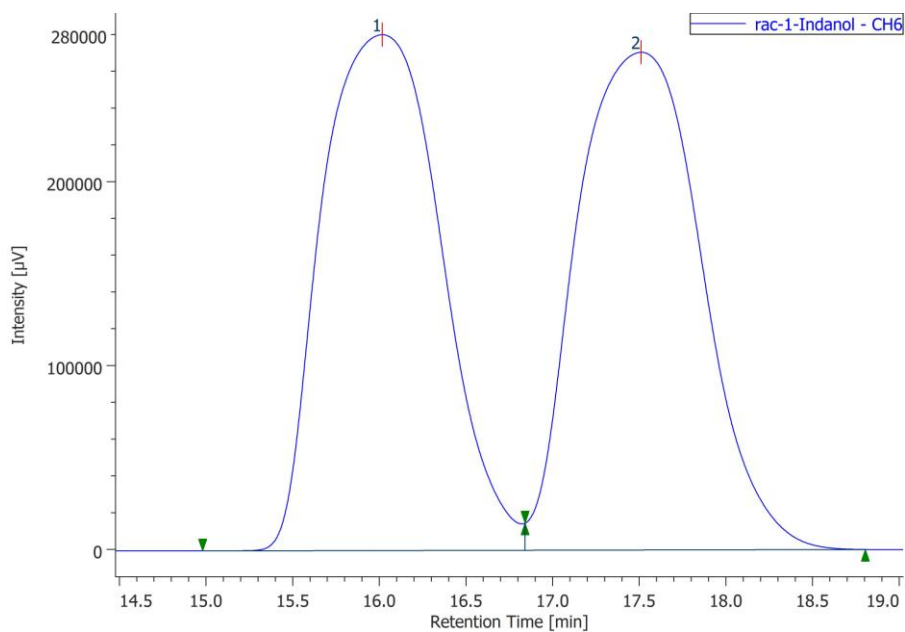
(R)-1-(*m*-Nitrophenyl)ethanol (1i)



#	Peak Name	CH	tR [min]	Area [$\mu\text{V}\cdot\text{sec}$]	Height [μV]	Area%	Height%	Quantity	NTP	Resolution	Symmetry Factor	Warning
1	Unknown	6	17.880	49062	2437	1.557	1.731	N/A	18107	1.791	N/A	
2	Unknown	6	18.880	3102139	138316	98.443	98.269	N/A	16475	N/A	1.330	

IE-3, Hexane:2-Propanol =95:5

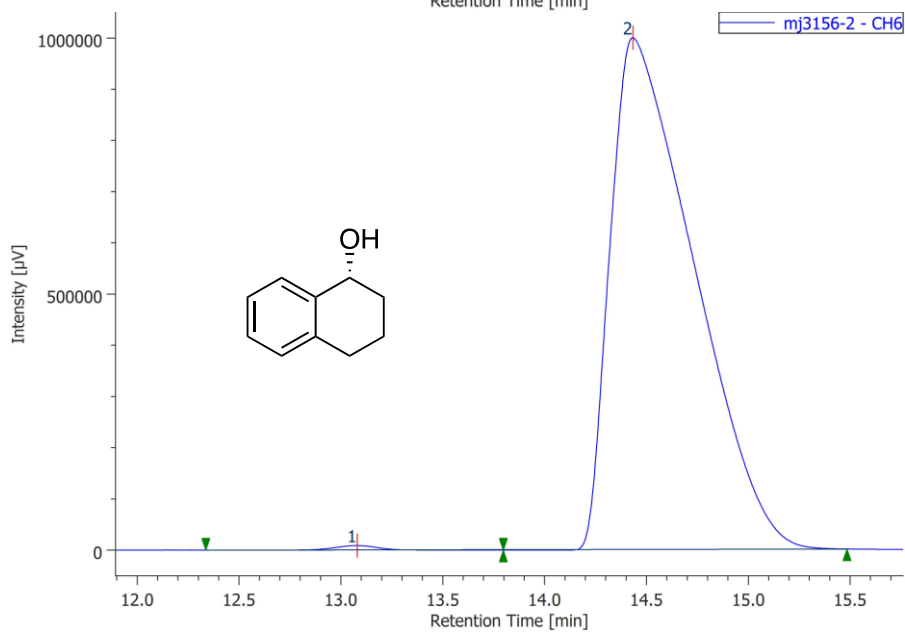
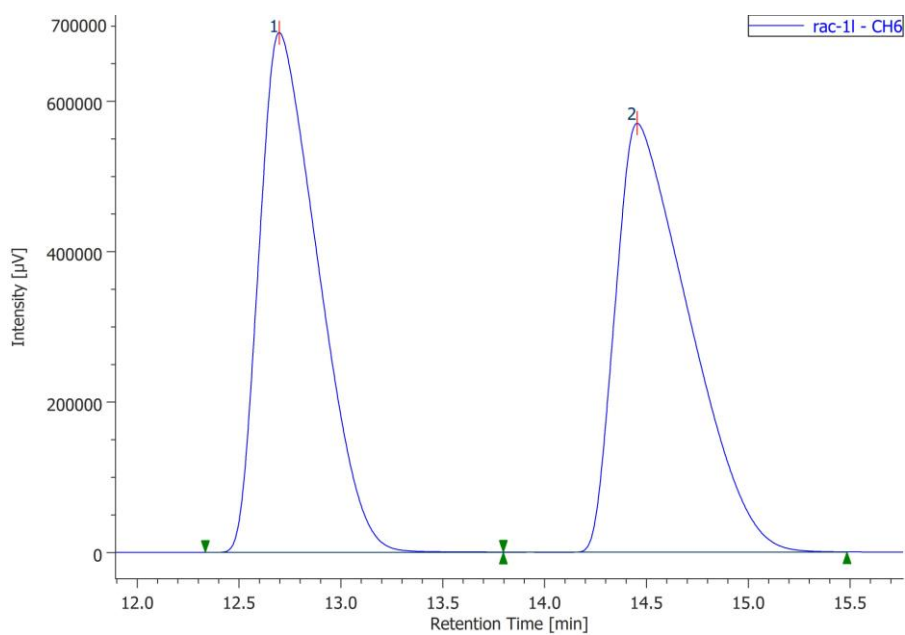
(R)-1-Indanol (1j)



#	Peak Name	CH	tR [min]	Area [$\mu\text{V}\cdot\text{sec}$]	Height [μV]	Area%	Height%	Quantity	NTP	Resolution	Symmetry Factor	Warning
1	Unknown	6	15.043	1197	16	0.023	0.015	N/A	2307	2.035	8.206	
2	Unknown	6	17.673	5197024	107727	99.977	99.985	N/A	2787	N/A	1.075	

IC-3, Hexane:2-Propanol =98:2

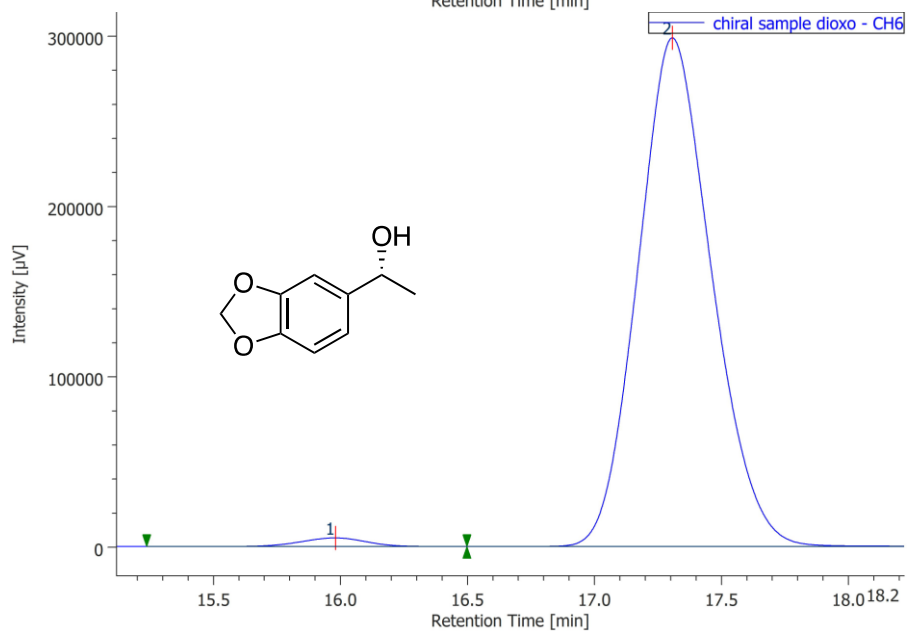
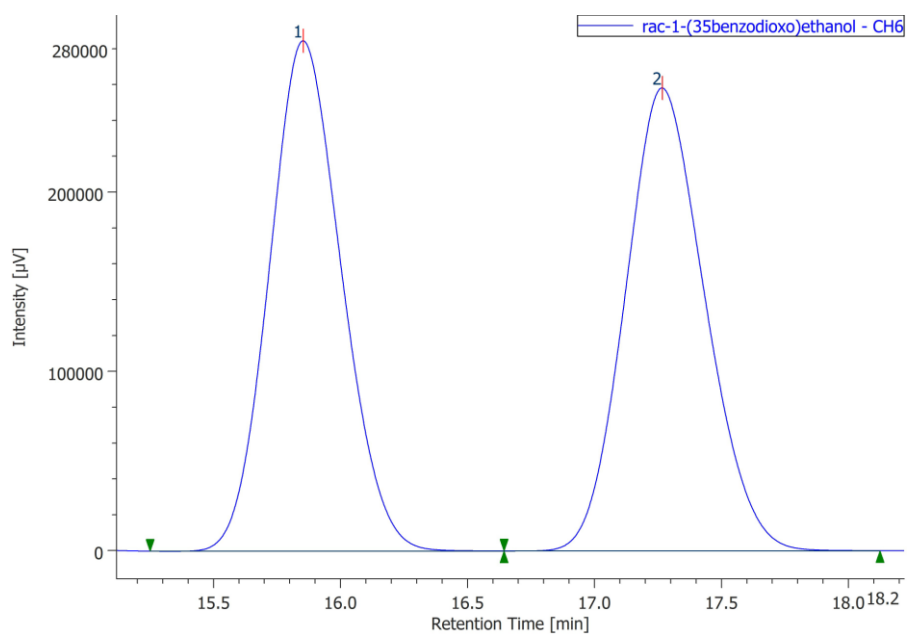
(R)-1-Tetralol (1k)



#	Peak Name	CH	tR [min]	Area [μV·sec]	Height [μV]	Area%	Height%	Quantity	NTP	Resolution	Symmetry Factor	Warning
1	Unknown	6	13.080	107753	8219	0.378	0.816	N/A	20947	2.366	0.929	
2	Unknown	6	14.433	28418276	998714	99.622	99.184	N/A	5402	N/A	2.057	

IJ-3, Hexane:2-Propanol =98:2

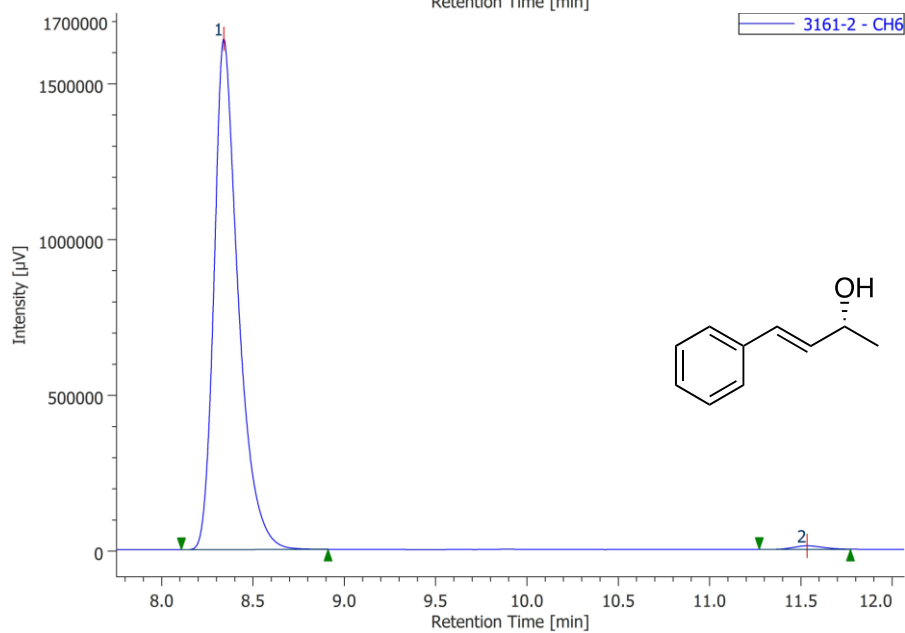
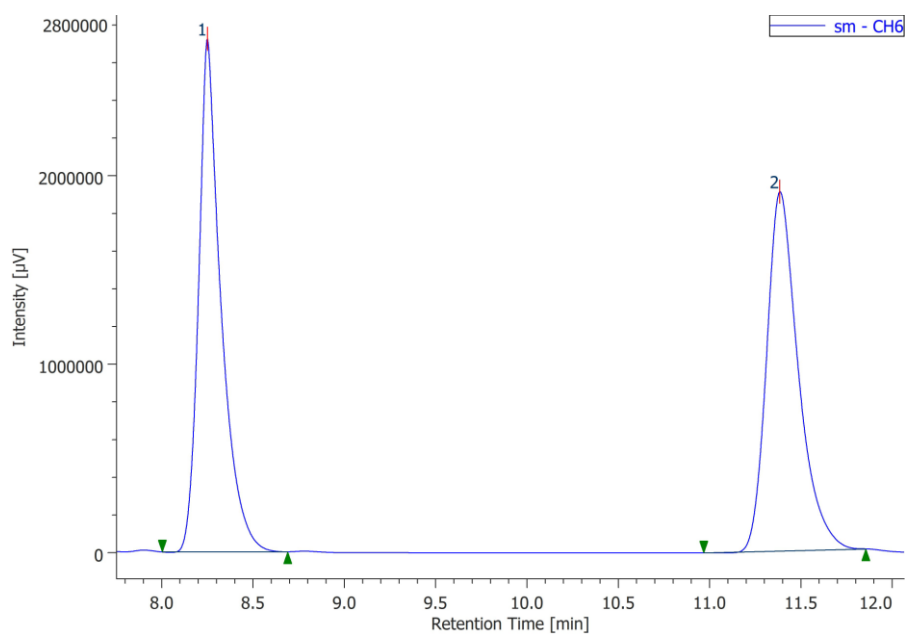
(R)-1-(Benzo[d][1,3]dioxol-5-yl)ethanol (11)



#	Peak Name	CH	tR [min]	Area [μV·sec]	Height [μV]	Area%	Height%	Quantity	NTP	Resolution	Symmetry Factor	Warning
1	Unknown	6	15.980	88913	5026	1.458	1.656	N/A	18199	2.650	0.941	
2	Unknown	6	17.307	6008123	298479	98.542	98.344	N/A	17049	N/A	1.127	

IJ-3, Hexane:2-Propanol =95:5

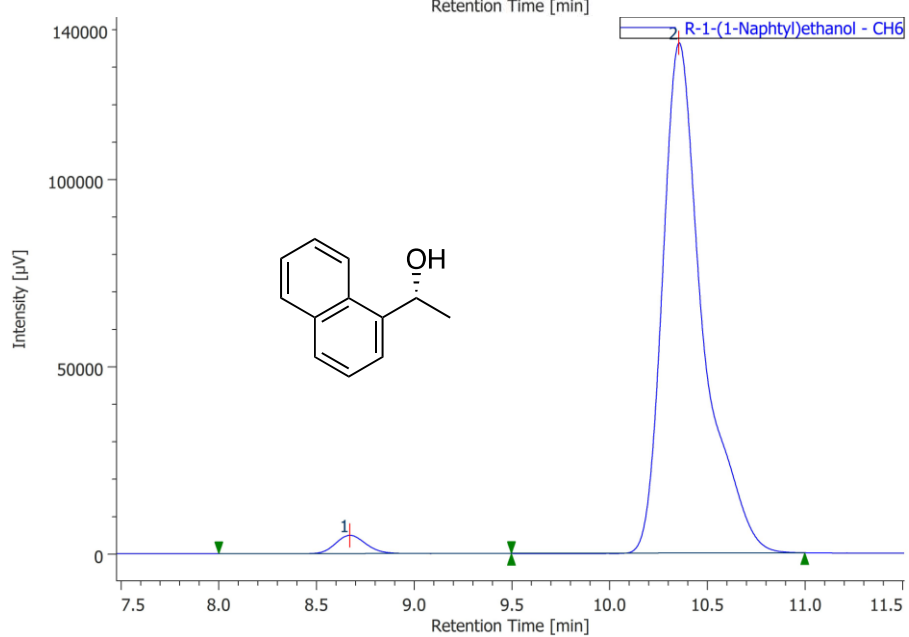
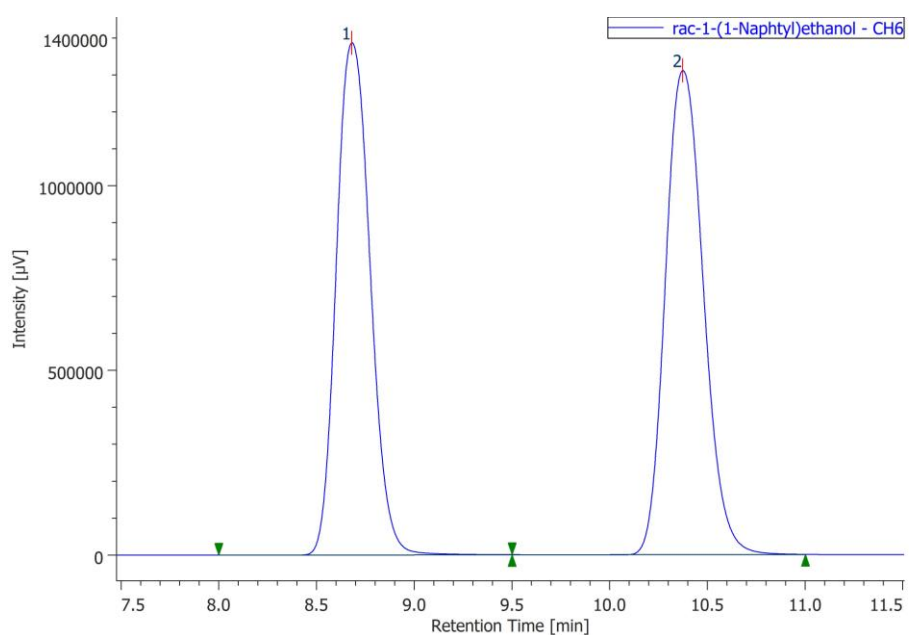
(R)- 4-Phenyl-3-buten-2-ol (1m)



#	Peak Name	CH	tR [min]	Area [$\mu\text{V}\cdot\text{sec}$]	Height [μV]	Area%	Height%	Quantity	NTP	Resolution	Symmetry Factor	Warning
1	Unknown	6	8.340	15125128	1639375	99.182	99.318	N/A	21197	12.230	1.420	
2	Unknown	6	11.533	124715	11249	0.818	0.682	N/A	24547	N/A	1.127	

IB N-3, Hexane:2-Propanol =90:10

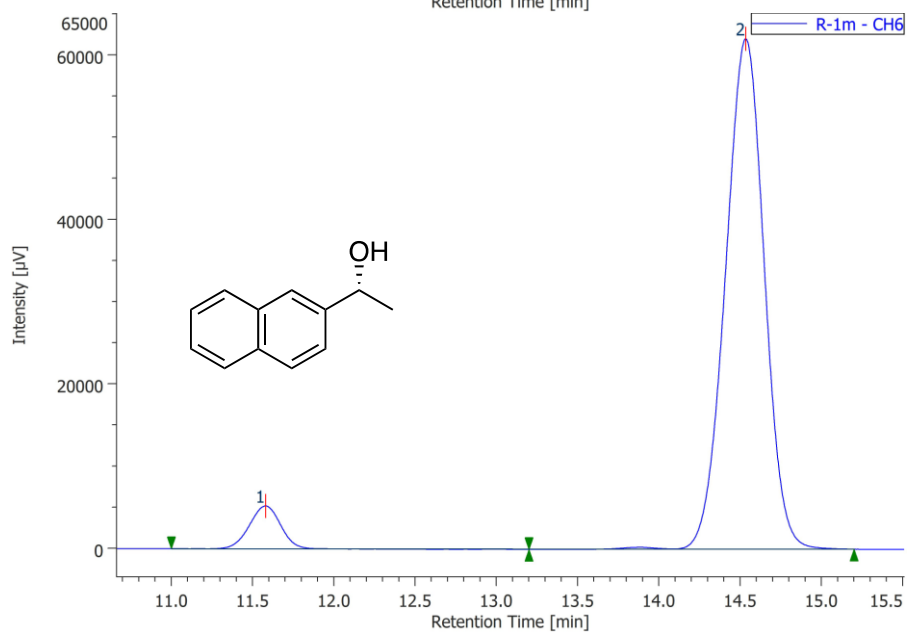
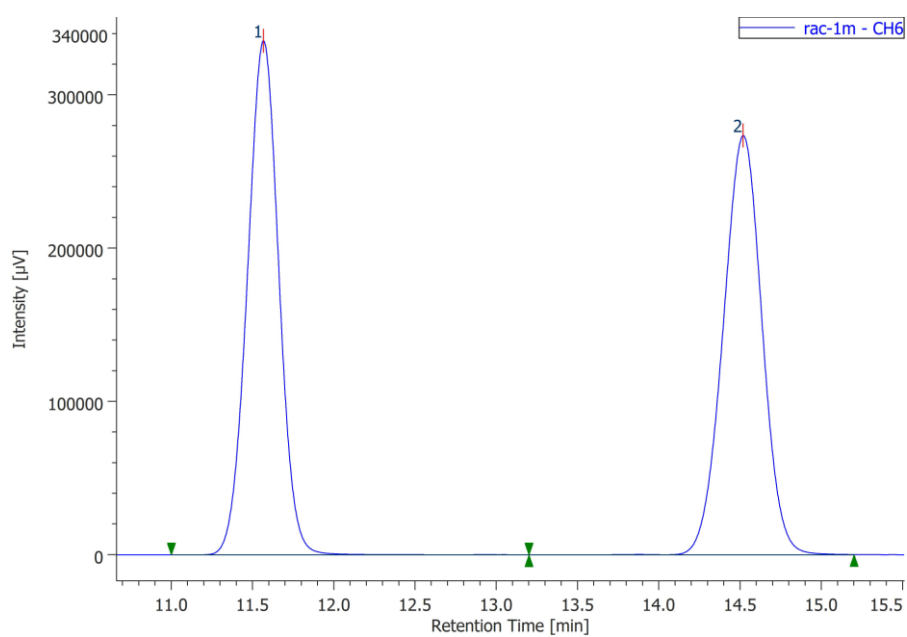
(R)-1-(1-Naphthyl)ethanol (1n)



#	Peak Name	CH	tR [min]	Area [μV-sec]	Height [μV]	Area%	Height%	Quantity	NTP	Resolution	Symmetry Factor	Warning
1	Unknown	6	8.670	51865	4872	2.601	3.454	N/A	15125	5.472	1.118	
2	Unknown	6	10.353	1942186	136202	97.399	96.546	N/A	15289	N/A	1.511	

IC-3, Hexane:2-Propanol =95:5

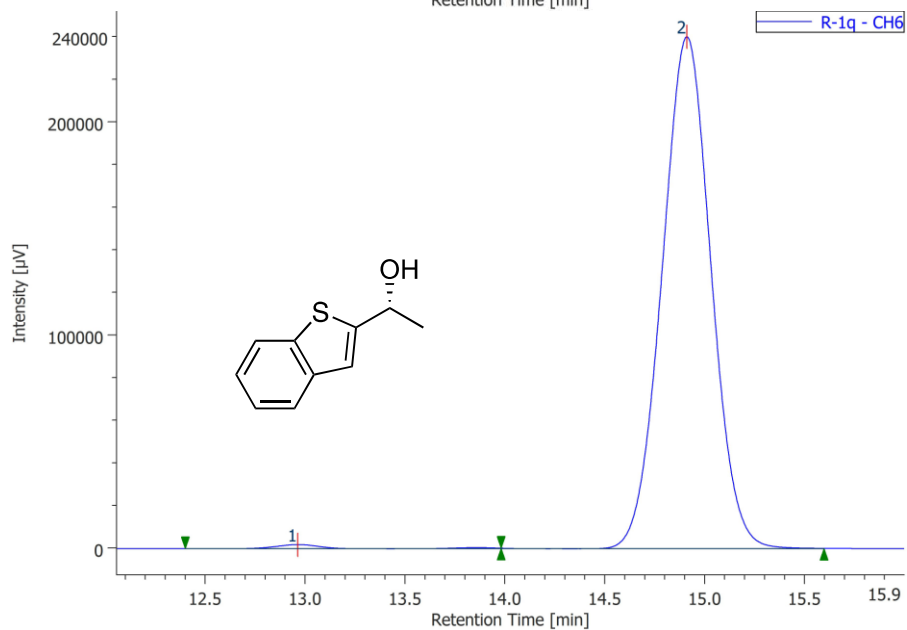
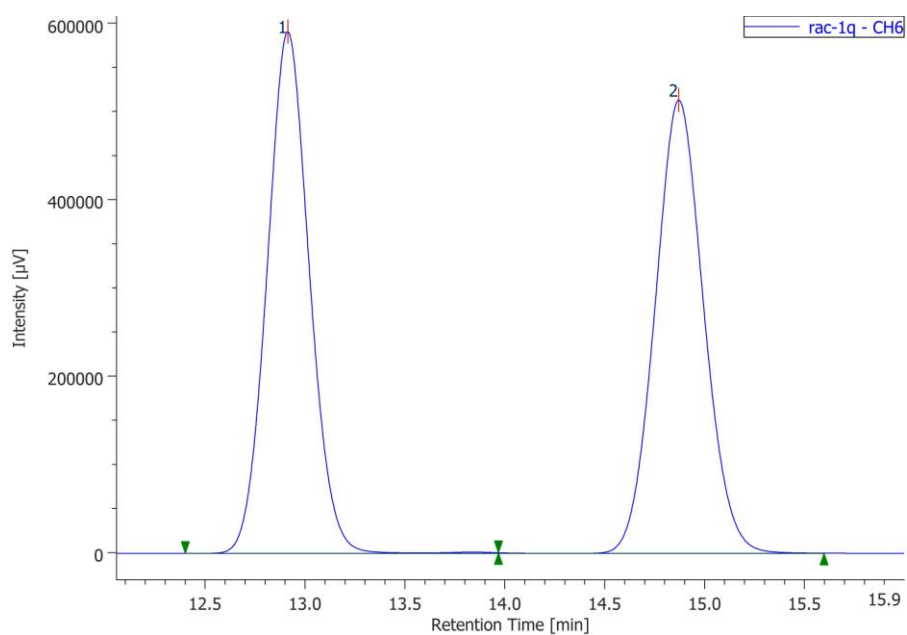
(R)-1-(2-Naphthyl)ethanol (1o)



#	Peak Name	CH	tR [min]	Area [$\mu\text{V}\cdot\text{sec}$]	Height [μV]	Area%	Height%	Quantity	NTP	Resolution	Symmetry Factor	Warning
1	Unknown	6	11.580	70094	5227	6.369	7.769	N/A	17145	7.491	0.982	
2	Unknown	6	14.533	1030383	62058	93.631	92.231	N/A	17711	N/A	0.977	

IJ-3, Hexane:2-Propanol =90:10

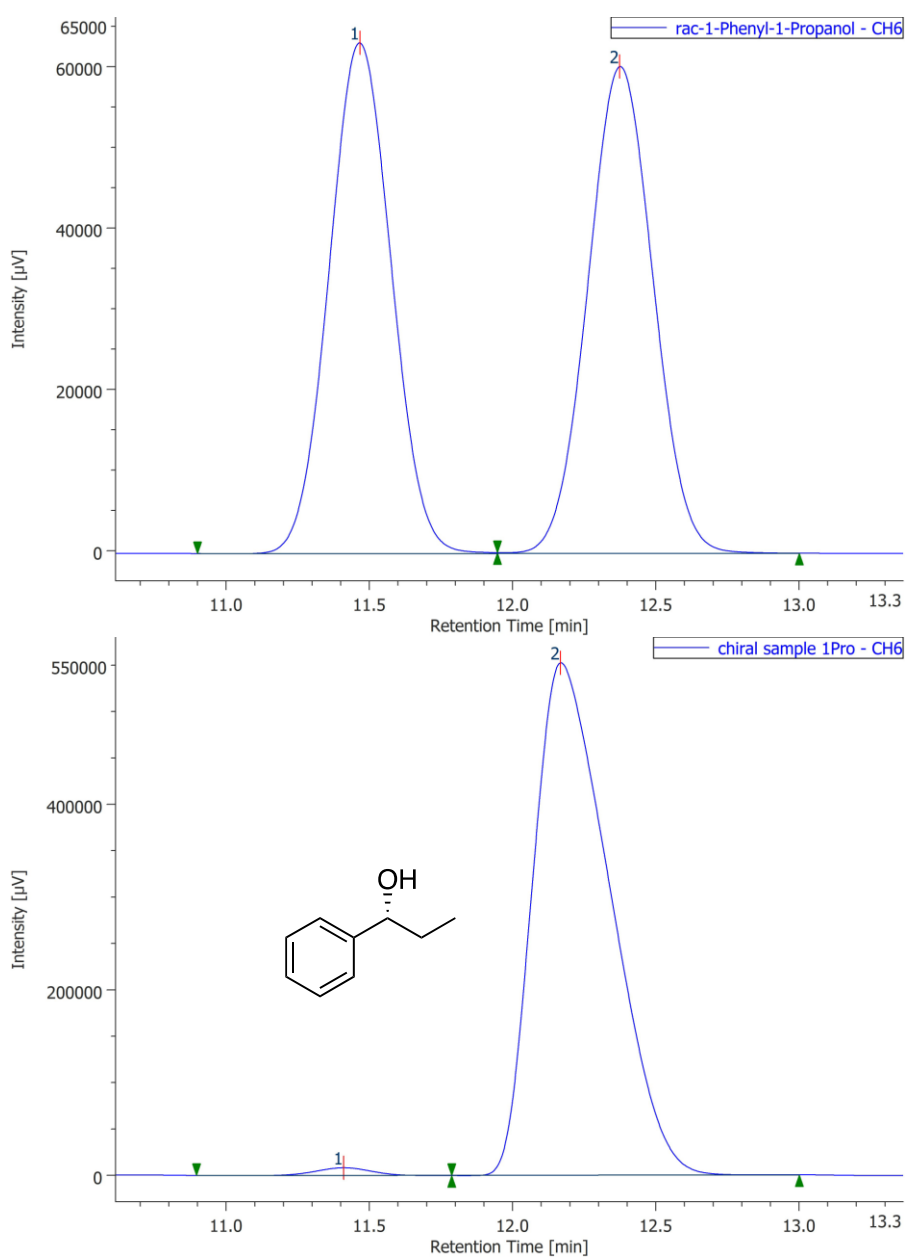
(R)-1-(Benzo[b]thiophen-2-yl)ethanol (1p)



#	Peak Name	CH	tR [min]	Area [μV·sec]	Height [μV]	Area%	Height%	Quantity	NTP	Resolution	Symmetry Factor	Warning
1	Unknown	6	12.963	32768	1891	0.796	0.782	N/A	17825	4.668	N/A	
2	Unknown	6	14.910	4082382	240040	99.204	99.218	N/A	17731	N/A	1.015	

IJ-3, Hexane:2-Propanol =90:10

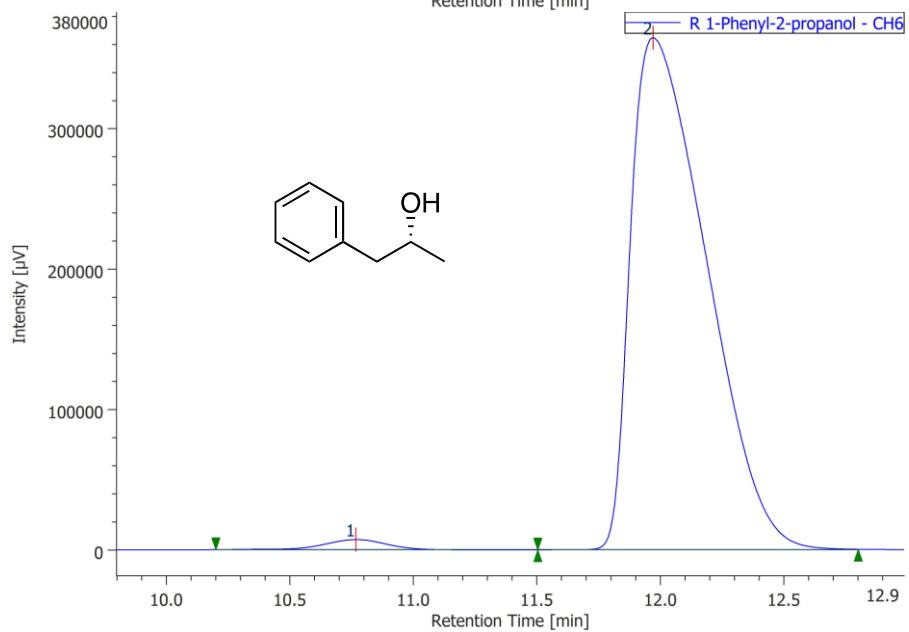
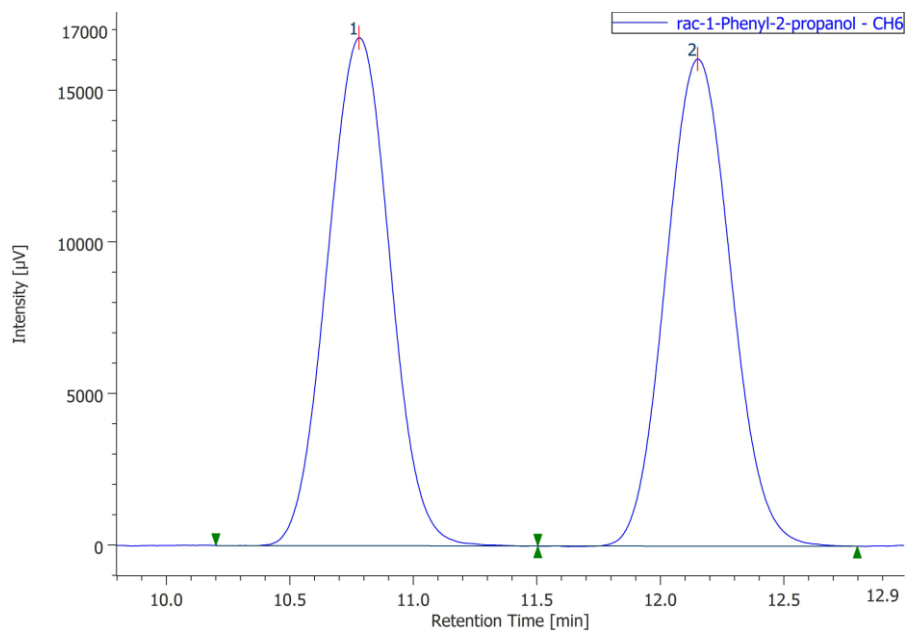
(R)-1-Phenyl-1-propanol (1q)



#	Peak Name	CH	tR [min]	Area [μV·sec]	Height [μV]	Area%	Height%	Quantity	NTP	Resolution	Symmetry Factor	Warning
1	Unknown	6	11.410	105237	8129	1.017	1.451	N/A	16689	1.760	0.973	
2	Unknown	6	12.167	10244424	552160	98.983	98.549	N/A	9143	N/A	1.472	

IJ-3, Hexane:2-Propanol =98:2

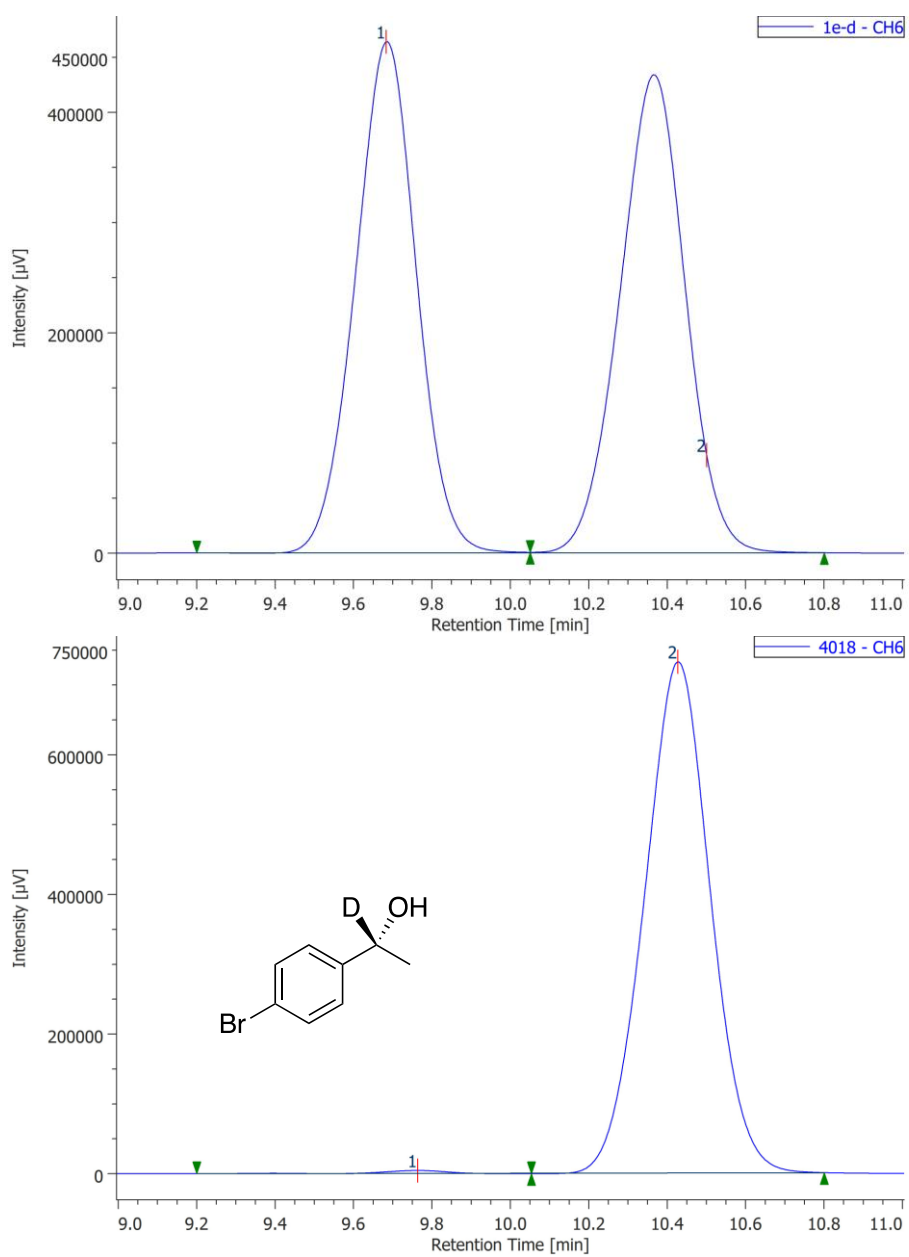
(R)-1-Phenyl-2-propanol (1r)



#	Peak Name	CH	tR [min]	Area [μ V \cdot sec]	Height [μ V]	Area%	Height%	Quantity	NTP	Resolution	Symmetry Factor	Warning
1	Unknown	6	10.767	125251	7130	1.591	1.920	N/A	8926	2.319	0.888	
2	Unknown	6	11.970	7746131	364224	98.409	98.080	N/A	6705	N/A	1.938	

IE-3, Hexane:2-Propanol =98:2

(R)-1-(p-Bromophenyl)ethan-1-d-1-ol (1e-d)



#	Peak Name	CH	tR [min]	Area [μ V·sec]	Height [μ V]	Area%	Height%	Quantity	NTP	Resolution	Symmetry Factor	Warning
1	Unknown	6	9.763	42947	4095	0.499	0.556	N/A	21281	2.314	0.641	
2	Unknown	6	10.427	8555980	732017	99.501	99.444	N/A	18451	N/A	1.014	

IJ-3, Hexane:2-Propanol =95:5